2019-09

STUDY OF MATERIAL AND PARAMETER IMPACTS ON THE PERFORMANCE OF A SIMPLE PARALLEL PLATE CAPACITOR WITH SUPER DIELECTRIC MATERIALS

Roman, Alexander J.

Monterey, CA; Naval Postgraduate School

NAVAL POSTGRADUATE SCHOOL

MONTEREY, CALIFORNIA

THESIS

STUDY OF MATERIAL AND PARAMETER IMPACTS ON THE PERFORMANCE OF A SIMPLE PARALLEL PLATE CAPACITOR WITH SUPER DIELECTRIC MATERIALS

by

Alexander J. Roman

September 2019

Thesis Advisor:	Jonathan Phillips
Second Reader:	Ibrahim E. Gunduz

THIS PAGE INTENTIONALLY LEFT BLANK

REPORT DOCUMENTATION PAGE			*Form Approved OMB No. 0704-0188*

1. AGENCY USE ONLY *(Leave blank)*	**2. REPORT DATE** September 2019	**3. REPORT TYPE AND DATES COVERED** Master's thesis

4. TITLE AND SUBTITLE
STUDY OF MATERIAL AND PARAMETER IMPACTS ON THE PERFORMANCE OF A SIMPLE PARALLEL PLATE CAPACITOR WITH SUPER DIELECTRIC MATERIALS

5. FUNDING NUMBERS

6. AUTHOR(S) Alexander J. Roman

7. PERFORMING ORGANIZATION NAME(S) AND ADDRESS(ES)
Naval Postgraduate School
Monterey, CA 93943-5000

8. PERFORMING ORGANIZATION REPORT NUMBER

9. SPONSORING / MONITORING AGENCY NAME(S) AND ADDRESS(ES)
N/A

10. SPONSORING / MONITORING AGENCY REPORT NUMBER

11. SUPPLEMENTARY NOTES The views expressed in this thesis are those of the author and do not reflect the official policy or position of the Department of Defense or the U.S. Government.

12a. DISTRIBUTION / AVAILABILITY STATEMENT
Approved for public release. Distribution is unlimited.

12b. DISTRIBUTION CODE
A

13. ABSTRACT (maximum 200 words)

This study explored the impact of the materials employed, particularly electrode material, on the performance of Novel Paradigm Supercapacitors (NPS). The main experimental focus was on the impacts of changing the identity of the electrode materials in Novel Paradigm Supercapacitors employing Distilled Deionized water (DI) or DI with 3.5 wt % dissolved NaCl. In sum, it was determined that i) some metals too easily corrode in this application (e.g., silver and lead) to be functional for more than a few hours, ii) titanium is an excellent electrode material that corrodes very slowly and the corrosion layer has an impact on performance, and iii) conductive carbon of any type is superior to all other materials in terms of net energy storage capability. The study also served the purpose of testing the Super Dielectric Material Theory (SDM-Theory). The main thrust of the "theory" component was to test the general SDM model of dielectrics against the standard model using appropriately designed experiments, specifically, experiments designed to measure the impact of dielectric material “outside” the volume between the electrodes. Traditional theory indicates the material outside the capacitor has no possible impact, whereas SDM theory says it can have a very significant impact. Results were only consistent with SDM theory.

14. SUBJECT TERMS
capacitor, dielectric, SDM, novel paradigm supercapacitors, supercapacitors

15. NUMBER OF PAGES
121

16. PRICE CODE

17. SECURITY CLASSIFICATION OF REPORT	**18. SECURITY CLASSIFICATION OF THIS PAGE**	**19. SECURITY CLASSIFICATION OF ABSTRACT**	**20. LIMITATION OF ABSTRACT**
Unclassified	Unclassified	Unclassified	UU

NSN 7540-01-280-5500

Standard Form 298 (Rev. 2-89)
Prescribed by ANSI Std. 239-18

THIS PAGE INTENTIONALLY LEFT BLANK

Approved for public release. Distribution is unlimited.

STUDY OF MATERIAL AND PARAMETER IMPACTS ON THE PERFORMANCE OF A SIMPLE PARALLEL PLATE CAPACITOR WITH SUPER DIELECTRIC MATERIALS

Alexander J. Roman
Lieutenant, United States Navy
BS, U.S. Naval Academy, 2012

Submitted in partial fulfillment of the
requirements for the degree of

MASTER OF SCIENCE IN MECHANICAL ENGINEERING

from the

NAVAL POSTGRADUATE SCHOOL
September 2019

Approved by: Jonathan Phillips
Advisor

Ibrahim E. Gunduz
Second Reader

Garth V. Hobson
Chair, Department of Mechanical and Aerospace Engineering

THIS PAGE INTENTIONALLY LEFT BLANK

ABSTRACT

This study explored the impact of the materials employed, particularly electrode material, on the performance of Novel Paradigm Supercapacitors (NPS). The main experimental focus was on the impacts of changing the identity of the electrode materials in Novel Paradigm Supercapacitors employing Distilled Deionized water (DI) or DI with 3.5 wt % dissolved NaCl. In sum, it was determined that i) some metals too easily corrode in this application (e.g., silver and lead) to be functional for more than a few hours, ii) titanium is an excellent electrode material that corrodes very slowly and the corrosion layer has an impact on performance, and iii) conductive carbon of any type is superior to all other materials in terms of net energy storage capability. The study also served the purpose of testing the Super Dielectric Material Theory (SDM-Theory). The main thrust of the "theory" component was to test the general SDM model of dielectrics against the standard model using appropriately designed experiments, specifically, experiments designed to measure the impact of dielectric material “outside” the volume between the electrodes. Traditional theory indicates the material outside the capacitor has no possible impact, whereas SDM theory says it can have a very significant impact. Results were only consistent with SDM theory.

THIS PAGE INTENTIONALLY LEFT BLANK

TABLE OF CONTENTS

THIS PAGE INTENTIONALLY LEFT BLANK

LIST OF FIGURES

THIS PAGE INTENTIONALLY LEFT BLANK

LIST OF TABLES

THIS PAGE INTENTIONALLY LEFT BLANK

LIST OF ACRONYMS AND ABBREVIATIONS

A	electrode area
Ag	silver
C	capacitance
[cm^3]	centimeter cubed
CVD	chemical vapor deposition
DI	deionized water
DMSO	dimethyl sulfoxide
dt	infinitesimal time
DT	discharge time
dV	infinitesimal voltage
E	energy
EC Lab	electrochemistry lab
EM Railgun	electromagnetic railgun
EU	European Union
ε	dielectric constant
ε_o	permittivity of free space
[f]	farad
FEL	free electron laser
gsm	grams per square meter
GTA	high purity grade (minimum 99.5% graphite)
HEL	high energy laser
I	current
[J]	joule
LaWS	Laser Weapons System
[mA]	milliamp
[mm]	millimeter
MATLAB	Matrix Laboratory (software)
NP	novel paradigm
NPS	Naval Postgraduate School

P	power
Pb	lead
[s]	second
SEM	scanning electron microscope
SM	standard model
SDM	super dielectric material / model
SW	salt water
NaCl	sodium chloride
NiCd	nickel cadmium
NiMh	nickel metal hydride
pH	power of hydrogen
q	charge
t	time
T	temperature
Ti	titanium
UUV	Unmanned underwater vehicle
UAV	Unmanned aerial vehicle
V s	volt seconds
W	watt
V	voltage difference
[V]	volts
Vol	volume
XRD	X-ray diffraction
wt	weight

ACKNOWLEDGMENTS

I would like to acknowledge my wife, Rachel, for all her support creating a strong environment for further education. I would like to thank my advisor Dr. Jonathan Phillips and all the professors who have taught me along the way.

THIS PAGE INTENTIONALLY LEFT BLANK

I. INTRODUCTION

A. SUMMARY OF FINDINGS

This study explored the impact of the material characteristics employed, particularly the electrode material, on the performance of Novel Paradigm (NP) Supercapacitors. The study identified a combination of carbon nanotube sheet electrode with a sodium chloride solution dielectric stored the highest energy and operated at the greatest constant current loading.

The study also served to show the super dielectric material theory (SDM) is more consistent with the tested experiments than the standard model of dielectrics (SM). In order to clearly distinguish two theories of dielectric operation an experiment for which each theory made diametrically opposite predictions was conducted. Specifically, the standard model (SM) of dielectrics found in all text books, predicts, mathematically, that the impact of dielectric located on the outside of the volume of a parallel plate capacitor will have no influence on performance. In contrast the SDM theory, a theory first proposed by Naval Postgraduate School (NPS) faculty, indicates that dielectric on the outside should have an impact on performance similar to the same dielectric between the plates. Extensive testing confirmed: Dielectric material on the outside of the plates of a parallel plate capacitor has a dramatic impact on all capacitive parameters [1].

In more detail, the tests, as we previously described [1], were as follows: Simple parallel plate capacitors with only ambient air between the plates behaved as per standard theory. To wit: The capacitance was very low, and the dielectric constant approximately 1.0. Once the same capacitor was partially submerged in deionized water (DI), or DI with low dissolved sodium chloride (NaCl) concentrations, still with only ambient air between the electrodes, the capacitance, dielectric constant, energy density, and power density, at low frequency, increased by more than seven orders of magnitude. This result is completely consistent with SDM theory [2]. Notably, conventional theory precludes the possibility that material outside the volume between the plates will in any fashion impact capacitive

behavior. Thus, conventional theory postulates no change in performance upon the capacitor being submerged in any material.

B. MOTIVATION AND BACKGROUND

The carbon footprint of the human race is a macro scale problem. The impact of every individual might not seem like much but combined makes a tremendous difference. The world today is connected on such a grand scale that it's hard to be disconnected. Just think about going to work, how many items that you interact which use electricity. When you wake up, your alarm clock uses electricity, you turn on the light to the bedroom and bathroom to see. You might have an electric toothbrush. Your water heater might use an electrical heating coil. You check your watch which uses a battery. You leave the house and turn on your electric or hybrid vehicle. The world we live in is connected to a power grid. We are driven and limited by electricity. Imagine if these energy materials could be made out of simple, safe and readily available products. Imagine that instead of when you get a new product that has a 20 page "properly disposal procedures" instruction manual that it's safe to dispose of in your garden. Instead of chemicals and rare minerals that are high energy density power sources for your phone and other devices, that these products are made up of salt water and carbon. A disruptive technology is NP Supercapacitors which use super dielectric material that have energy densities greater than current commercial products [2].

1. U.S. Navy

The U.S. Navy is moving towards electric ships, electric catapults on ships and electric autonomy. In order to enable these proposed technologies, the Navy must find improved modalities of electric energy storage and electric power delivery. Improved capacitors are part of the roadmap. High energy density capacitors are needed to deliver power to weapon systems. Only capacitors can deliver electric energy on the time scale, that is high electric power, needed to enable rail guns and other systems. Batteries cannot, intrinsically, provide power on the needed scale. Also, improved capacitors could 'smooth out' power demand made to batteries, and this is known to significantly increase battery lifetime. Moreover; there is some basis for considering capacitors as a substitute for

batteries for electrical energy storage. Initial data, optimistically extrapolated, indicates that fully developed NP Supercapacitors will have energy density significantly better than the best batteries, will charge far faster, and will be less expensive; hence, NP Supercapacitors could ultimately replace batteries in many systems [3].

2. Alternative Energy Storage

Alternative electrical energy storage is a concept of using simple technologies to store energy when "alternative energy" sources such as wind and solar, are periodically "off-line" due to natural limits such as night fall, low wind, etc. Electrical energy storage is most commonly battery based. Given the increasing reliance on these alternative energies, as well as the replacement of combustion engines in cars, trucks, ships, etc., with electric/battery engines, the growth of battery production is dramatically increasing. In turn, increased battery use is already stressing supplies of necessary materials such as cobalt for the cathode and lithium for the anode. The price of cobalt, which is needed for these batteries, rose over 270 percent from 2016 to 2018 [4].

Also, battery disposal is a major problem because batteries contain environmentally unsafe materials. Harnessing the power from batteries means having dangerous chemicals. Harnessing solar power gives us clean air. Utilizing and structuring theses alternative energies in conjunction with a storage device can revolution the world.

The ultimate goal of this research is providing the information required to assess NPS capacitors as a potential replacement technology for batteries in many applications. Can NP Supercapacitors be superior to batteries in terms of energy density, charge more rapidly, charge rate, power delivery, cost and longevity? Should this potential be pursued through further research?

3. Environmental Impact

Based on extrapolation of data collected regarding the performance of prototypes it is possible NP Supercapacitors will not only outperform batteries, but will be cheaper, less toxic, less hazardous. They will also only employ materials available virtually everywhere, such as salt water for the dielectric and carbon for the electrodes. Current

batteries use a wide swath of technologies. Some common used batteries are alkaline based batteries in disposable electronics, or lead acid batteries in cars. The batteries used in large electric vehicles and hybrids are lithium ion or NiMH (nickel metal hydride) or NiCd (nickel cadmium) [5]. The list goes on to be Lithium Cobalt Oxides, Manganese Oxide, Nickle Manganese, Iron Phosphate and Cobalt Aluminum Oxide. The combination of complex chemical and there uses has been regulated in the European Union (EU) to be branded with a "do not dispose" of label. All of these minerals and materials used for these complex technologies are limited in their availability.

4. Energy Weapon Supply (EM Rail Gun/HEL/FEL/LaWS)

Energy is the next frontier for future weapons. Bridging the divide between science fiction and the battle field can give any country a tactical advantage. Weapons, and military systems, based on electrical energy are potential game changers because they will be more powerful, more readily controlled, better able to deliver power precisely on target, more compact. High energy weapons such as electromagnetic (EM) rail guns, high energy lasers (HEL), focused energy lasers (FEL) or laser weapon system (LaWS) all need high concentrations of energy that need to be delivered in a short time [6]. One aspect of creating a mature, dependable technology for electric weapons are the power sources. Batteries cannot deliver sufficient power over the time frames required by these weapons. That is, they have an upper limit on power. Indeed, it is generally understood that capacitors are superior 'power' sources. Capacitors have far lower energy density than batteries, but can deliver all the energy in a far shorter time than batteries. There is evidence that NP Supercapacitors can not only potentially match battery energy density, a real leap in capacitor capability, but also deliver the power needed for weapons. In addition, capacitors can be re-charged far faster than batteries.

C. RESEARCH OBJECTIVES

There were both engineering and scientific objectives to the work conducted. The engineering objective was to further understand the effects of changing parameters for NP Supercapacitors. To identify the best combination of materials/parameters for a simple parallel plate capacitor using super dielectric materials. In particular, to determine if the

material identity of the electrodes has any impact and to determine which materials are superior. In brief, carbon based material is superior to all metals tested. Limited tests of different dielectrics were also conducted, and it was shown simple 'salt water' is an exceptional dielectric.

The scientific objective was to conduct a test with an outcome which could definitively determine if the Standard model (SM) or the Super Dielectric model (SDM) model of dielectric behavior is correct. It was demonstrated, in brief, that the mathematical and narrative forms of the SM, that only dielectric material in the volume between the electrodes can impact behavior, is incorrect. The finding that dielectric on the outside has a significant impact is only consistent with the SDM theory.

D. CAPACITOR THEORY/GOVERNING EQUATIONS

The theory studies were designed to test SDM theory: Dielectrics increase capacitance by 'cancelling everywhere' the field created by charges on the electrodes of a parallel plate capacitor. Cancelling the field reduces the energy (voltage) required (integrated line integral of field strength) to bring a charge from anywhere to either electrode. Thus, according to theory, any material that allows large dipoles, in high density in the dielectric to form upon the application of the electrode field will be a super dielectric. Salt water is clearly one such material, as the ions formed by salt dissolution in the water can 'swim' apart macroscopic distances upon field application. Moreover, the dipole density is within an order of magnitude of that found in solid dielectrics. In contrast, only sub angstrom dipole length is possible in a solid. One example of a theory test: According to SDM dielectric (e.g., salt water) outside the area between the plates of a parallel plate capacitor will be as effective as the same dielectric between the plates. According to conventional theory, dielectric outside the volume between the plates will have no effect.

E. SDM THEORY

The main hypothesis of the SDM theory can be explained in a five-part model [1], [2], [6], [7].

1. Dielectric Polarization

Dielectric material polarizes in the opposite direction to any field applied to it. This occurs because the positive charge in a dielectric move toward the negative electrode and negative charge moves toward the positive electrode.

2. Opposing Field

Placed between the electrodes of a standard parallel plate capacitor, the dielectric material creates a field opposite in direction to the electric field created by charges on the electrodes, in all space, not just the region between the plates.

3. Field Interaction

As the field at any point in space is the vector sum of the fields of all individual charges. Thus, given the opposite polarization of dielectric and charges on the electrodes, the fields produced by each at all points 'cancel'. That is, the dielectric in a parallel plate capacitor reduces the field, at all points, created by charges on the electrodes.

4. Overall Reduced Field

As "voltage," a state property, is the scaler line integration of the electric field, and the dielectric reduces the field at all points, the dielectric necessarily reduces the "voltage" between any two points, including any path from infinity to an electrode.

5. Increased Storage

It follows that as in the presence of a dielectric it takes more charge on the electrodes to reach a given capacitor voltage, dielectrics increase the electrode charge/voltage ratio. Thus, by definition, dielectrics increase capacitance:

$$C = \frac{q}{V} \tag{1}$$

where C is capacitance, q amount of charge on electrodes and V the voltage between the plates.

F. MEASUREMENT METHODOLOGIES

All data, dielectric constant, energy, and power density, were computed from the constant current discharge leg of charge/discharge cycles collected using a programmable galvanostat. The device, in constant current discharge mode, was operated over the range of 0 to +/-10 volts. The rate of electrolysis of water was minimal for most configurations at these voltages. Significant electrolysis is discussed in following sections.

1. Capacitance

The constant current measurement method was the only method employed to measure capacitance in this work. There is a simple relationship between capacitance and measured discharge rate assuming capacitance is independent of voltage

$$C = \frac{I}{(\frac{dV}{dt})} \tag{2}$$

where C is capacitance, I is current, V is voltage, and t is time. Capacitance, once measured, can be used along with easily measured geometric factors to determine the non-dimensional, engineering parameter, dielectric constant (ε). This is the mathematical expression of the standard theory of dielectrics applied to parallel plate capacitors:

$$C = \frac{\varepsilon\varepsilon_o A}{t} \tag{3}$$

where t is the thickness of the dielectric layer, A is the area of the electrode, and (ε_o) is the permittivity of free space [3].

Problem: Equation 3, that is the standard theory of dielectrics applied to parallel plate capacitors, is based on the assumption that only the dielectric material between the electrodes contributes to the capacitance. This was clearly demonstrated to be an incorrect assumption in the present study, and an earlier study by our team [1], [7]. Yet, for the capacitive values obtained when the dielectric is only present outside the volume between the plates there are no geometric constants to be used in equation 3. Hence, for the 'dielectric on the outside' configuration, a dielectric constant cannot be computed. Instead an 'effective' dielectric constant is reported. This value is computed employing the same

geometric parameters employed for the case of the dielectric between the plates: the area of the electrodes and the distance between them. Similarly, 'effective' energy density, and power density were computed/reported below "as if" the only volume of significance is that between the plates [1].

2. Dielectric Constant

Solving from Equation 3 to solve for the dielectric constant

$$\varepsilon = \frac{Ct}{\varepsilon_o A} \tag{4}$$

3. Energy Density

Energy was computed as the integral of the area under the voltage time data (V s) multiplied by current (amps).

$$Energy = E = I\int_{t_i}^{t_f} Vdt \tag{5}$$

Energy density was computed as the Energy (E) divided by the volume of the internal dielectric.

$$Energy\_Density = \frac{Energy}{length \times width \times thickness} \tag{6}$$

4. Power

Power was computed as the total energy of the discharge divided by the total discharge time.

$$P = \frac{E_{total}}{t_{discharge}} \tag{7}$$

5. Capacitors in Parallel

Capacitance in parallel was calculated using the addition of each individual capacitor.

$$C_{Parallel} = C_1 + C_2 + ... + C_{Final} \tag{8}$$

6. Capacitors in Series

Capacitance in series was calculated using

$$C_{series} = \frac{1}{\frac{1}{C_1} + \frac{1}{C_2} + \ldots \frac{1}{C_{Final}}} \tag{9}$$

G. CAPACITOR FABRICATION/ TEST APPARATUS CONFIGURATION

The standard configuration was a simple parallel plate capacitor. The design was modular and consisted of interchangeable electrodes and dielectrics. The designed parallel plate capacitor was the combination of two electrode sheets 4.5 cm x 4.5 cm with an air gap of 2.5 cm x 2.5 cm. That is, only the center area consisted of an air gap. The edges of the sheet were used to hold it in place. The electrode pieces were clamped in with layers of acrylic and commercial gasket rubber. The rubber was 1.5 mm thick. The gasket was used to create a watertight seal from the inside to outside and reverse.

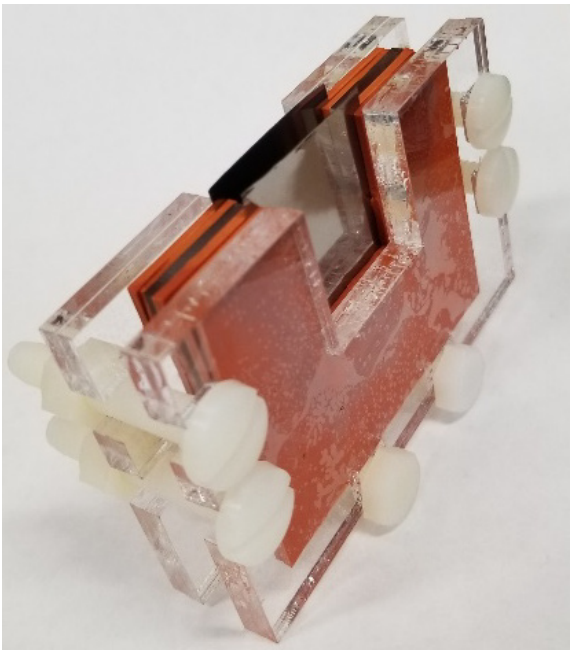

Figure 1. Parallel Plate Capacitor Rig

1. Configuration

Two separate configurations were tested.

a. Dielectric on the Inside (DI)

The volume between the electrode sheets, 2.5 cm x 2.5 cm x 6 mm, was filled with dielectric liquid. Outside was simply ambient air.

b. Dielectric on the Outside (DO)

The volume between the electrodes, 2.5 cm x 2.5 cm x 6 mm, contained only ambient air. The apparatus was submerged in a liquid dielectric of approx. 700 ml volume. The liquid level reached to the top of the external 2.5 cm x 2.5 cm area. Thus, dielectric material was only present *outside* the volume between the plates.

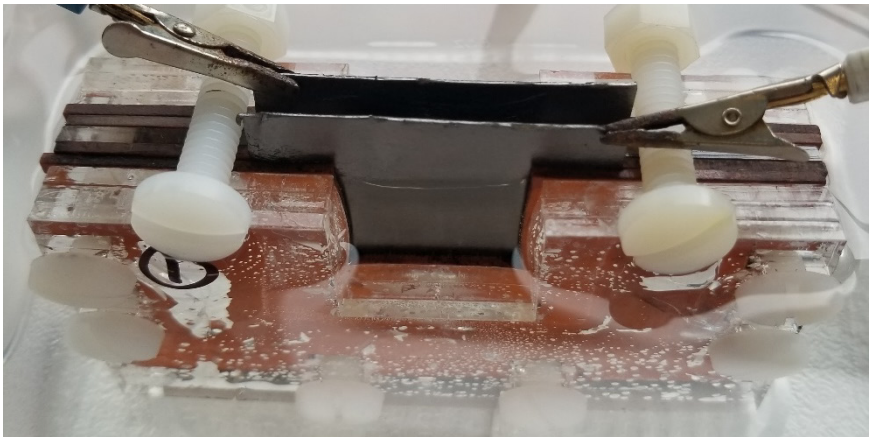

Figure 2. Dielectric on the Outside

2. Electrode Materials

All electrodes were cut to 4.5 cm x 4.5 cm squares.

a. Titanium Thin (0.05 mm)

Titanium electrodes were cut out of Ti GR2 0.05 mm thick foil sheets.

b. Titanium Thick (0.10 mm)

Titanium electrodes were cut out of Ti GR2 0.10 mm thick foil sheets.

c. Silver

Silver electrodes were cut out of Goodfellow Cambride Limited 0.5 mm thick 99.95+% purity silver foil. Its temper was “As rolled”.

d. Lead

Lead electrodes were cut out of Goodfellow Cambride Limited 1.0 mm thick 99.5% lead foil. Its temper was “As rolled”.

e. Grafoil

Carbon electrodes were cut out of GTA grade Grafoil flexible sheets (0.76 [mm] thick, minimum 99.5% graphite). Grafoil, manufactured by Graftech, is “prepared by chemically treating natural graphite flake to form a compound with and between the layers of the graphite structure” resulting in very thin (0.0762 to 1.651 [mm]) and flexible carbon-based material.

f. Carbon Nanotube Sheet

Carbon Nanotube Sheet electrodes were cut out of Nanocomp Sheet “Acetone 20–30 grams per square meter (gsm).” This material is also referred to as “Miralon.” It is a non-woven material manufacture via chemical vapor deposition [8].

3. Dielectric Materials

a. Air (Control)

Ambient air was used for experiments. Room temperatures would range from 60–80 degrees Fahrenheit.

b. Deionized water (Polar)

Deionized water was Weber Scientific brand Reagent water/ Deionized Water designed for scientific and laboratory research. Water is a polar molecule based on its covalent bond between hydrogen and oxygen.

c. Mineral Oil (Non Polar)

The mineral oil was a combination of generic mineral oils from Johnson and Johnson corporation [9] and Exchange Select Brand. These oils did contain fragrance added for consumer use. The fragrance showed no impact on performance. The mineral oil was tested for polarity by a solubility test where DI water and mineral oil were placed in a same container. They two solutions stayed separated.

d. Ionic (3.5 % NaCl Solution)

Ionic solutions were created using by weight measurements. Sodium chloride was measured to the desired weight then combined with deionized water to make a homogenous solution. The solution was heated and mixed with a magnetic mixer till not no large solids were visible. Sigma Aldrich branded 58.44 g/mol NaCl was combined with deionized water.

H. GALVANOSTAT SETUP

The galvanostat used was the BioLogic Model SP 300, made by Bio-Logic Science Instruments SAS, in Claix, France. As we described in [1], “notably, the device is regularly tested by using it to measure the marked capacitance of both commercial supercapacitors and electrostatic capacitors.”

1. Testing Protocol

The standard protocol for testing was a five step process. First would be to charge to an initial voltage, hold for a set time, discharge at a constant current, switch polarity and then repeat. An example is shows in Figure 3.

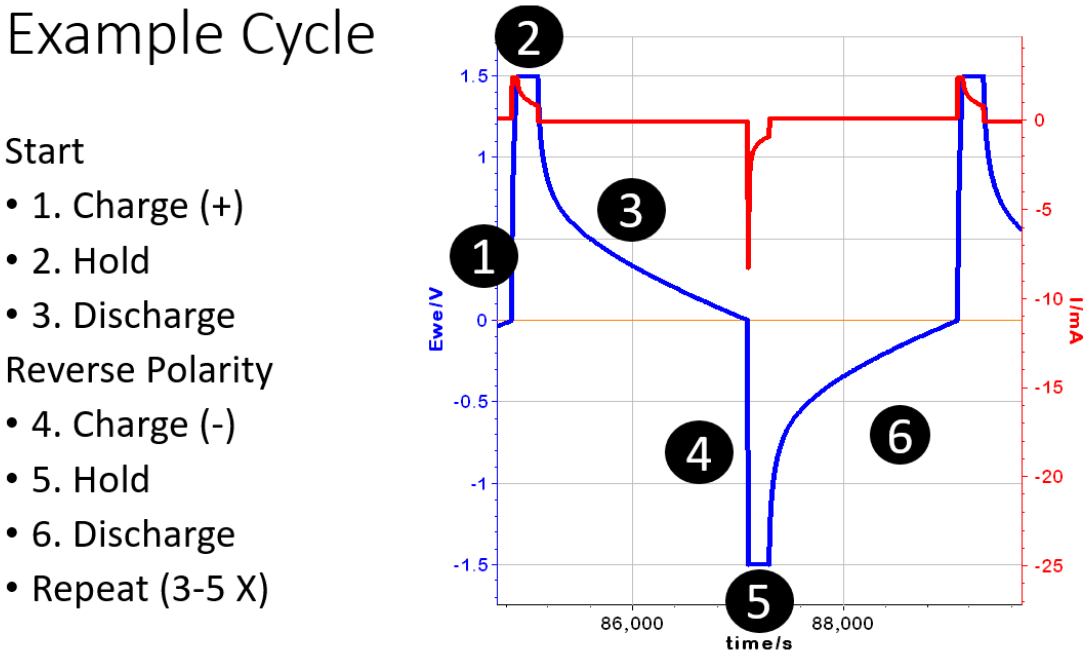

Figure 3. Example Cycle of Typical Testing Protocol

a. Charging

A range of 1 to 50 mA charging was selected. This allowed for a quick charge on the electrodes to reach its initial desired voltage with minimal impact to its hold time.

b. Constant Voltage Hold

A constant voltage hold time was determined for each material. This voltage was based on material characteristics and its ability to reach the desired voltage with the desired charging amperage. The material would be raised to the desired voltage and then held for a determined time.

c. Constant Current Discharge

A constant current discharge was used to measure the stored charge. These values ranged from 0.025 mA up to 5 mA.

d. Cycle/Repeat

Each capacitor was set up to charge, hold, discharge, reverse, charge, hold discharge and repeat for 3–5 cycles for each desired discharge current. The report typically lists the average of 3–5 cycles. After completing the cycles, the discharge current was changed and the process repeated. Changing the discharge current allows for a change in "period/ frequency."

2. EC Lab Software

BioLogic Science instruments EC-Lab Software V10.44 released Aug 31, 2015 and V11.27 released Feb 15, 2019 were used to collect and process the data.

I. PH INDICATION

A measure of the pH value was conducted using General Hydroponics pH Indicator with small samples and visual comparison of color. This pH indicator is rated for pH of 4.0 to 8.5. The lighter and closer to orange the indicator turns the lower the pH.

Table 1. pH Indicator Color Chart

pH	Color
4.0	Red
5.0	Orange
6.0	Yellow
6.5	Mustard Yellow
7.0	Light Green
8.0	Dark Green
8.5 and higher	Blue Green

J. SCANNING ELECTRON MICROSCOPE

Scanning Electron Microscopy (SEM) was conducted on using a Zeiss Neon 40 Scanning electron microscope with SMARTSIM 5.07 Software for analysis.

K. X-RAY DIFFRACTION(XRD)

XRD measurements were conducted using a Rigaku MiniFlex 600 machine and both MiniFlex Guidance and MDIJADE9 XRD pattern processing, identification, and quantification software.

THIS PAGE INTENTIONALLY LEFT BLANK

II. RESULTS

A. CHARGING AMPERAGE

The first step in each experiments was to choose an initial voltage and charge the electrodes to that voltage. This seems trivial in theory. The issue is for each combination of materials; these characteristics change dramatically. There are several phenomena which occur with the electrode or dielectric or combination. Based on the paring there were many considerations and parameters needed to be changed to meet these. 1) An ageing process would occur. This in most cases of metals consisted of an oxidation layer occurring on the surface. 2) Ageing oxide growth and material break down into the dielectric. 3) Delamination and expansion of the electrode. 4) Dielectric electrolysis and a change of pH. 5) Pitting corrosion and ultimate failure. For each material there was a maximum voltage that a combination of electrode and dielectric would reach at a set amperage. Table 2 lists the combination. The required amperages would change for some materials as an artifact of an aging process of a thin surface oxide layer or a change in the dielectric. The desired charging amperes and voltages was a function of the two variables.

Table 2. Material Charging Voltage Plateau and Associated Current

Material	Dielectric	Location	Charging Amperage (mA)	Maximum Voltage (V)
Ag	DI	Inside	2.4	7.3
Grafoil	DI	Inside	1.0	8.7
Grafoil	DI	Inside	2.4	9.2
Grafoil	SW	Inside	2.4	1.8
CNT Sheet	SW	Inside	4.5	1.32
CNT Sheet	SW	Inside	10	1.4
Ti Thick	SW	Inside	2.4	6.7

A final charging amperage was selected to have minimal effect on the initial charging and not induce increased hold time.

B. INITIAL VOLTAGE DISCUSSION

The original intention was to use a constant voltage of 10 V for all electrodes. This changed for three reasons. 1) The desired charging amperage would need to be increased dramatically. The initial range was set to 1 mA and upon further configurations was increased as high as 50 mA. 2) Electrolysis of the dielectric would occur for some materials at higher voltages. Specifically, electrodes would cause electrolysis of the DI water and dramatically change its pH altering its ionic concentration observed by bubbles forming on the surface. 3) The increased voltage and electrolysis would cause material break down and even failure.

Left: Electrolysis of water with titanium electrodes. Right Lead oxide saturation in DI water showing a glitter effect.

Figure 4. Electrolysis of Water with Ti and Lead Oxide Formation in DI Water

C. HOLD VOLTAGE EFFECT

1. Hold Voltage Current Plateau

The initial charging current set to maintain a voltage is a function of the dielectric and the material. Examining three cases, 1) Air –Ti charges almost instantaneously. 2) Water - Ti takes a large initial amperage and then over time it will require less amperage to maintain and steady over time. 3) Ionic Solution (Salt water) – Ti charges slower than water and air but reaches its desired voltage quickly based on the appropriate amperage.

For each desired voltage, the required current to reach it would peak and then begin to decrease as the hold time continued. In order to maintain the desired voltage there was less current needed. This process would occur over large hold times. In many cases the minimum current required to maintain a voltage was not reach even after 2000 seconds.

Table 3. Initial Voltage Required Amperage.

Material	Dielectric	Location	Voltage(V)	Hold Time(s)	Minimum Amperage observed (mA)
Ti Thin	DI	In	10	2000	~0.075
TI Thin	DI	Out	10	600	~0.09
TI Thick	DI	In	10	600	~0.50
TI Thick	DI	Out	10	600	~0.26
Grafoil	DI	In	10	200	~0.37
Grafoil	DI	Out	10	600	~0.77
Grafoil	SW	In	1.5	2000	~0.22
Grafoil	SW	Out	1.5	2000	~0.30

2. Electrolysis of the Dielectric

A side effect of higher voltages between plates and using water based dielectrics was the electrolysis of the water. The breakdown of the water at higher voltages was observed by bubbling on the electrodes (Figure 5). This bubbling on the electrodes caused a change in the pH of the dielectric (Figure 6). An increased pH of the dielectric lead to increased performance. The increased performance was observed by gradual increase in discharge times for each cycle in some cases. Mitigation of the electrolysis was managed by operating at lower testing voltages.

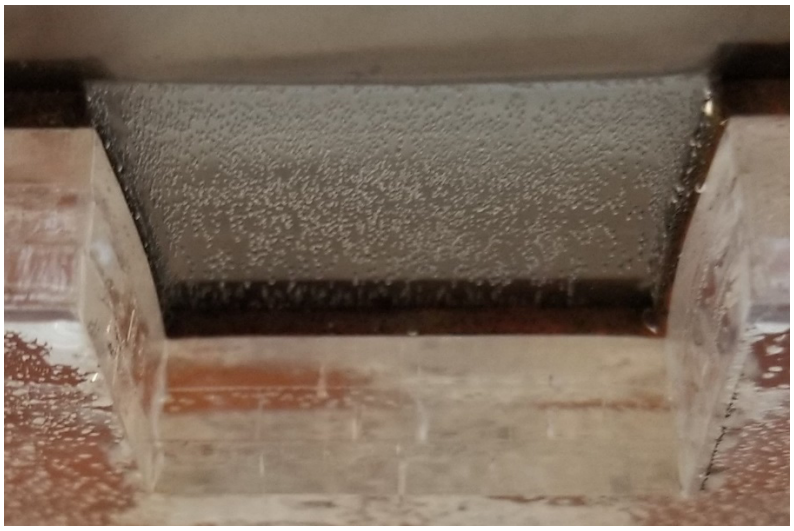

Figure 5. Electrolysis Occurring on the Electrode Surface

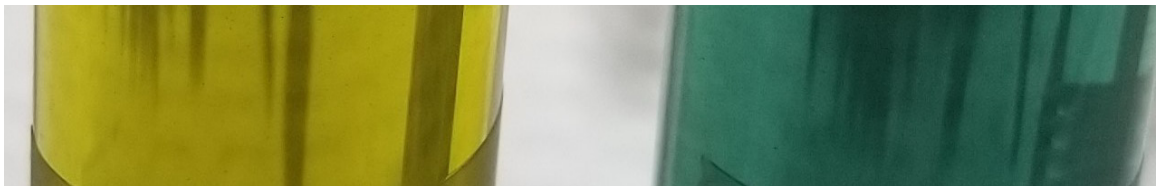

Left- Deionized water pre experiment, yellow hue indicating a pH of ~ 6. Right – Deionized water post experiment; dark green hue indicating a pH of ~7.5 – 8.

Figure 6. pH Color Change

D. IMPACT OF HOLD TIME

For each experiment a desired voltage and hold time were chosen. For most cases an increased hold time showed increased energy storage. Based on increased discharge rates the energy storage was becoming less variable and converging. It is believed that the individual plate oxidation and performance would give deviations and in some cases better performance. The overall trend is that an increased hold time leads to greater energy storage. This relationship is nonlinear based on 3X increase hold time giving a 1.6 X energy storage and a 10 X increase in hold time giving only 2 X the energy storage as observed in (Figure 7).

The increase in stored charge is hypothesized by allowing greater time for alignment of dielectric. The greater alignment, the greater the reduction of the field. This increased alignment was also noted by an increase in discharge time.

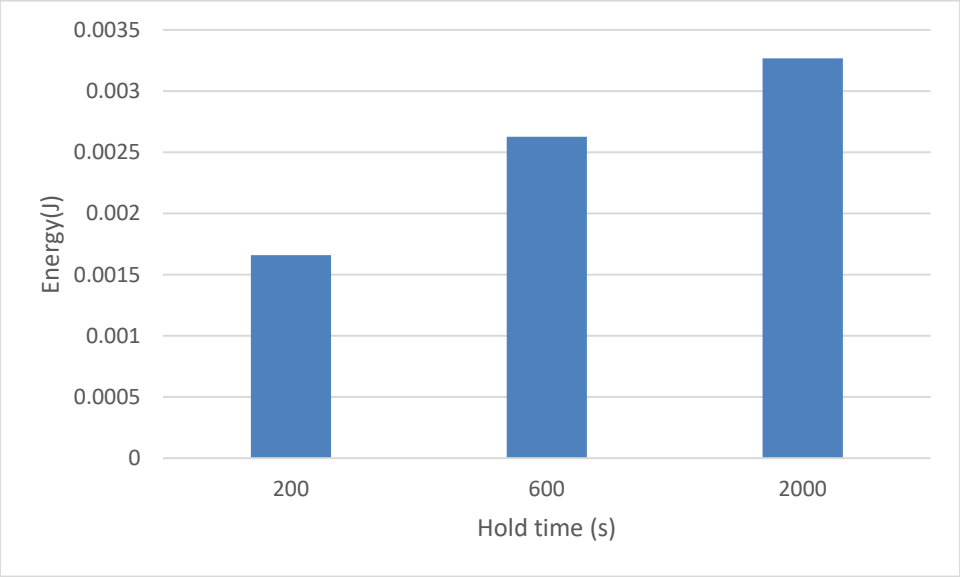

Hold time has a relatively small impact (~2 X) energy storage

Figure 7. Energy Storage vs. Hold Time of Ti Thin and DI water at 0.1 mA Discharge Rate

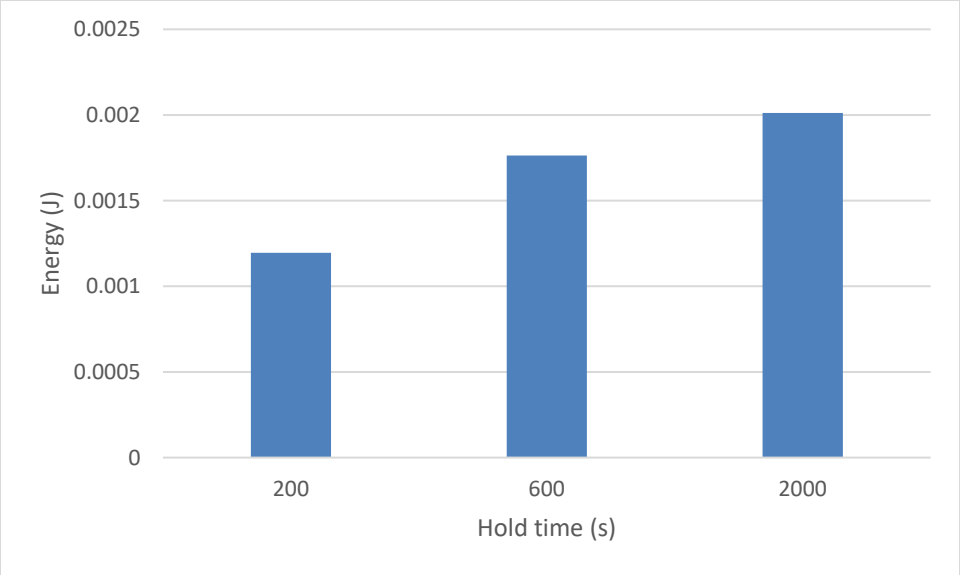

Hold time has a relatively small impact (~2 X) energy storage

Figure 8. Energy Storage vs. Hold Time of Ti Thin and DI Water at 0.25mA Discharge Rate

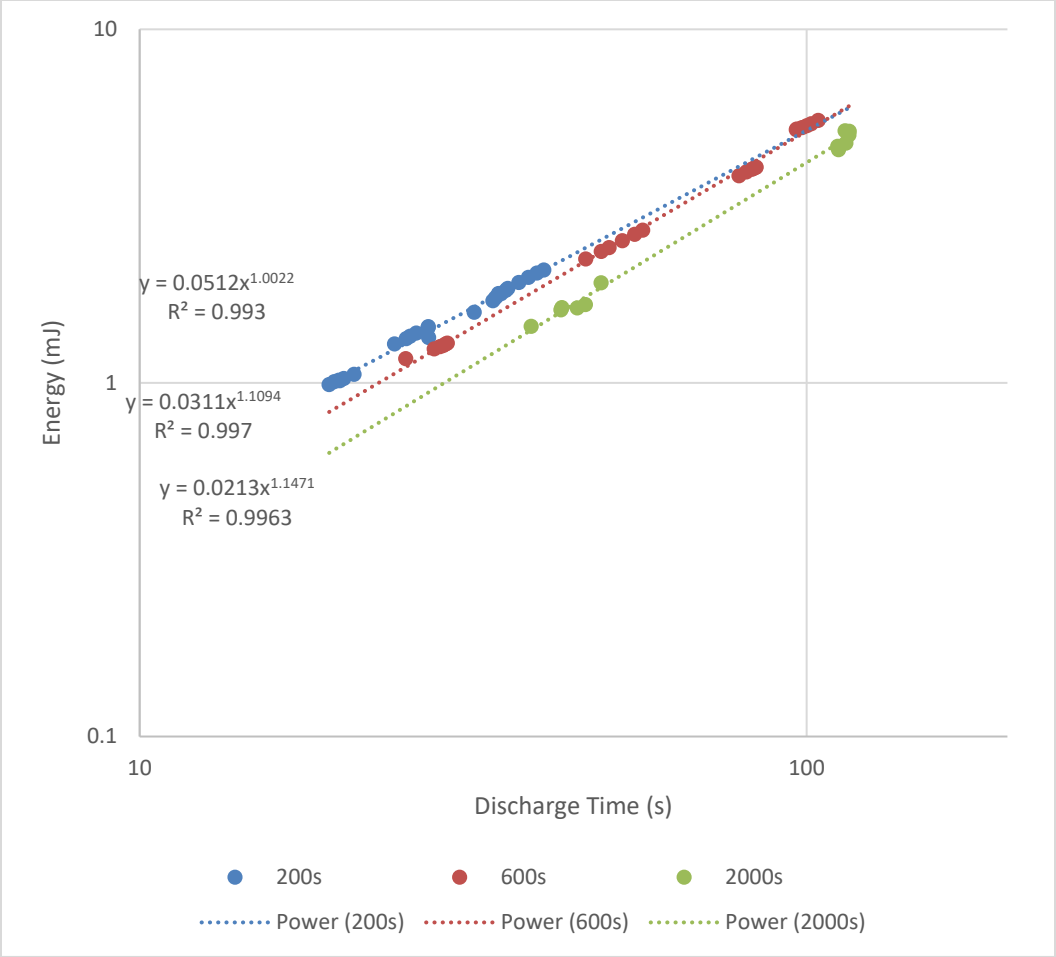

Impact based on 0.1 mA discharge rate

Figure 9. 200 vs. 600 vs. 2000 Second Hold Time Comparison Energy Storage vs. Discharge Time Ti and DI Water at 0.1 mA

Using titanium sheets there is a significant impact on the discharge time, and energy density in relation to the voltage hold time. This relationship is not specific to the electrode material. Increased hold time also gives increased energy storage as seen in changing the electrode to Grafoil and dielectric to salt water. Grafoil and SW showed and increased energy storage indication that an increased hold time allows greater energy storage.

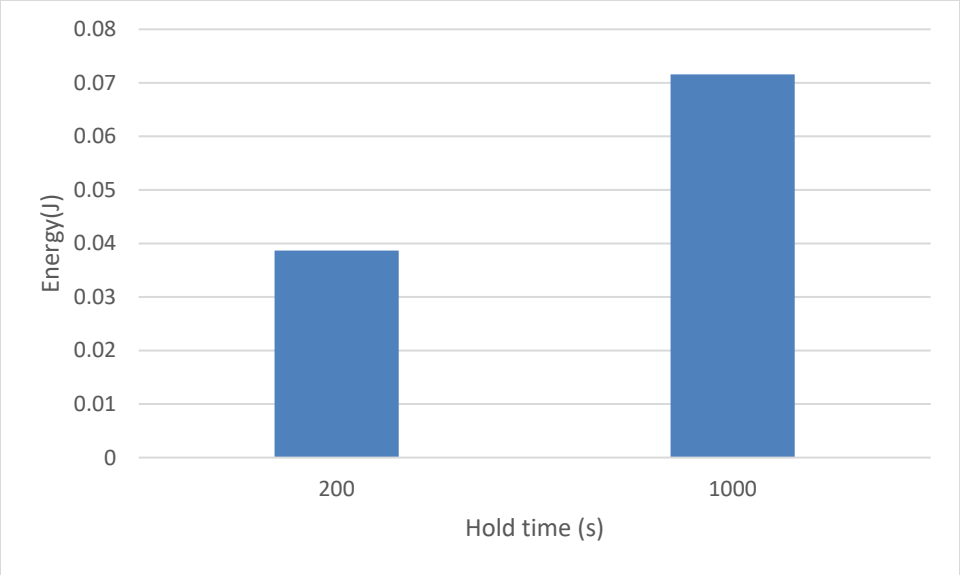

Figure 10. Energy Storage 200 s vs. 1000 s Hold Time at 1.0 mA Discharge Grafoil with SW Inside

E. POLAR VS NON POLAR DIELECTRIC DISCUSSION

The selected polar dielectric was deionized water and the non-polar was mineral oil. The premise for super dielectric materials is that they are able to reduce the overall electromagnetic field between two plates. This allows for an overall reduction of the forces brought upon storing a charge and allowing for more electrons to gather on an electrode. One test of the theory is to explore the difference in the impact of polar and non-polar liquids on measured capacitive behavior. That is, according to the theory non-polar liquids will have no effect on observed behavior, whereas polar liquids, because they will create fields oppositely polarized to the fields created by charges on the electrodes, will "cancel field" at all points in space. This will lead to a significant increase in capacitance, dielectric constant, energy density, power density.

The use of mineral oil, which has no dipoles, as a dielectric is predicted to have no impact, similar to air on capacitance. This recorded results are in alignment with the theory and match those taken with only air in-between.

Table 4. Polar vs. Non Polar Discharge Time and Energy Storage.

	Discharge Time (s)	Energy Stored (J)
Polar Inside DI In Ti 10V 0.1mA	41.1471	0.0021759
Polar Outside DI Out Ti 10V 0.1mA	1.02446	0.0001203
Non-Polar Inside	No measurable time	~ 0
Non-Polar Outside	No measurable time	~ 0

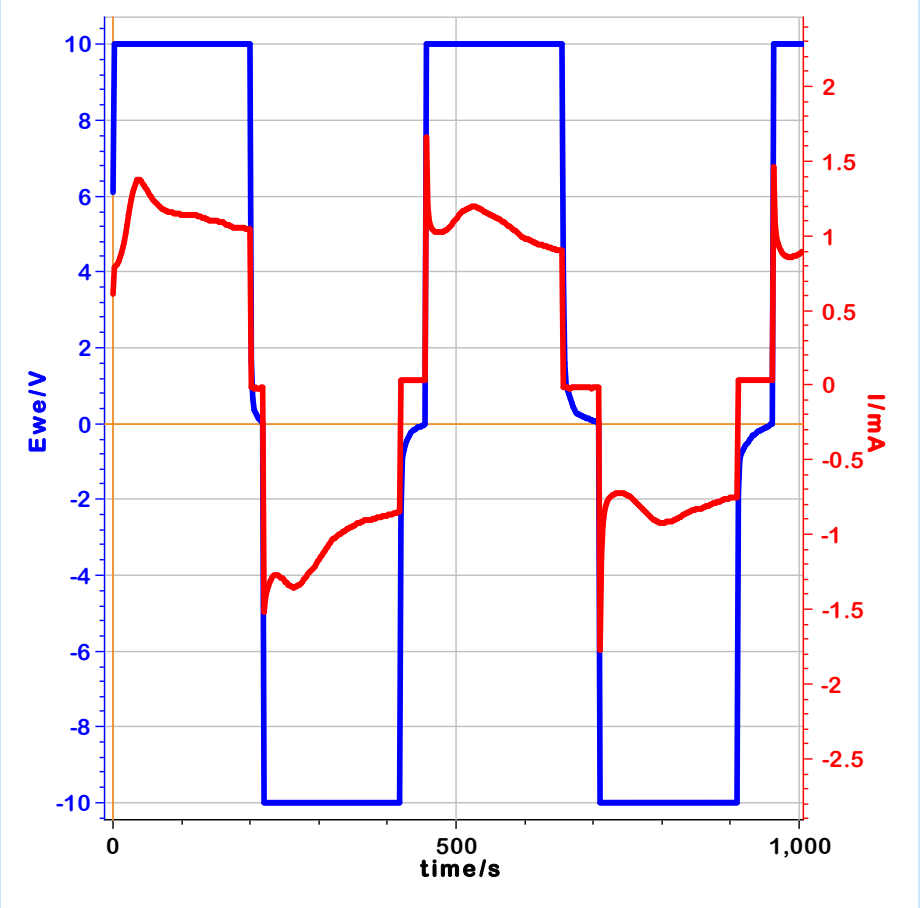

Polar discharge example: measurable discharge times and current readings

Figure 11. Polar Discharge Example

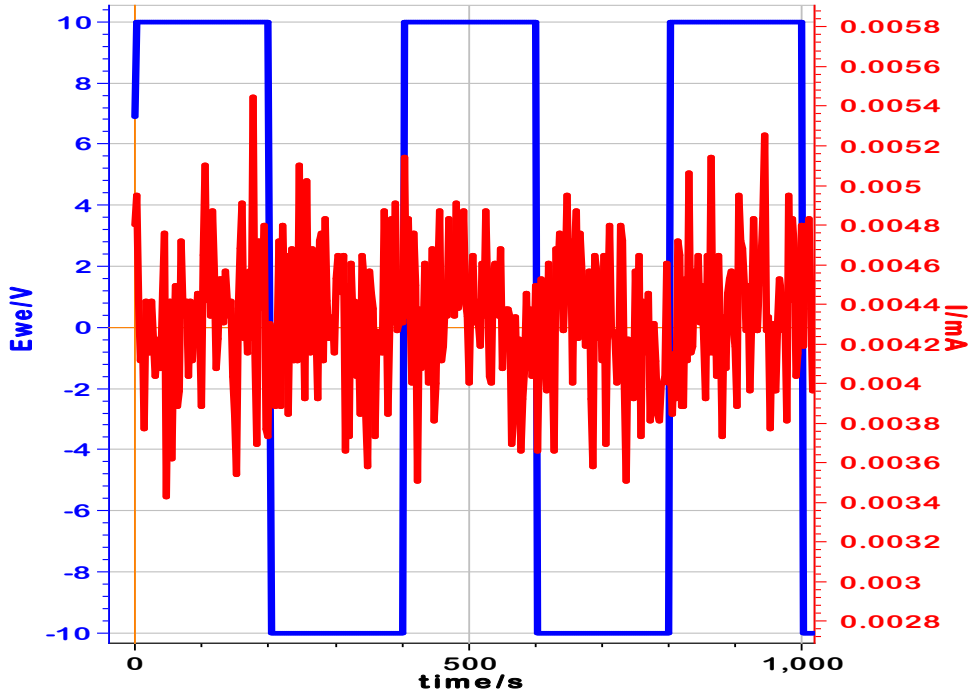

Non-polar- No measurable discharge times or currents, within the noise of the system setup

Figure 12. Non-Polar Example Discharge

The non-polar solution would record similar to air, where the internal noise of the system would dominate the program. The readings were negligible compared to an internal polar dielectric or external where measurable values were received.

F. POLAR VS POLAR IONIC

Two liquids with polar characteristics were tested; Deionized water (DI) and the DI with 3.5% dissolved NaCl by weight ("Salt Water" (SW)). Comparing DI water to Salt water there is a remarkable difference. Based on the SDM theory the alignment of the polarities will reduce the internal field between the place. Based on an addition of free ions this increased the internal field and increases the charge storage on each plate. Even though the salt water inside was only raised to 1.5 V instead of 10 V the energy stored in the ionic solution held much more energy.

Table 5. 200 s Hold Grafoil Polar Ionic (SW) vs. Polar (DI)

Discharge Current (mA)	SW IN Energy (J)	DI IN Energy (J)
0.025	0.040649231	0.006197751
0.025	0.043085704	0.004634019
0.1	0.052646395	0.000276487
0.1	0.049393794	0.000208469
0.25	0.05775418	2.70104E-07
0.25	0.05028029	6.44758E-08

The addition of ions into the solution allows for a greater energy storage. This was first noted with a dramatic increase in the required amperage to reach desired voltages as well as dramatic increases in discharge times.

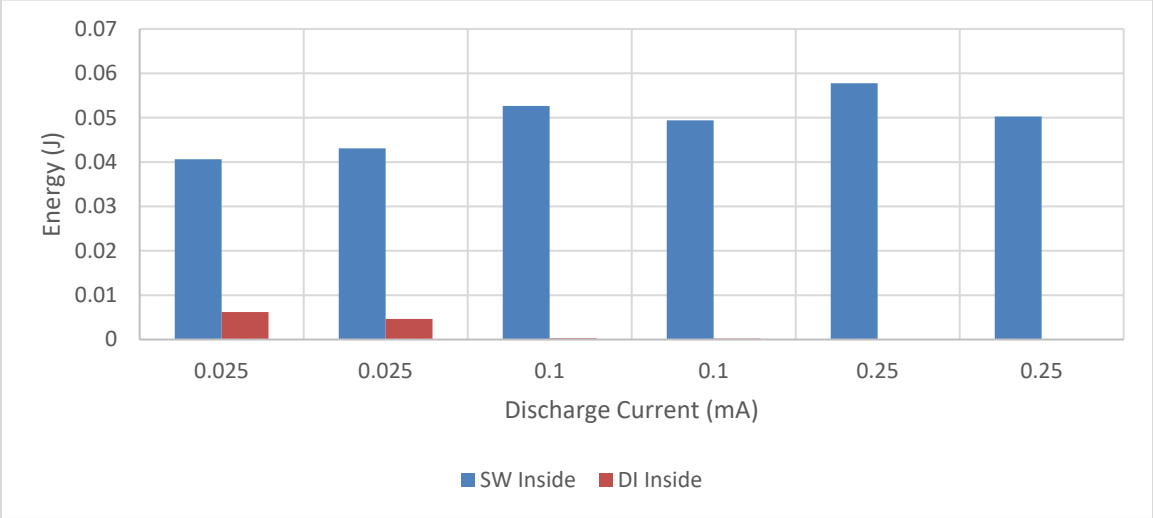

Figure 13. 200 s Hold Time Grafoil with SW vs. DI Water Comparison Energy vs. Discharge Current

G. DISCHARGE DISCUSSION

The discharge portion can be broken into two major sections. The first being a dramatic drop. The second being a gradual near linear decay down to zero. These two stages are different for the electrode materials and dielectric.

To discuss the case of Thick Ti with DI water inside there is a dramatic drop from 10 volts down to approx. 1.5 volts. Then it begins its near linear decent down to zero. This drop from 10 to 1.5 took approx. 8 seconds. This was similar for all tested currents. This was also repeatable for different hold time, a combination of electrode and dielectric had repeatable results. The discharge pattern was similar.

Comparing two separate hold times the discharge curves had very similar profiles with the exception where a longer hold time correlated to a greater discharge time. This corresponds to an increased energy storage.

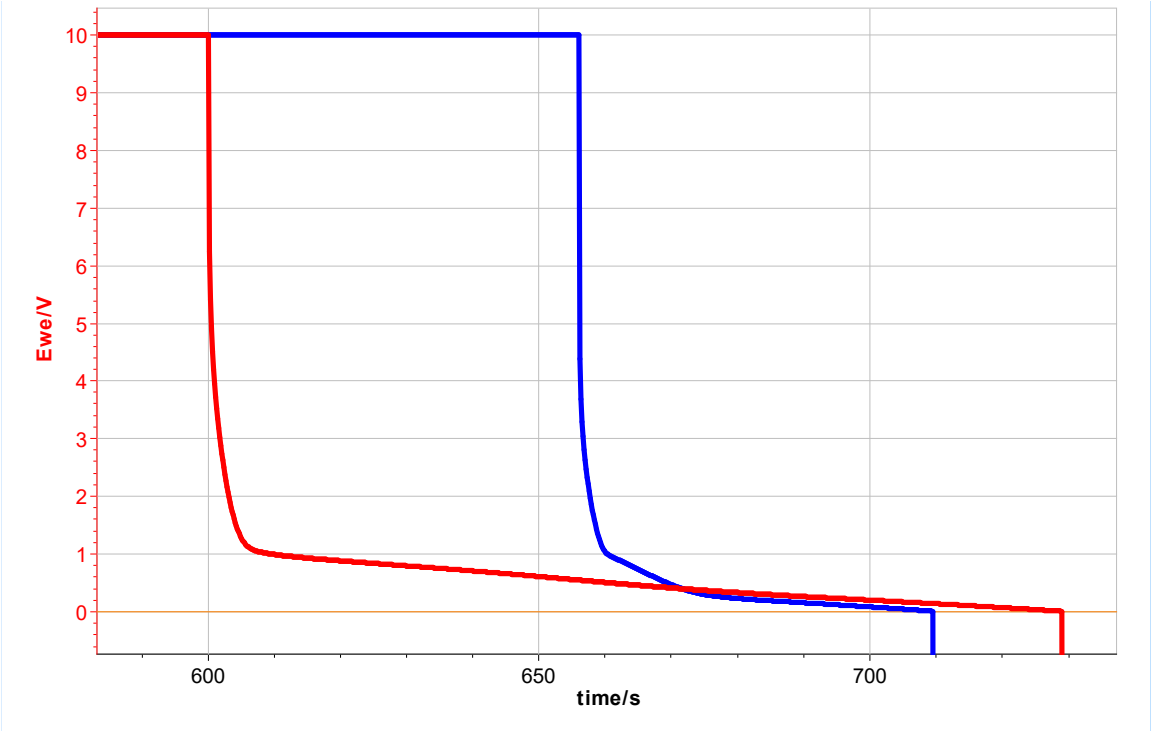

200s hold time (Blue) vs 600 hold time (Red): Similar discharge profiles, however the increased hold time give a longer discharge time.

Figure 14. DI and Titanium 200 vs. 600 s Hold Time

DI water and salt water operated extremely differently. The addition of salt with the same hold time dramatically increased the discharge times. Making them much longer.

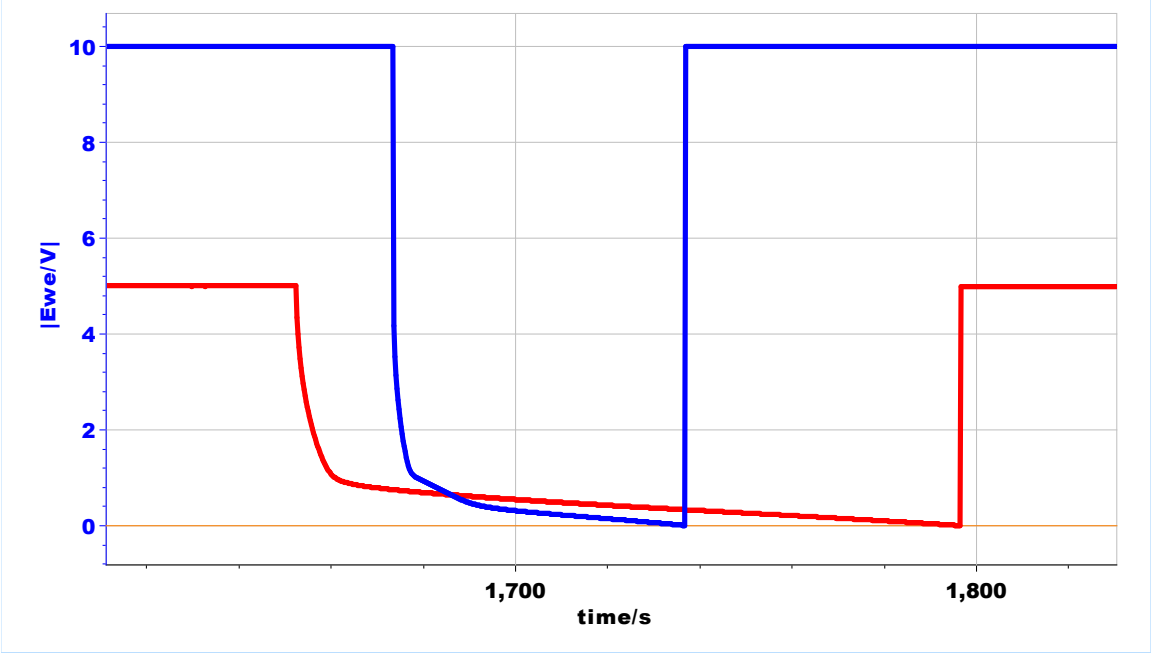

Blue- DI discharge cycle after 200 s from 10 V to 0 V. Red- SW discharge cycle after 200 s hold from 5 V to 0.

Figure 15. DI Water vs. SW Discharge Example

Lead electrodes dropped dramatically down from 10 V to approx. 0.1 V and then showed a linear discharge slope from approx. 0.025 V and below.

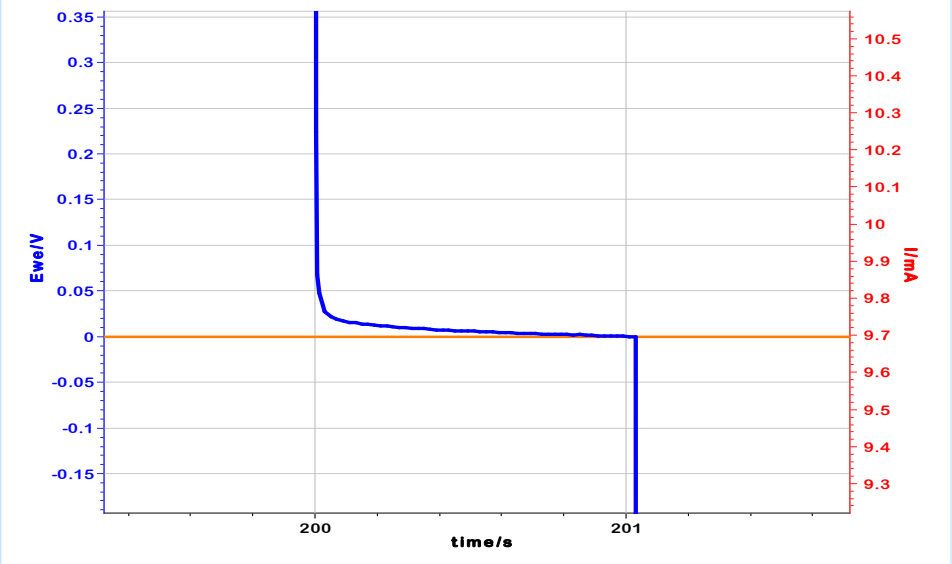

Figure 16. Lead Discharge Example

The location of the plateau seems to be a characteristic of the material electrode or the dielectric but not the initial voltage. Based on the inside or outside configuration there is the same drop from initial charge voltage to the plateau and then begins its linear descent. The linear portion seems to be a function of the discharge current.

Table 6. Material Discharge Current Plateau

Material	Dielectric	IN/Out	Discharge Current	Initial Voltage	Major drop change Plateau Voltage
TI	DI	IN	0.025 - 0.1	10	1.2-.07
TI	DI	OUT	0.025 - 0.1	10	~.45-0
TI	SW	IN	0.025 - 0.1	5	1.2-.7
TI	SW	OUT	0.025 - 0.1	5	1.4-1.1
Grafoil	DI	IN	0.025 - 0.1	10	1.7-1.1
Grafoil	DI	OUT	0.025 - 0.1	10	2.0-0.5
Grafoil	SW	IN	0.025 - 0.25	1.5	0.85-.8
Grafoil	SW	OUT	0.025 - 0.1	1.5	0.9-0.85
Silver	DI	IN	0.025	10	1.5-.07
Silver	DI	IN	0.025	10	Not Tested
Lead	DI	IN	0.025	5	0.04-0.02
Lead	DI	OUT	0.025	5	0.1-0.02
CNT	DI	IN	0.025 - 0.25	5	1-.016
CNT	DI	OUT	0.025	5	~0
CNT	SW	IN	0.25-1	1.5	1.4-1.3
CNT	SW	OUT	0.25-1	1.5	1.5-1.3

H. ELECTRODE THICKNESS DISCUSSION

As shown in Figures 17 and 18 the data for different Ti thicknesses virtually overlaps for discharge times greater than 10 seconds. Shorter “pulse” data, discharge less than 10 seconds, suggests there may be a very limited advantage to thin Ti electrodes for rapid discharge. This is not clear as the apparent difference may be an artifact. Indeed, the absolute energy densities are at the “low end” of the detectable range of the galvanostat in this range. Further investigation is required.

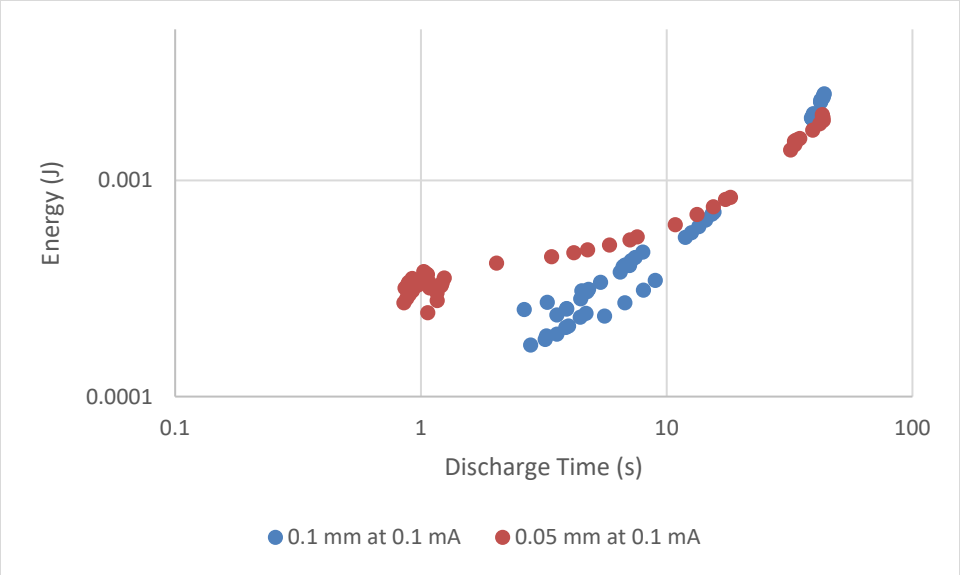

Figure 17. Ti Thickness Comparison (0.1 mm vs. 0.05 mm) Energy Storage vs. Discharge Time at 0.1 mA Discharge

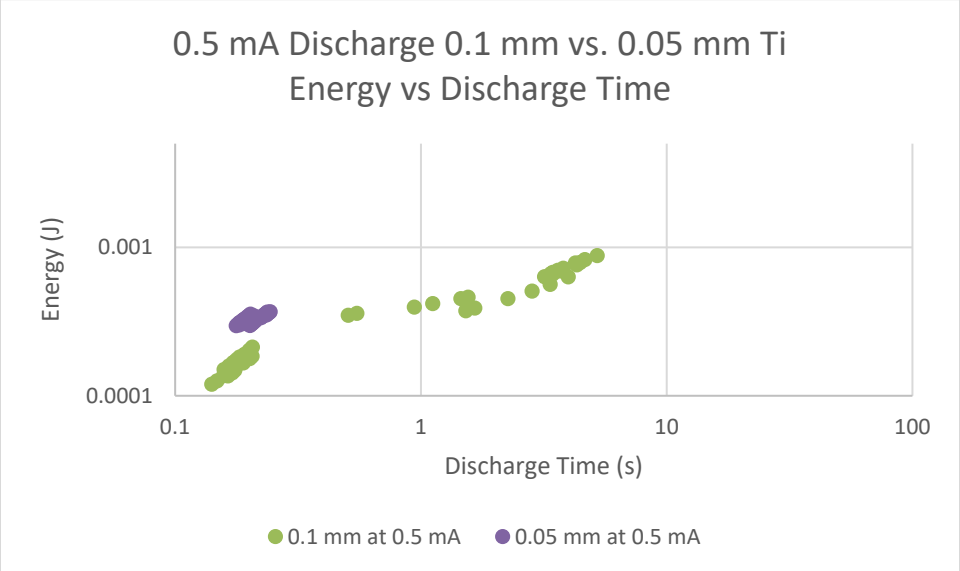

Figure 18. Ti Thickness Comparison (0.1 mm vs. 0.05 mm) Energy Storage vs. Discharge Time at 0.5 mA Discharge

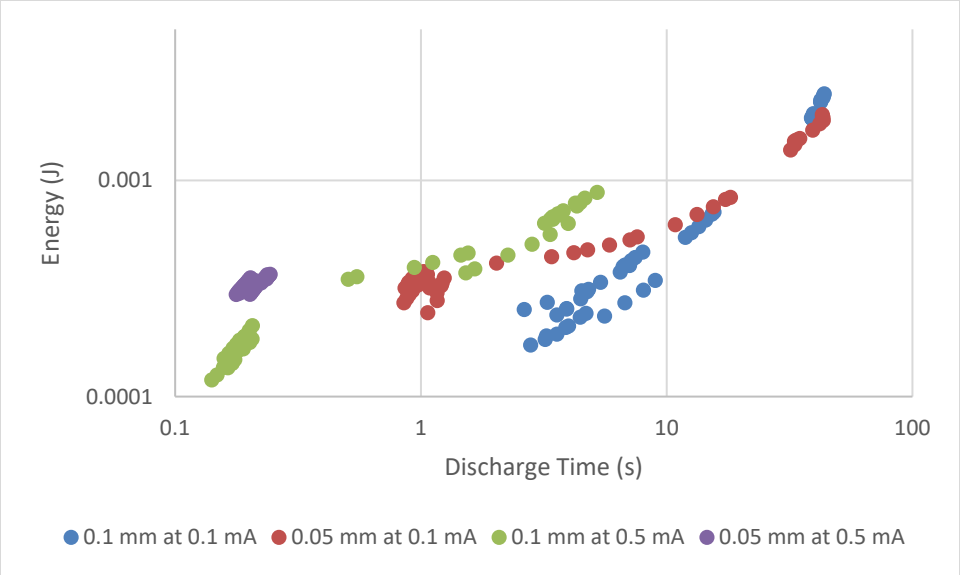

Figure 19. Ti Thickness Comparison (0.1 mm vs. 0.05 mm) Energy Storage vs. Discharge Time at 0.1 mA and 0.5 mA

I. IMPACT OF INSIDE VS OUTSIDE DI VS SW AND TI

The location of the dielectric has an impact on the performance of the capacitor. If the dielectric is polar (DI) (Figure 21), the inside energy storage is much greater than the outside. If the dielectric is polar and ionic (SW) (Figure 22), the energy storage inside is greater than that outside. Both polar and polar ionic store energy, both inside or outside.

A direct comparison would be Ti-DI inside 600 s hold time gives a 150 second discharge at 0.025 ma while Ti-DI outside 600 s hold time gives a 1–5 seconds discharge. Ti-SW inside 200 s hold gives a 150~500 second discharge at 0.025 ma. TI-SW outside 200 s hold gives a 100 second discharge. SW inside gave a much more comparable energy storage to SW outside compared to DI inside vs DI outside.

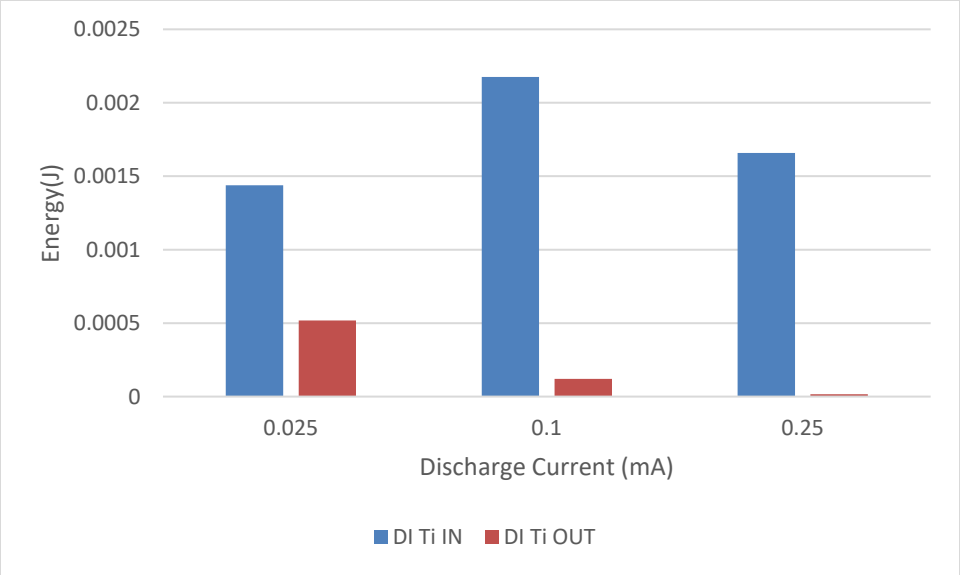

The dielectric performance in the dielectric outside configuration is inferior to the DI dielectric in the inside configuration.

Figure 20. Energy Storage Inside vs. Outside Comparison Ti Electrode and DI Dielectric

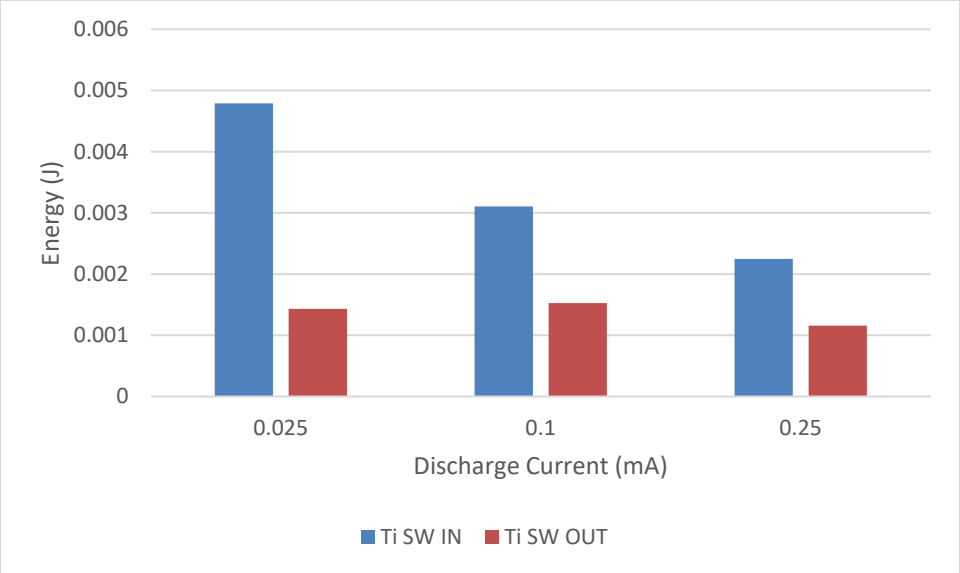

The performance of SW is a function of configuration, always superior in the inside configuration, however, the difference is relatively modest.

Figure 21. Energy Storage Inside vs. Outside Ti Electrode and SW Dielectric

J. IMPACT OF INSIDE VS. OUTSIDE SW AND GRAFOIL

The location of the dielectric does make a difference. The salt water dielectric inside configuration did show a slightly greater energy storage than outside. The major takeaway from this comparison though is that there is similar performance either with the dielectric located inside or outside for ionic solutions. SW Inside configuration is also superior to the SW outside configuration, but the difference as a function of configuration is less significant than that observed using DI as the dielectric. Further discussion in detail is discussed in Chapter III.

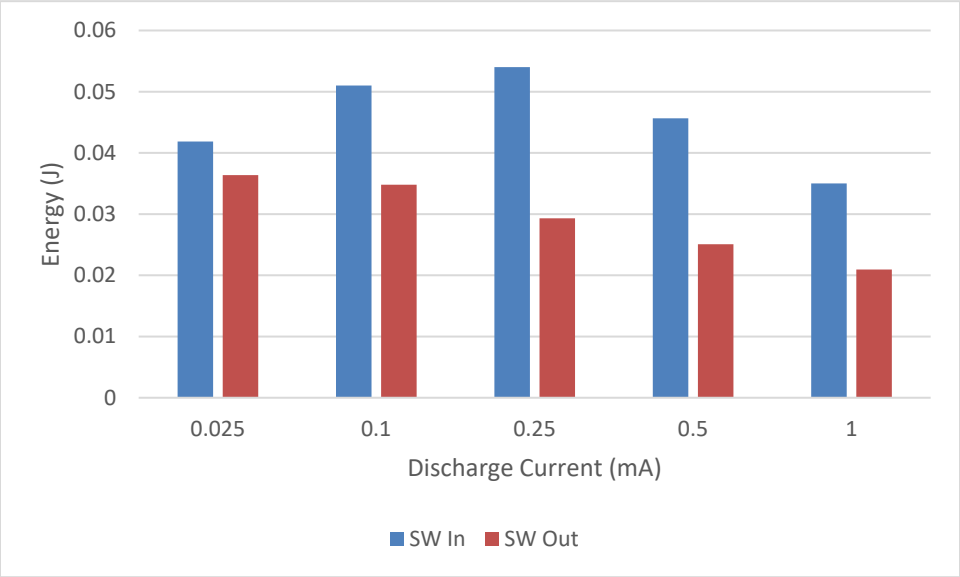

Figure 22. 200 s Hold Time Grafoil SW Inside and Grafoil SW Outside, Energy vs. Discharge Current

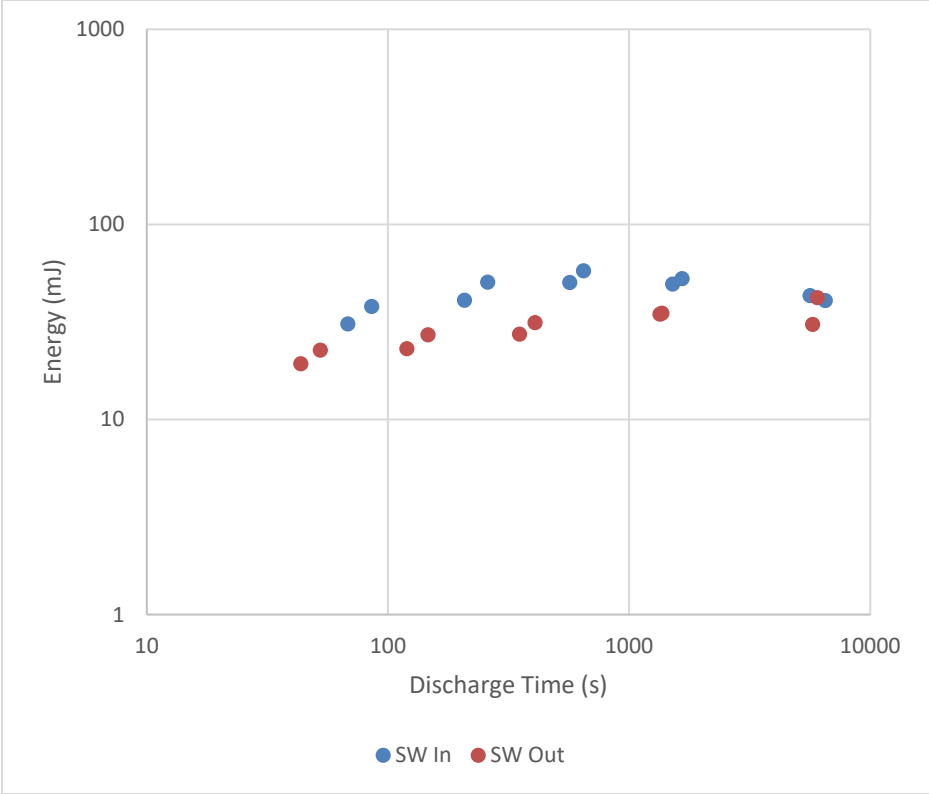

Figure 23. Grafoil 200 s Hold Time Energy vs. Discharge Time Comparison SW Inside vs. Outside

For SW, the energy density is always higher for the dielectric inside configuration. In particular, as shown in (Figure 21), for all discharge currents this is always true. However; it is also true that the energy density for the two configurations, given identical charge and discharge parameters, is always within a factor of two. On a log-log plot it is clear that the difference is not greatly significant (Figure 23).

K. DI VS. SW AND TI VS. GRAFOIL COMPARISON

There is a clear difference in net energy storage as a function of the identity of the electrodes and dielectric. Comparing four configurations the tested samples demonstrated SW in Grafoil is the best, then SW Ti second and then DI Ti followed by DI Grafoil. Comparing the four configurations a clear separation is determined and visible in the energy storage vs. discharge time comparison.

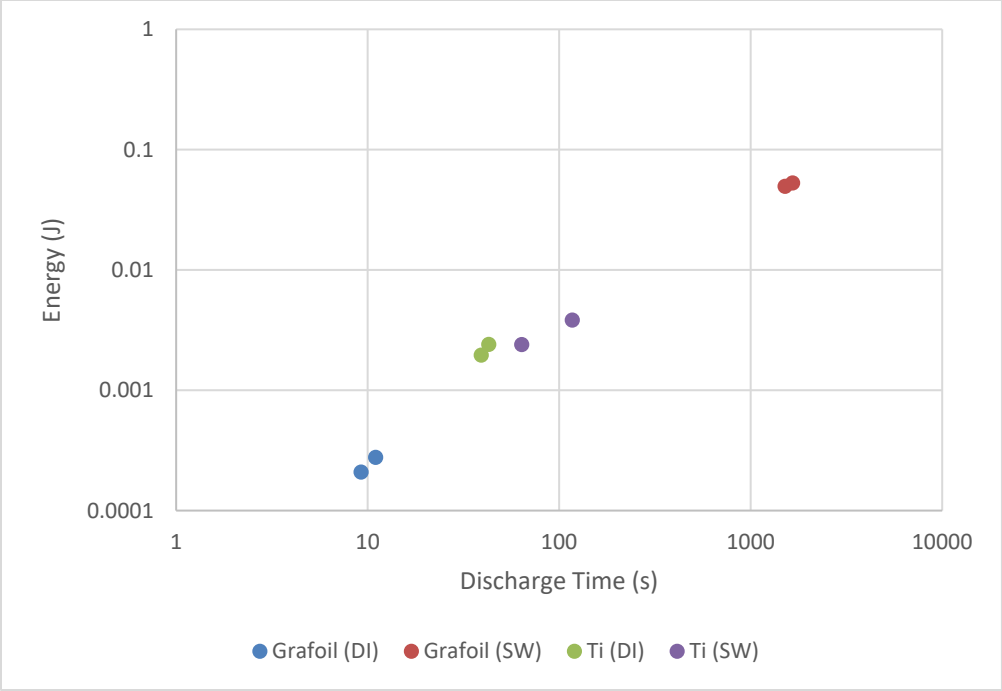

Figure 24. Grafoil and Ti Comparison SW and DI Dielectric, Energy vs. Discharge Time at 0.1 mA Discharge Rate

L. TITANIUM PLATE OXIDATION

Based on the oxidation layer of the plate a measurable difference in performance can occur. Running the "same" experiment with two rigs set up identically. The "same" rig comprised of different freshly cut electrodes from the same parent sheet of titanium metal. Results could vary by as much as a factor of 10. This level of difference deserves further investigation. The experiment shows the comparison of the four total plates. Rig 1 Sheet A and B and Rig 2 Sheet A and B. The greatest difference was between Rig 1 and 2. After testing, the rigs were disassembled and a clear difference in color between Rig 1's sheets and Rig 2's sheets was visible. The coloration of a plate is an indication of different oxidation layer thickness [10]. That is the coloration of the sheet is an indication of the degree of oxidative aging and has an impact on performance.

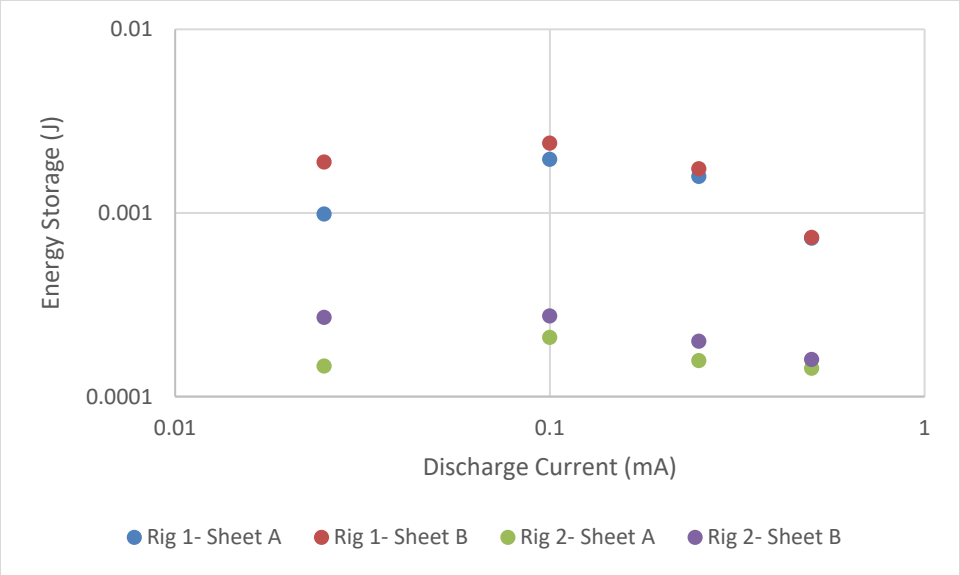

Same configuration, four different results

Figure 25. Ti and DI Inside Energy Storage vs. Discharge Current

M. DIFFERENT ELECTRODE DISCUSSION DISCHARGE TIMES

Different electrode materials gave significantly different results. Of the several materials tested, carbon based materials performed the best.

Table 7. Voltage vs. Discharge Time Comparison

Initial Voltage	Dielectric	Electrode Material	Approximate Discharge Time (s) At (~0.025 mA)	Approximate Discharge Time (s) At (~0.25 mA)
5	DI	Lead	0-1.2	
10	DI	Ti Thin	3-5	
5	DI	Ti Thick	4-10	
10	DI	Ti Thick	10-50	
10	DI	Silver	120	
10	DI	Grafoil	200-300	0-3
5	SW	Ti Thick	200-500	20-40
1.5	DI	CNT Sheet	700+	1-25
1.5	SW	Grafoil	5500-6500	550-650
1.5	SW	CNT Sheet		500-700

N. MATERIALS AGING

1. Titanium

Titanium clearly ages. After cycling (+/- 10 Volts) for approximately 48 hours in either DI or SW a surface oxide layer is evident to the naked eye in the form of color change. The color is an indication of thickness [10]. The two observed colors seen during testing were an orange color hue and a blue color hue. The color changes were also found to vary as a function of position. In particular, the greatest color changes appear to occur around the edges of the gasket interaction as seen in Figures 26 to 28. Localization of the oxide layer thickness is evidence of crevice corrosion.

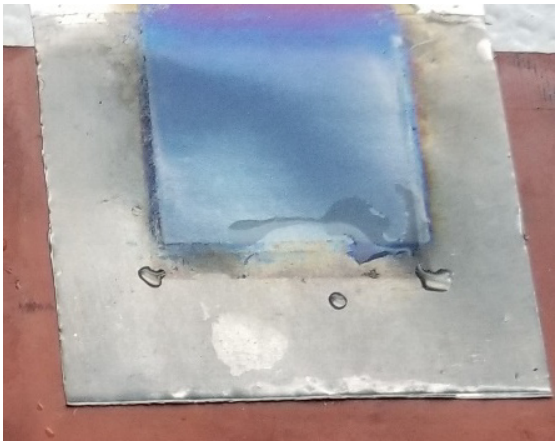

Note the deepest color change is evident at the top of the electrode. Ti 0.05 mm thick after approx. 6+ hours of testing with DI water.

Figure 26. Ti Blue Oxide Layer

Note the deepest color change is evident at the bottom of the electrode. Ti 0.05 mm thick after approx. 6+ hours of testing with DI water.

Figure 27. Ti Orange Oxide Layer

Note the deepest color change is evident at the bottom of the electrode. Ti 0.1 mm thick after approx. 6+ hours of testing with DI water.

Figure 28. Localized Oxidation, Higher Near Bottom Edge

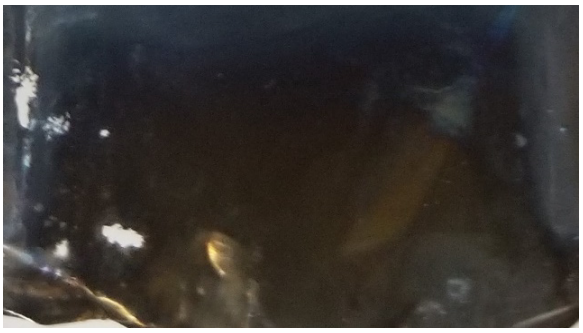

Figure 29. Complete Failure of Ti Sheet with Small Pitting and Holes

2. Silver

Silver was chosen as a potential substitute for titanium because is a good conductive metal, and like all noble metals more resistant to corrosion than base metals and copper. During testing with silver and DI water at 10 volts it was deemed unviable for continued testing. During the first testing a breakdown of silver formed a floating surface layer seen in (Figure 30).

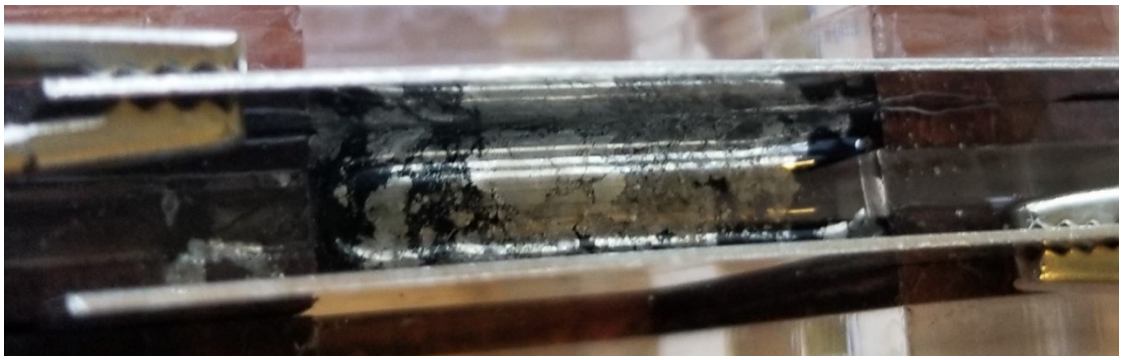

Figure 30. Floating Silver Film

During initial testing (Figure 31), the capacitor went through its initial charge and discharge cycles but failed to reach the return voltage of 10 V. This test was then manually continued and an increased amperage was needed to reach 10 V.

The first cycle created a naked-eye-visible black surface layer, typical of silver oxide. Some of this black material clearly “entered” the liquid material (Figure 30). As the

number of cycles increased the oxide layer appeared to create a low resistance path through the liquid, requiring ever higher currents to reach any given voltage difference between the electrodes (Figure 31).

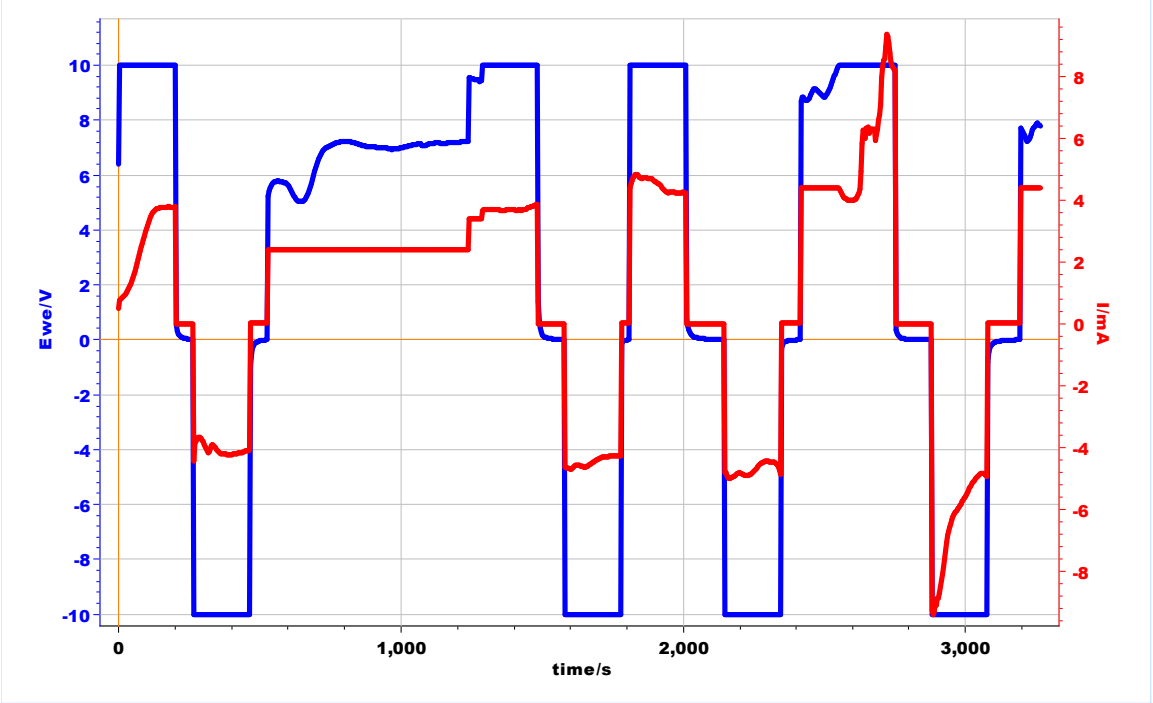

Figure 31. Silver Cycle Example

The test was stopped and the rig was disassembled and the surface cleaned with a paper towel and then reassembled and continued.

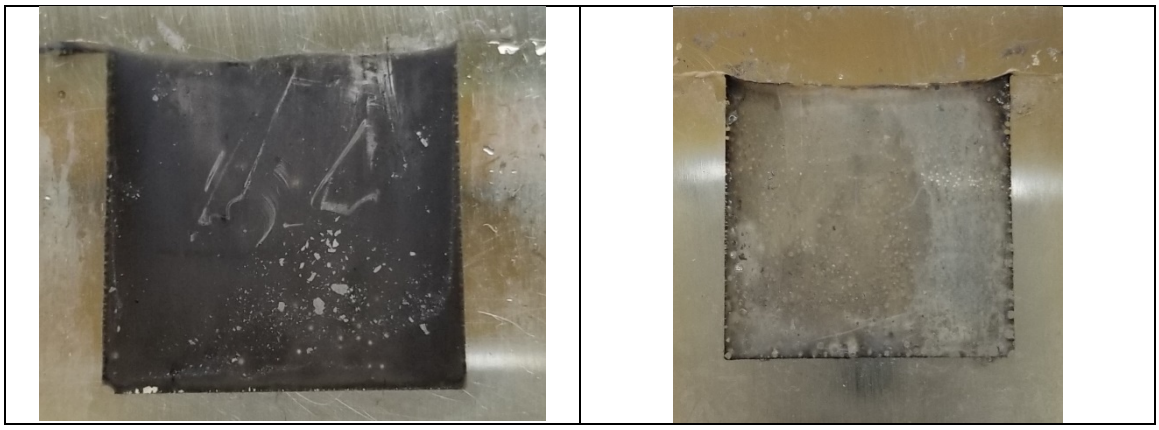

Figure 32. Silver Plate Oxidized and Cleaned.

The same electrodes were used for second test. The corroded electrodes were wiped clean after the first test to remove most of the top layer of oxide growth. Also, the water was replaced with clean/new DI water. Below, performance is discussed in terms of discharge time at the same current in all cases, 0.025 mA.

Performance in terms of discharge times at 0.025 mA provides a quantitative indicator relating the status of the oxide on the electrode surface and/or in the liquid phase. In the first test discharge times started at 30–60 seconds and then increased to a maximum, before complete breakdown, of approximately 120 seconds, before the leakage current became extremely high. During the tests of the "cleaned" electrodes, discharge in all cases took approx. 120 seconds (Figure 34). Yet, again, after a five cycles, the current required to charge the capacitor, just like the failure noted in the test of the fresh silver electrode, was indicative of a "leaky" dielectric (Figure 33). It was clear that a new silver oxide layer formed and that some of that oxide material entered the liquid dielectric, dramatically reducing the resistance of the liquid phase. The capacitor at that point was "very leaky"/ "failed." The test was stopped after six cycles as it was determined silver is not a viable electrode material.

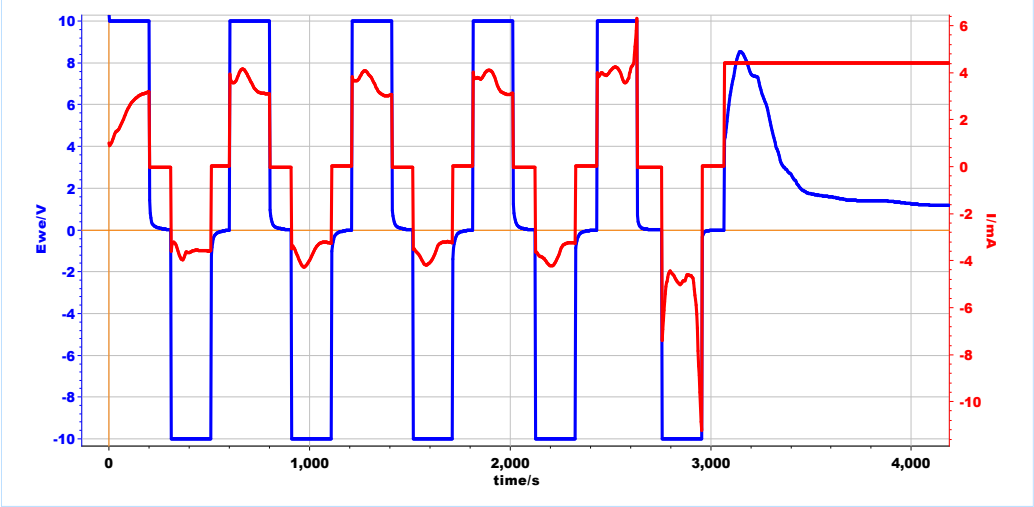

Figure 33. Silver Failure Example

The internal solution was collected and examined. XRD data indicated a combination of silver and silver oxide (Appendix, Part D).

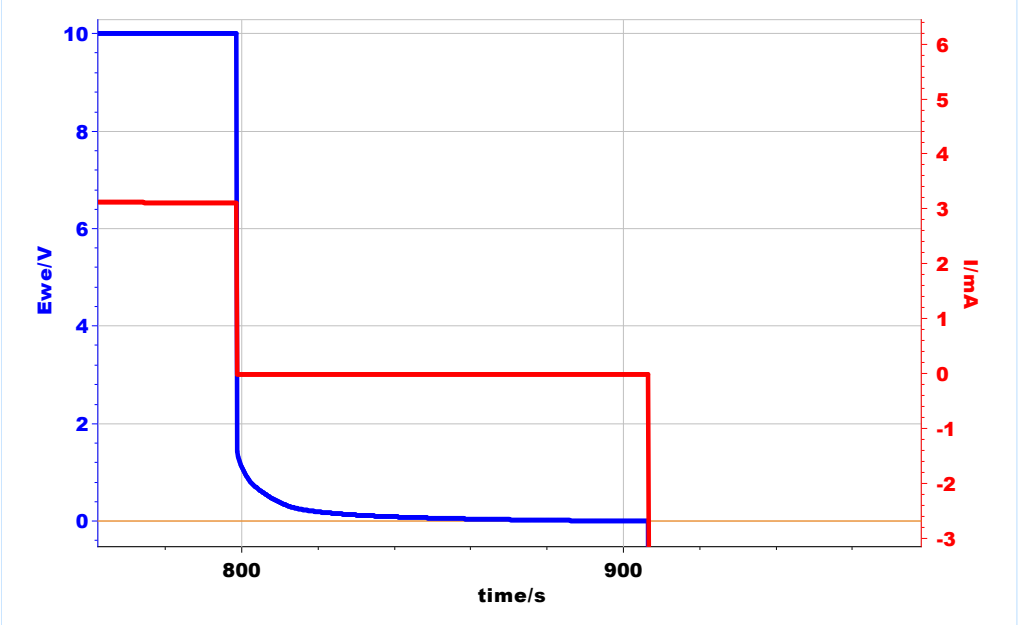

A typical discharge is shown in Figure 34 for the second test, first five cycles. The voltage discharge starts from 10 V and drops dramatically to approx. 1.5 volts, then there is a more extreme decay until it reaches approx. 0.5 volts and then shows linear behavior. This is not like that observed for titanium electrodes.

Figure 34. Silver Discharge Example

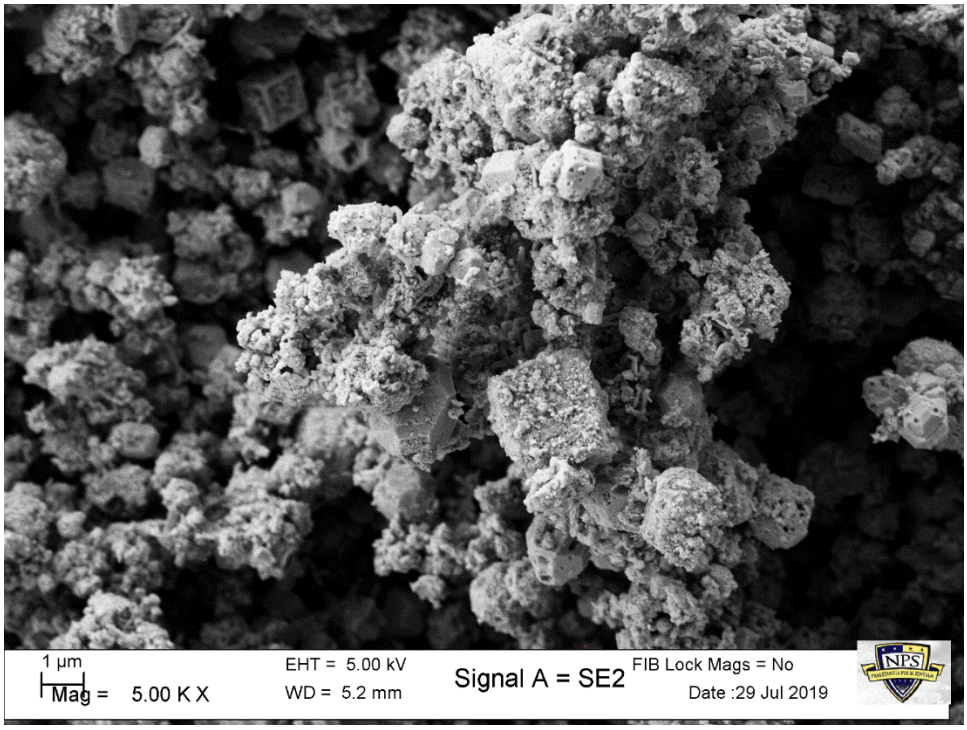

Figure 35. SEM IMAGE of Silver Oxide Particulates 5,000x Magnification

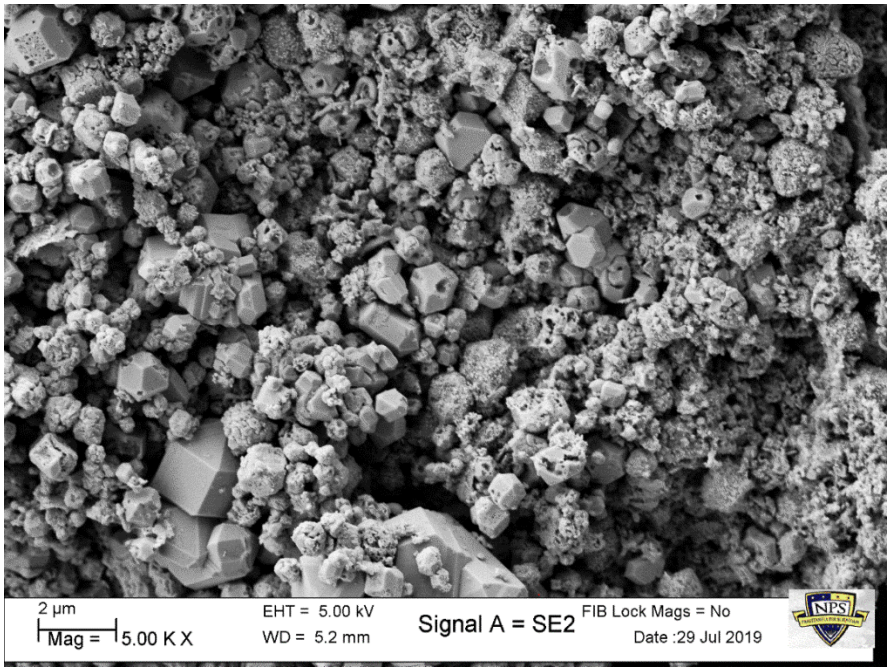

Figure 36. SEM Image of Silver Oxide Particulates 5,000x Magnification

3. Lead

Aging of the lead gave an increased discharge time but also required an increased amperage to maintain 5 volts. The first cycle charged to 5 volts with a maximum amperage of 1.5 mA while the last cycle was peaked at 2.4 mA. As the cycles continued there was increased performance as seen in (Figure 38) by an increased discharge time.

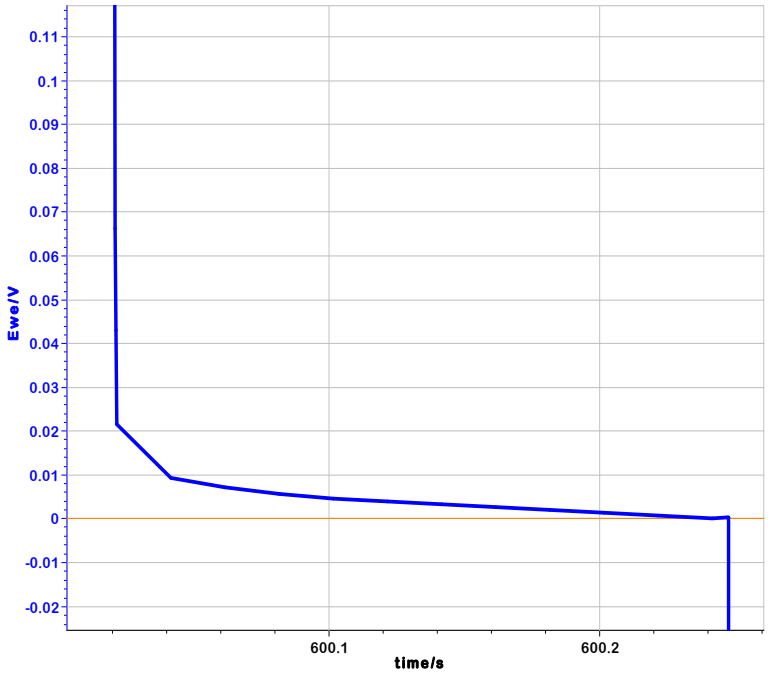

Figure 37. Lead Discharge at 600 Seconds

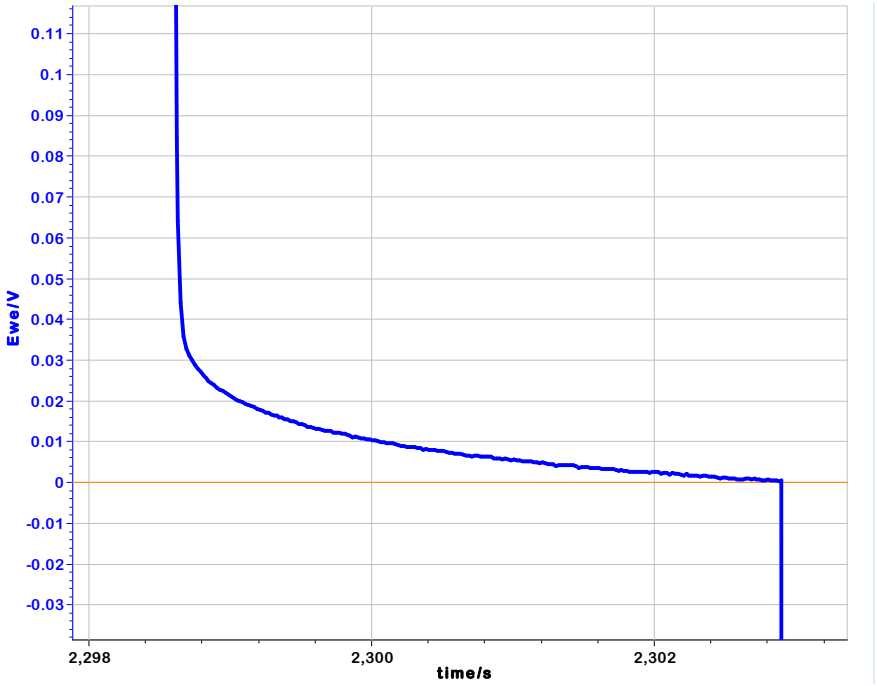

Figure 38. Lead Discharge at 2300 Seconds

During the first cycle with lead, the material was generating a surface oxide layer. As this layer grew and became more homogenous, the amperage needed to reach its desired voltage increased as well.

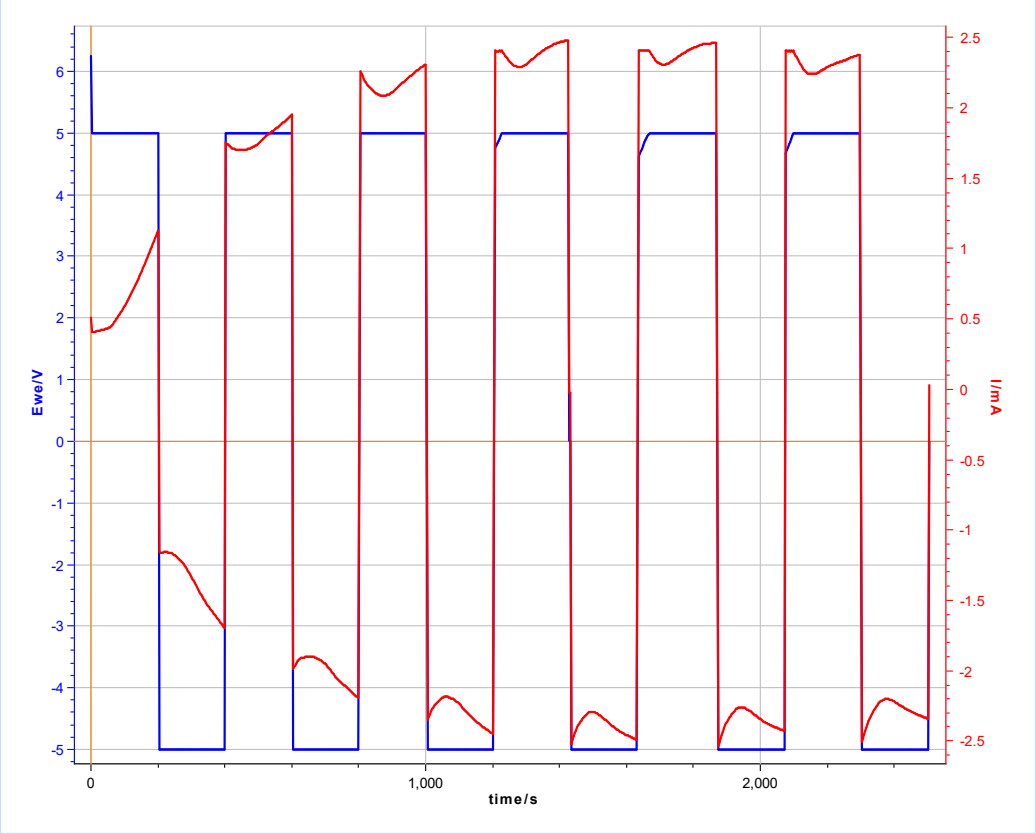

Figure 39. Amperage Cycle Demonstration

Lead outside showed a similar result as the internal. But it occurred much faster. The sample only made three cycles before not being able to reach the desired voltage with a max amperage of 2.4 mA. This aging characteristic still need much more investigation based on increased performance with the aging. The result of the aging, is increased current needed to reach the same desired voltage. But this also seems to give an increased discharge time.

The steady discharge linear portion seems to begin similar to the inside 5 volts while the inside configuration showed a 0.1 volts. The discharge times increased as the number of cycles continued. The first discharges were in the range of 1 second while the later discharges were 4–7 seconds.

Table 8. Comparison of Plate A and B

Time	Plate	Discharge Current
7.39859981309559	A	0.02-0.03 mA
15.3953996110795	A	0.02-0.03 mA
1.03059997396480	B	0.02-0.03 mA
7.73119980469346	B	0.02-0.03 mA

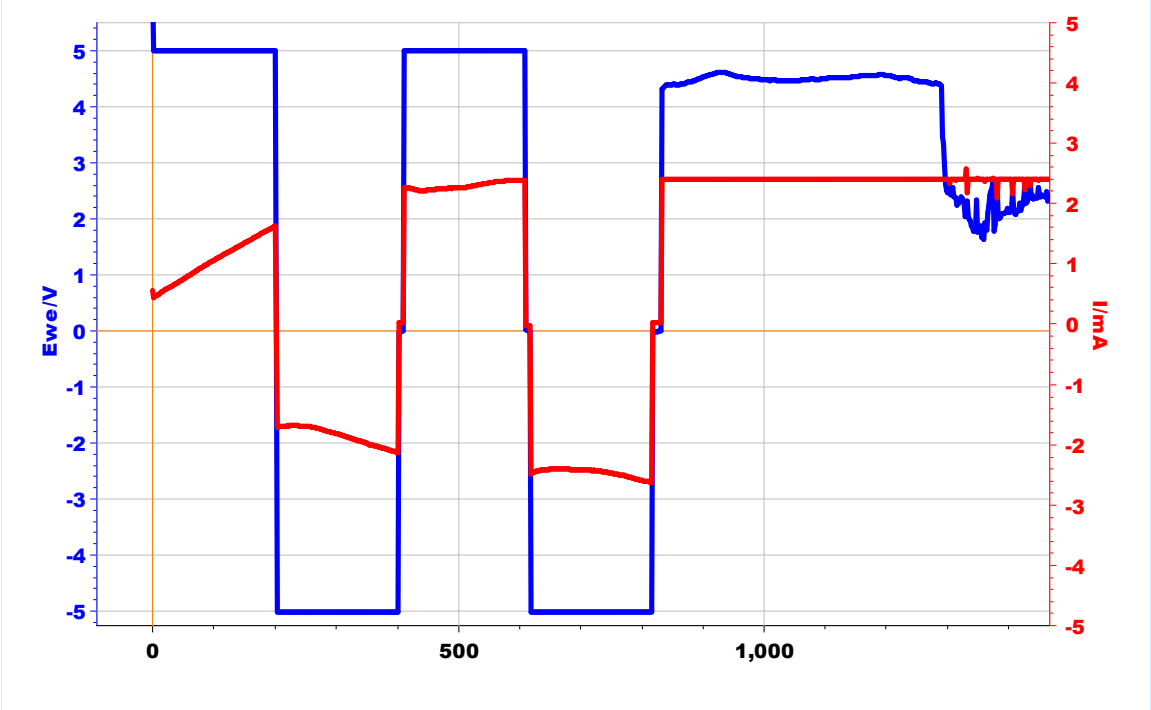

Figure 40. Lead DI Outside Failure after Two Cycles

The particle decomposition formed a breakdown into the water. This solution was deemed to be lead oxide. Under high magnification this oxide looks to be planar and film like, thin and even transparent in some cases.

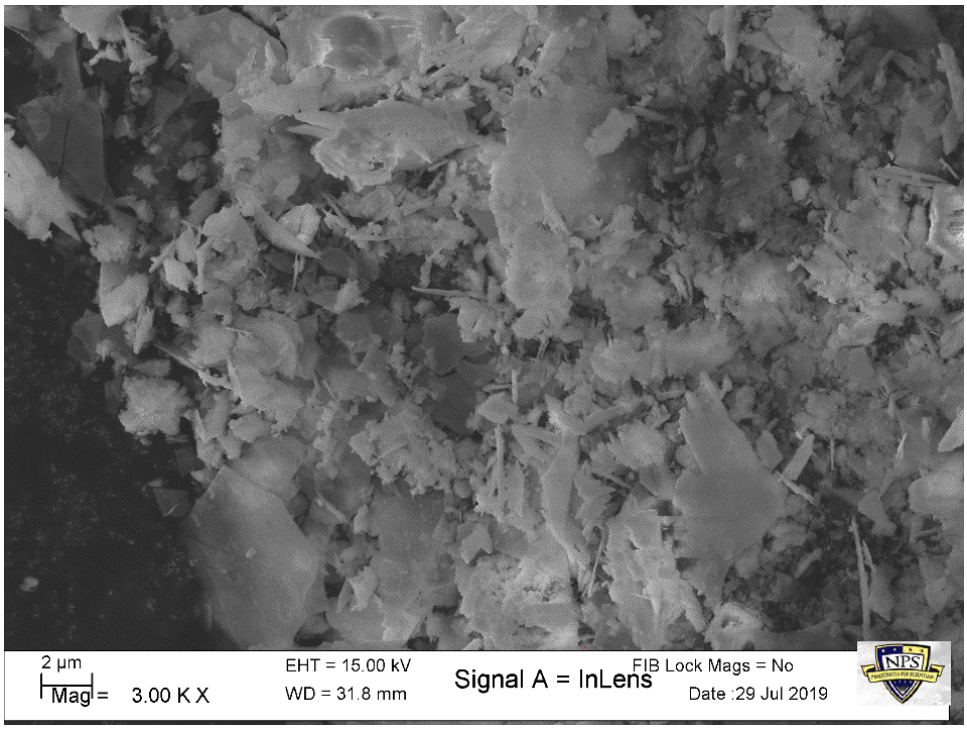

Figure 41. SEM Lead Oxide 3,000x Magnification

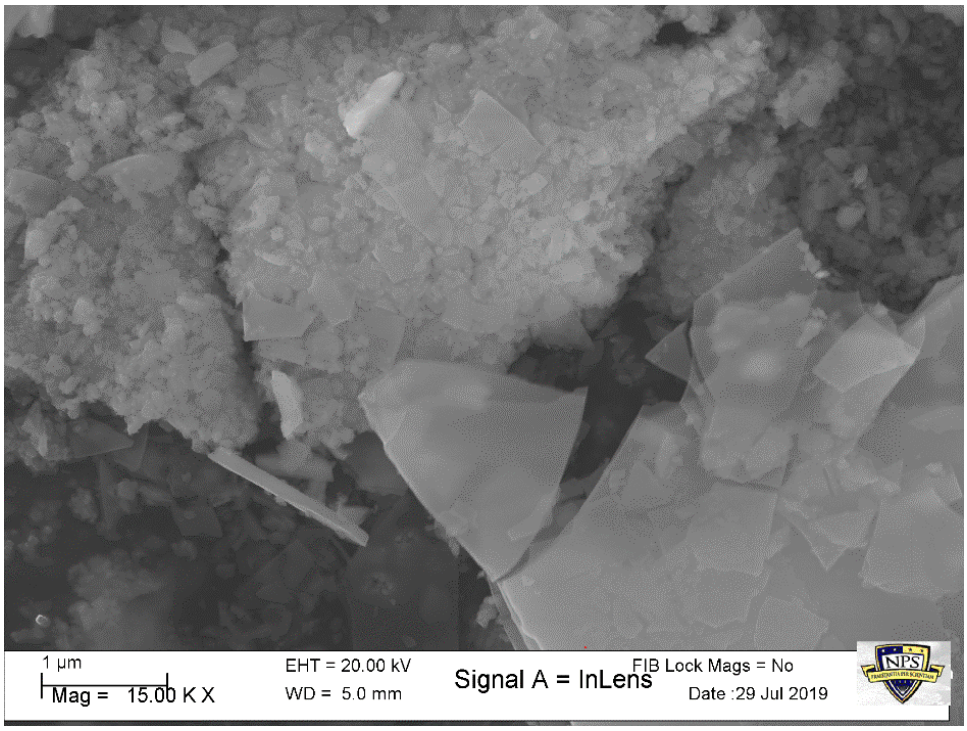

Figure 42. SEM Lead Oxide 15,000x Magnification

4. Grafoil

Grafoil electrodes faced two observable changes. The first was a “swelling” of the electrode. The exposed area showed a visual increase in size as if it became saturated. This was confirmed as well during the SW experiments of salt crystal formation on areas that were not exposed to the SW solution indicating saturation and transport of the NaCl. The second change with Grafoil was observed as complete delamination. The material after operating at higher voltages and increased cycles would eventually delaminate and show thin flake layers.

Figure 43. Grafoil Saturated and Swollen

Figure 44. Grafoil Delaminated

During initial trail testing with the electrodes, this was placed in high NaCl bath and charged at extremely high currents to verify the transition of pH observations. These sample testing produced delamination which were viewed in the SEM had small whisker nucleation of carbon on NaCl particles. An interesting side effect of these whiskers was there susceptibility to being broken with the electron beam.

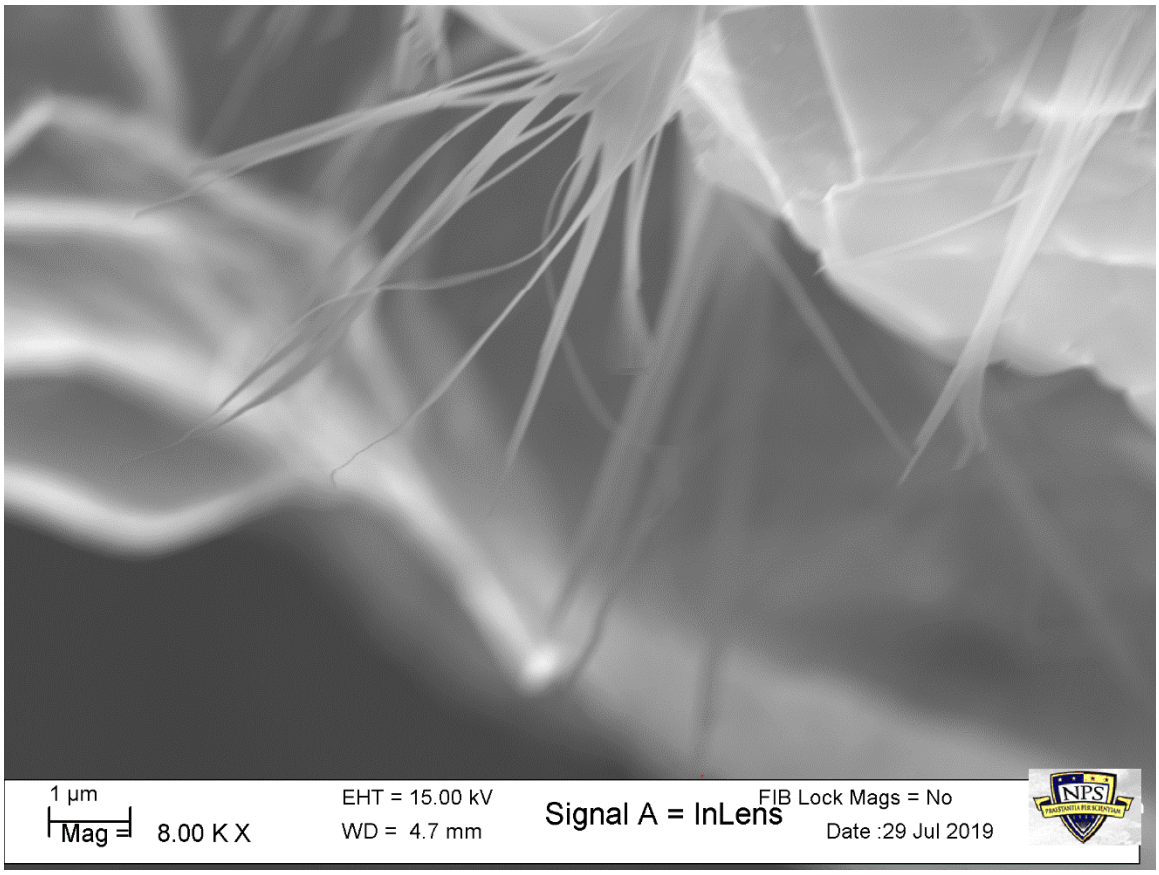

Figure 45. SEM Image of Grafoil Byproduct

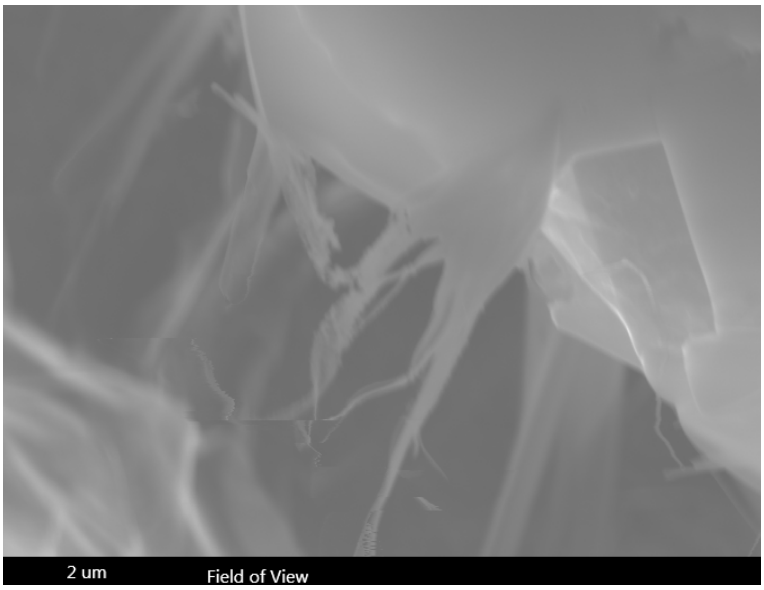

Figure 46. Image After Whisker was Broken with Electron Beam

5. Carbon Nanotube (CNT) Sheet

CNT sheet was a very good electrode material. The material itself did face some breakdown which was observed by a wicking characteristic. Where the galvanostat leads were placed was originally dry and as the number of cycles increased, the sheet seemed to become saturated and wicking caused slight corrosion on the electrical leads.

When testing was conducted with DI water, the inside showed significant and measureable reads. There was an increase in energy storage from 0.025 mA to 0.1 mA and then a decrease again above 0.25 mA discharges. This was a characteristic for 1.5 and 5 V charges. When testing was conducted with DI Outside, there was no measure readings. For SW there was measurable readings on the inside and outside. The SW configuration was tests at 0.25 – 1 mA discharges and showed increased performance on the outside rather than inside. However, the inside showing continued increased energy storage for all tested parameters.

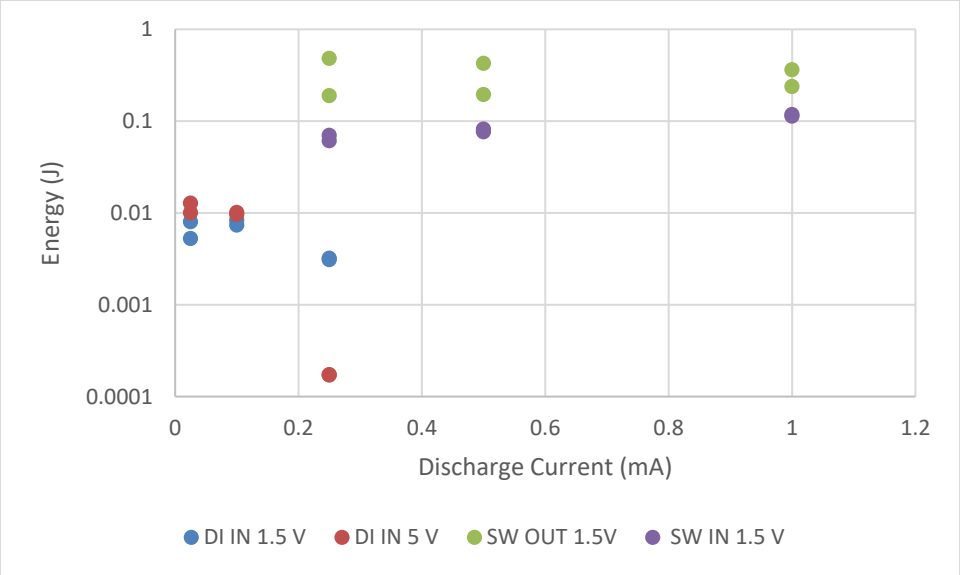

Figure 47. CNT Sheet DI vs. SW Comparison Energy vs. Discharge Current

6. Electrolysis of Dielectric/pH Changes for Dielectric

Electrolysis occurred when operating at voltages above the breakdown voltage (>1.5 V) and was observed by bubbling on the surface of the electrode. This was typically neglected based on the magnitude scales of currents. The energy storage and measured discharge times gave discernable separations. The increase of pH of the dielectric mostly gave increased performance based on increased polarity of the solution. Operating at lower voltages gave more reliable and repeatable results with less electrolysis.

In the case of silver DI water showed a pH increased from a neutral 6.5 to 7 to over 8.5. This continual increase in pH of the dielectric can attributed to an increase discharge times for the first tests. As the initial pH started at 7 and the finals at 9+ a greater polar dielectric would demonstrate increased performance.

Figure 48. pH Change from Before to After Silver and DI water.

The electrolysis mostly occurred with the DI water. The addition of NaCl salt to the dielectric increased the amperages which was required to bring the electrodes to a desired voltage and made higher voltages a place for further research. The SW test were conducted mostly at lower voltages 1.5 V instead of 10 V which did not show changes in the pH of the dielectric.

O. CIRCUIT DISCUSSION

These SDM capacitors do follow traditional capacitor circuity trends. The capacitance measured for Ti with DI inside was tested in series and parallel.

1. Parallel

The parallel testing consisted of two rigs set up in parallel. The overall set up was charged to 10 V and then discharged. The measure capacitance followed the expected trend of the addition of each capacitance and as expected like with Equation 8. Complete the calculations shows results very similar and in the correct order of magnitude.

Table 9. Capacitance Parallel Data 10 V

Discharge Current (mA)	10V Rig 1 Alone Capacitance (mF)	10 V Rig 2 Alone Capacitance (mF)	Parallel Calculation Capacitance (mF)	Parallel Measured Capacitance (mF)
0.025	0.891362	0.260035	1.151396	1.678561
0.025	1.207207	0.378263	1.58547	2.483555

2. Series

The series testing consisted of two rigs set up in series. The overall set up was charged to 10 volts and then discharged. The measured capacitance follows the trend of lower overall capacitance for two capacitors in series. The setup of charging the entire configuration to 10 volts created a voltage divide, creating a total capacitor of two charged to 5 volts. Conducing the calculations in Equation 9 show the results in the appropriate order of magnitude.

Table 10. Capacitance Series 5 V

Discharge Current (mA)	5V Rig 1 Alone Capacitance (mF)	5 Rig 2 Alone Capacitance (mF)	Series Calculation Capacitance (mF)	Series Measure Capacitance (mF)
0.025	0.067194	0.053268	0.029713	0.024245
0.025	0.237747	0.038074	0.032818	0.086601

P. SUMMARY

In summary it is clear that the electrode material strongly impacts performance. In fact, due some electrode materials, in particular lead, and silver are not viable electrode candidates because they age quickly and fail. The tested electrode materials that age slowly, and hence are candidates for long term use, include titanium and carbon in various forms. It must be noted that the "effective" electrodes produce different outcomes. In all cases, carbon based electrodes demonstrated greater energy storage than titanium.

The data presented here permitted a preliminary assessment of the aging and failure mechanism of silver and lead electrodes. In both cases two problems arise. First, an oxide forms on the electrode surface due to the challenging electrochemical environment. Second, in each case some electrically conducting particulate material leaches off the surfaces of these metals, and eventually creates a short between the electrodes. The lifetime of the electrodes is no more than a few hours.

Those materials shown to be effective also suffer forms of aging; however, that aging has limited impact on performance. The only metal shown effective, titanium,

clearly, like lead and silver, develops an oxide layer. This layer, unlike the lead and silver oxide layers, does not bleed particulate material into the liquid phase but does impact performance. No short evolves.

Carbon of two types was shown, one composed of graphite flakes compressed, and the other composed of compressed nanotubes. The energy density of capacitors was somewhat better for the latter. Both were 2 or 3 X more energy dense than titanium at the similar conditions. Both types of electrodes tended to swell with time and gradually leaked fluid.

III. UNDERSTANDING DIELECTRICS: IMPACT OF EXTERNAL SALT WATER BATH

This chapter was previously published as a journal article by A. Roman and J. Phillips (thesis advisor) in *Materials* a MDPI product [1]. Contributions made by Alexander Roman include fabrication and manufacturing of the capacitor rig, experimental procedures, data collection, post processing, and discussion contributions to the result analysis.

A. INTRODUCTION

In this paper a novel experiment was conducted to test further a new theory of dielectrics, the so-called super dielectric material (SDM) theory. The experimental design of this work was intended to provide a contrast between conventional dielectric theory, as presented in physics texts, and SDM theory. That is, the experiments were designed such that the outcome could only be consistent with one of these theories.

The basic arguments of the SDM theory are not widely disseminated, hence there is value in a brief review. To wit: The central hypothesis of the SDM theory is that dielectrics increase capacitance by polarizing opposite to the polarity of charges on the electrodes. This can be understood from a five-part argument [2] - [7]. (1) Dielectric material polarizes in the opposite direction to any field applied to it. This occurs because the positive charge in a dielectric moves toward the negative electrode and negative charge moves toward the positive electrode. (2) Placed between the electrodes of a standard parallel plate capacitor, the dielectric material creates a field opposite in direction to the electric field created by charges on the electrodes, in all space, not just the region between the plates. (3) As the field at any point in space is the vector sum of the fields of all individual charges, the dielectric in a parallel plate capacitor reduces the field, at all points, created by charges on the electrodes. (4) As “voltage,” a state property, is the scaler line integration of the electric field, and the dielectric reduces the field at all points, the dielectric necessarily reduces the “voltage” between any two points, including any path from infinity to an electrode. (5) It follows that as in the presence of a dielectric it takes

more charge on the electrodes to reach a given capacitor voltage, dielectrics increase the electrode charge/voltage ratio. Thus, by definition, dielectrics increase capacitance. There are some inherent predictions of the SDM model. One example is the prediction that the effectiveness of a dielectric is the product of the length of charge separation within it (dipole length), and the density of charges (dipole density). This was tested and found accurate in earlier work [3] , [11] . Other work showed that, as predicted by the model, high dielectric constants would be found for saltwater saturated fabric [12] ,for salt water saturated nano-tubes on the surface of anodized titania [13], for porous solids saturated with various salts [14] , [15], for fumed silica gels containing salt water [16], for water saturated with salts other than NaCl such as KOH and NH_3Cl [17]. Other studies show that both metal and carbon can be used as the electrode material [7] , and for non-aqueous polar fluids such as DMSO containing dissolved salts, etc. Each of the existing SDM studies [3], [2], [7], [11]–[20] adds to the corpus of data supporting the SDM hypothesis.

Another prediction of the model is that any mechanism that reduces the field at all points in space around a capacitor will increase the capacitance. This implies that in a standard parallel plate capacitor dielectric material need not be between the plates in order to impact capacitance. Indeed, dielectric material outside the volume between the electrodes should, under correct circumstances, increase capacitance. Consistent with this prediction of SDM theory, our team recently demonstrated that a parallel plate capacitor with high dielectric material only outside the volume between the plates acts “as if” there is a high dielectric constant material between the plates [7]. As shown in that study, a simple capacitor composed of titanium electrodes and a thin plastic dielectric had, as anticipated, a very low capacitance. Second, the control capacitor, still the same plastic dielectric, was modified on its outside only. Specifically, it was covered on the outside in a continuous thin layer (<1 mm thick) of a particular gel type super dielectric material. This increased measured capacitance by as much as seven orders of magnitude higher than the control below ~1 V. This finding is consistent with SDM theory, and completely contrary to standard theory.

Further experiment is needed to demonstrate the generality of the SDM hypothesis, particularly as it applies to the “dielectric on the outside” prediction. In the present study

simple parallel plate capacitors containing only air in the volume between the titanium foil plates were (1) immersed in air, (2) immersed in distilled deionized water (DI), (3) immersed in deionized water containing 0.5% NaCl (8.5 x 10^{-2} mol/L). The results confirm SDM predictions regarding the efficacy of "dielectric on the outside." That is, contrary to standard theory that immersion in any material cannot impact measured capacitance, it was found, in agreement with the SDM model, that immersion in salt water increased capacitance by more than seven orders of magnitude.

In addition to these experiments, studies of the behavior of (1) DI, and (2) DI containing ~5.0 wt % NaCl the dielectric between the electrodes is presented. The finding that the dielectric constant of DI water is remarkably high, in fact >10^9 in particular circumstances, confirms earlier studies showing pure water, at low frequency, has a remarkably high dielectric value [21], [22]. These results suggest, according to SDM theory, that well organized dipole formation must occur in water exposed to electric fields, and suggest there is value in continuing research on the dielectric behavior of water.

B. EXPERIMENTAL

Two different parallel plate capacitors, with electrodes made of Ti sheets (0.1 mm thick) 3 cm x 3 cm, covering an air gap of dimension 2.5 cm x 2.5 cm were employed. The only difference between the two was the size of the gap between the electrodes: 6 mm in one case and 20 mm in the latter. As shown in Figure 49, the Ti sheets were held between materials known to have low (<100) dielectric constants; rubber layer to grip the titanium sheets, and the gap created by layers of clear Acrylic sheet.

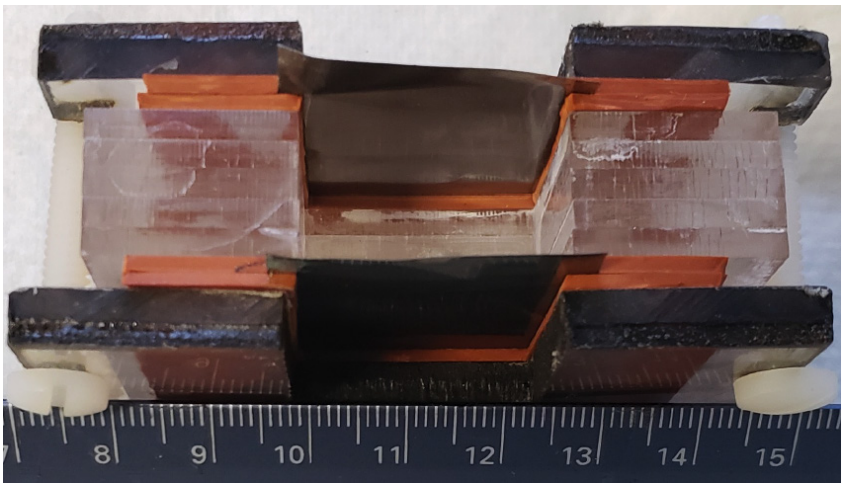

Unlike most modern studies of the dielectric properties that employ micron-scale devices, herein a multi-centimeter device (see ruler) was used.

Figure 49. Figure 1 -Standard 20 mm Capacitor Source: [1].

Several different capacitor configurations were studied. In all cases two different dielectric must be specified; an inner dielectric, that is the dielectric material between the electrodes and an outer dielectric, that is the dielectric material surrounding/outside the volume between the electrodes. The distance between electrodes was also specified below, because capacitors were virtually identical but for the distance between electrodes were studied. Specifically, the behavior observed for a capacitor in which the electrode distance was 20 mm (20 mm capacitor) was contrasted with one for which the electrode separation was 6 mm (6 mm capacitor).

1. Control

In the control cases the capacitor was simply placed on the lab bench in the ambient air (AIR). Both the inner and the outer dielectric were ambient air. There were two controls: One in which the titanium sheet electrode separation was 20 mm and one in which it was 6 mm.

2. Dielectric on Outside

In the “dielectric on the outside” configuration (DOC), the inner dielectric was the same as in the control case; ambient air. The outer dielectric was a super dielectric material,

either DI or DI with dissolved NaCl, generally 0.5% by weight. The bath surrounding the capacitor in all cases was about 500 cm^3. In the DOC configurations ~95% of the electrode surface was covered in liquid. The remainder was in the ambient environment. Two cases were studied: (1) The capacitor was partially submerged in DI water (DI-DOC), or (2) The capacitor was partially submerged in DI water containing dissolved NaCl (S-DOC), that is salt water.

3. Parameter Computation

The fact that the dielectric is on the "outside" leads to a conundrum in terms of computing and labeling parameters. That is, the standard nomenclature requires a volume, and that volume is always assumed to be that of the dielectric "inside" the electrodes. To address this conundrum, the computations were conducted "as if" only the volume between the electrodes is contributing, and the resulting values are called "effective dielectric constant," and "effective energy density".

4. Dielectric on the Inside

In the distilled water-dielectric on the inside configuration (DI-DIC) distilled water was used to fill the space between the electrodes, which is the inner dielectric. The capacitors were placed on the lab bench; hence the outer dielectric was simply ambient air. In essence this is the standard geometry for testing the dielectric properties of a material. In the salt water-dielectric on the inside configuration (S-DIC) salt water, generally DI water containing 0.5 wt % dissolved NaCl, was used to fill the space between the electrodes, hence salt water is the inner dielectric. The capacitors were placed on the lab bench, hence, again, the outer dielectric was simply ambient air.

5. Testing Protocol

All data, dielectric constant, energy, and power density, were computed from the constant current discharge leg of charge/discharge cycles collected using a programmable galvanostat (BioLogic Model SP 300 Galvanostat, Bio-Logic Science Instruments SAS, Claix, France). Notably, the device is regularly tested by using it to measure the marked capacitance of both commercial Supercapacitors and electrostatic capacitors. The

agreement with nominal capacitance is always excellent. The device, in constant current discharge mode, was operated over the voltage range, 0 to 10 V. The rate of electrolysis of water was minimal at these voltages, insignificant bubble formation even after twelve hours of continuous running. Capacitance is defined in constant current to be:

$$C = \frac{I}{(\frac{dV}{dt})} \tag{2}$$

where C is capacitance, I is current, V is voltage, and t is time. Clearly, if capacitance is not a function of voltage, voltage should decline linearly with time. As noted below and elsewhere [2], this is not always the case, particularly at "higher" frequencies.

The constant current method has advantages relative to more commonly employed methods for measuring capacitance. Constant current data is far easier to deconvolute than that obtained with cyclic voltammetry [23] - [24]. The constant current method also provides direct measures of energy and power density. In contrast, impedance spectroscopy [2], [25]–[27] is limited to providing values based on measurements conducted over a very small voltage range, ±15 mV, thus is clearly not able to directly measure energy or power. In impedance spectroscopy a voltage independent capacitance (ideal) also is assumed; although, it is clear from a review of the literature that this is generally only true at a very low frequency [2]. For the capacitors studied in this work, as with most capacitors, the "ideal" behavior was not observed.

Capacitance is generally used to compute dielectric constant (ε) by Equation (2) for a parallel plate capacitor. This is the mathematical expression of the standard theory of dielectrics applied to parallel plate capacitors:

$$\varepsilon = \frac{Ct}{\varepsilon_o A} \tag{4}$$

where t is the thickness of the dielectric layer, A is the area of the electrode, and (ε_0) is the permittivity of free space [28]–[30]. Equation (4), that is the standard theory of dielectrics applied to parallel plate capacitors, is based on the assumption that only the dielectric material between the electrodes contributes to the capacitance. This was clearly

demonstrated to be an incorrect assumption in the present study, and an earlier study by our team [7]. Thus, following the precedent set in earlier work, dielectric constant, energy density, and power density were computed/reported below "as if" the only volume of significance is that between the plates. Energy was computed as the integral of the area under the voltage time data (V x s) multiplied by current (amps), and power was computed as the total energy of the discharge divided by the total discharge time

On the discharge leg, two distinguishable ranges of capacitance as a function of voltage were found. In the first range from 10 V to ~1.2 V the capacitance was relatively low and not a subject of significant inquiry in this study. The capacitance and dielectric values reported were only reported based on data for the discharge between ~1.0 and 0 V. Over this range the voltage vs. time relationship was nearly linear in all cases for discharge times greater than ~1 s, indicating constant capacitance over this voltage region [7].

The standard protocol for testing involved three steps. The first step was charging to 10 V, generally at 1.5 mA. The second step was to hold the voltage for a period of time, for example 200 s. All parameters were derived from the third step, discharge of the capacitor from 10 V to 0 V at a constant current. Next, the polarity was reversed in all cases, and a mirror "negative" voltage studied. Thus, the capacitor was charged quickly to -10 V, held at that voltage for the same time as during the positive voltage sequence (e.g., 200 s) and then discharged to zero volts at the same current as the positive voltage discharge step. Generally, the reported values of parameters are the average of four cycles (circa Figure 50). In many cases, after four cycles, the value of the discharge current was changed, and the process repeated with the charge step, voltage, and voltage hold times unchanged. Changing the discharge voltage is the only means to change the discharge period/ "frequency." This permits an approximate analysis of the impact of frequency. Note: This three-step protocol is very similar to that employed to characterize the capacitance of commercial supercapacitors [31] - [32] also previously explored in [7].

C. RESULTS

The experiments were designed to collect capacitance, and "effective" values of dielectric constant, energy, and power density. This data was then employed for several

purposes: (1) To validate the SDM hypothesis. Specifically, dielectric material outside the volume between the electrodes significantly impacts all capacitor performance parameters. (2) To provide a check of earlier studies indicating that distilled water has a remarkably high dielectric value at low frequency (ca. 1 Hz). (3) To determine if these parameters impact capacitor behavior: Maximum charging voltage, hold time, discharge current, salt concentration, and electrode separation distance.

1. Control

The discharge time, given the smallest allowed discharge current, for the galvanostat connectors simply placed just above the bench in ambient conditions and that obtained when the electrodes are connected to the capacitor in the AIR configuration are the same. The charging current shows the same pattern as well. This indicates that the galvanostat is not able to measure discharges that occur more rapidly than 5 $x10^{-4}$ V/s as this is the current an instrument leakage minimum. Thus, the measurements made for this study confirm that the capacitance was extremely low for the AIR configuration, but the measurement method employed was not sufficient to determine the actual capacitance. Assuming the standard dielectric constant for "air," approximately 1, yielded a capacitance of 2 x 10^{-13} Farads (F) for the 20 mm separation capacitor, and 1.9 x 10^{-12} F for the 6 mm separation capacitor. In contrast, the capacitance measured below 1 V for the S-DOC 20 mm capacitor was ~4.5 x 10^{-3} F (discharge current 0.02 mA) and 9 $x10^{-3}$ F for the S-DOC 6 mm capacitor, or more than eight orders of magnitude higher than the AIR configuration in both cases.

2. Raw Data Outside Configuration

In Figure 50 the results for the DI-DOC of the 20 mm capacitor are illustrated with the raw data. The discharge time, on the order of three seconds from 1 V to 0 V, was many orders of magnitude higher than that observed in the control studies (<0.5 ms) of the same capacitor sitting in ambient air.

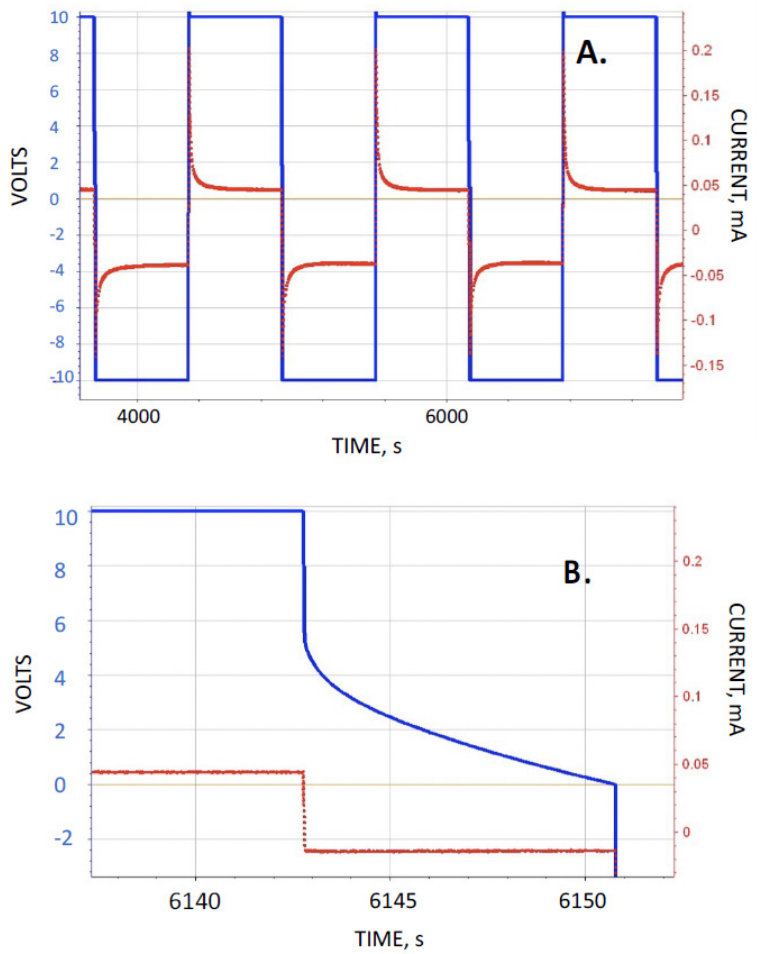

(A) Four positive (10 V to 0 Volts) and three negative (-10 V to 0 V) voltage cycles shown with a 600 s hold time and 0.02 mA discharge current. (B) An expansion of one positive discharge. (Lines: Red current, Blue voltage).

Figure 50. Discharge of DI-DOC for a 20 mm Separation Capacitor Source: [1].

One key result was that the hold time had almost no impact on the discharge time, a result dramatically different from that observed for salt water. That is, the discharge time for a ten second, a two hundred second, and a six hundred second discharge were not distinguishable.

Discharge to about 2 V in all cases took place in less than five seconds, and then in some cases (e.g., long hold times) slowed dramatically. An example of the latter was the impact of hold time. In the discharge to about 2 V in all cases took place in less than five seconds, and then in some cases (e.g., long hold times) slowed dramatically. An example

of the latter was the impact of hold time. In the case of DI-DOC the hold time at 1 s and 600 s was nearly equal, whereas for the S-DOC hold time had a considerable impact. As shown in Figure 51, the S-DOC the discharge time for a hold time of 600 s was 35 X longer than for a hold time of 1 s.

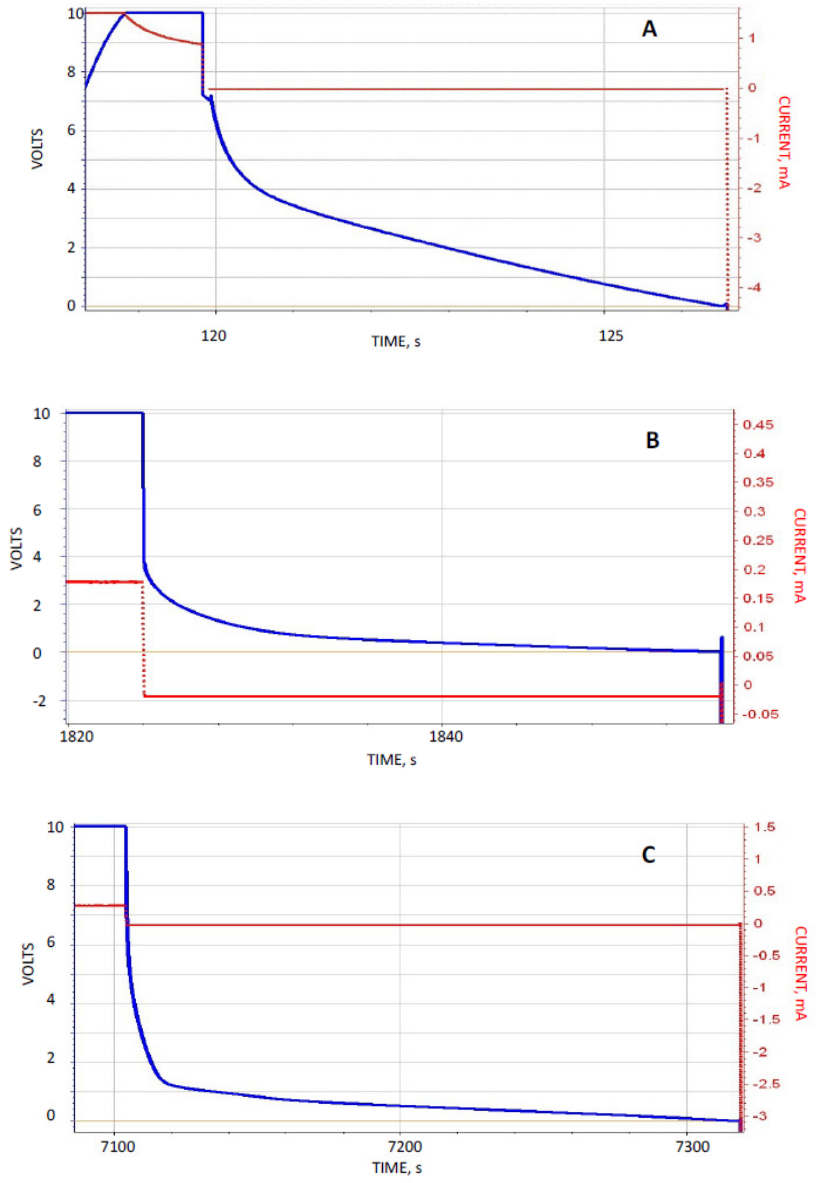

Impact of the hold time for dielectric, 0.5 wt % NaCl in deionized water (DI), only on the outside 20 mm capacitor. (A) Shown: Discharge, current 0.02 mA, 1 s hold at 10 V. (B) Discharge current 0.02 mA, 200 s hold at 10 V. (C) Discharge current 0.02 mA, 600 s hold at 10 V.

Figure 51. Impact of the Hold Time for Dielectric, 0.5 wt % NaCl in Deionized Water (DI), Only on the Outside 20 mm Capacitor Source: [1].

3. Dielectric Values

In Figure 52 the effective dielectric constant below one V (20 mm electrode separation) for three different salt concentration (DI-DOC and S-DOC) of the outer dielectric, with ambient air, all cases, as the inner dielectric. Clearly the S-DOC configurations had higher effective dielectric values than the DI-DOC configuration, but it was also clear that the DI-DOC was displaying effective dielectric values at least five orders of magnitude higher than the classically reported dielectric value for water, ~80 [33]. These high values of the dielectric constant for DI at a low frequency/long discharge period were similar to those reported elsewhere [21], [22] for distilled water.

Figure 52 also indicates that the effective dielectric constant for S-DOC was a function of the dissolved salt concentration. For example, the effective dielectric constant for a 250 s discharge of the 5 wt % NaCl solution was about 7 x larger than for the 0.5 wt % NaCl solution.

Finally, Figure 52 indicates that the dielectric constant for discharge times greater than ~0.5 s were relatively constant, given all other protocol parameters constant. This suggests an effective "saturation" limit, where saturation in this study meant that the number of charges released through the circuit, that is the capacitance, was not impacted by current levels/discharge time. The finding that dielectric values were relatively flat as a function of discharge current, was not consistent with previous studies of SDM [3], [2], [11]–[20] on the "inside." The physical basis for saturation of a dielectric was postulated to relate to full alignment of the dipoles in the dielectric. That is, at a particular voltage all the dipoles in the material were fully aligned, hence further increasing the voltage on the electrodes had no impact on the field generated by the dielectric [2] , [34] hence increasing voltage above the saturation voltage did not increase the amount of charge on the electrodes.

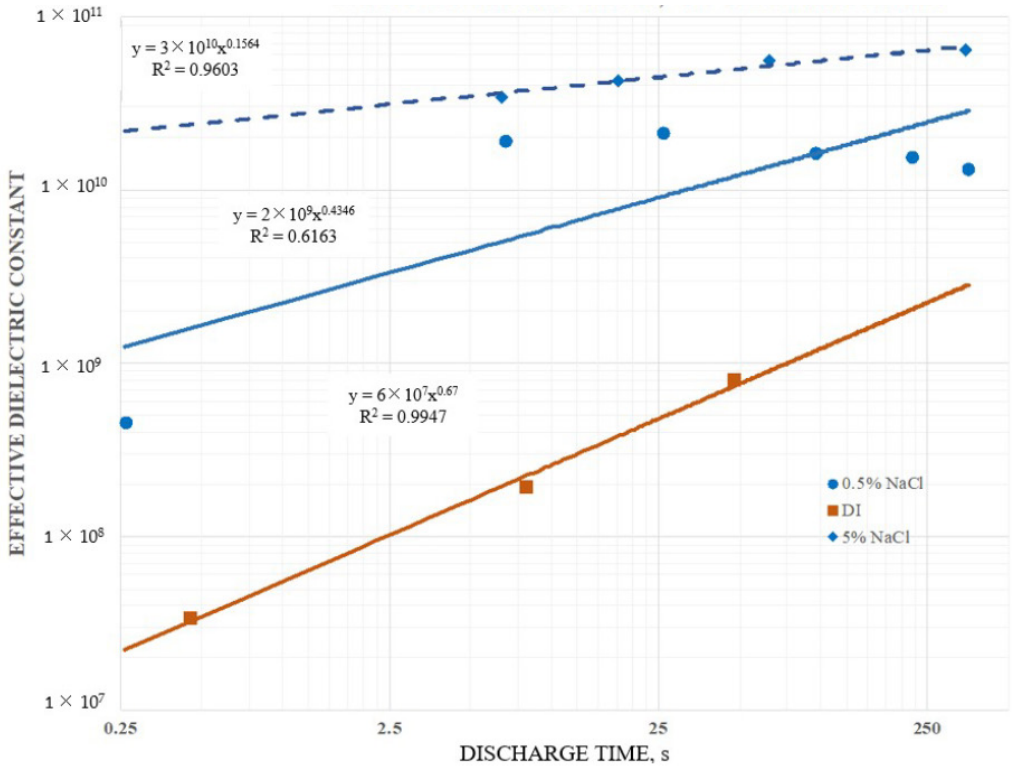

20 mm Capacitor. Based on capacitance below 1 V. As the salt concentration increases, the effective dielectric constant does.

Figure 52. Effective Dielectric Constant as a Function of the Salt Concentration Source: [1].

It was also clear that not all data was reasonably fit with a power law curve. The data for the 0.5 wt % NaCl case was nearly flat above a discharge time of 2.5 s, and clearly fell sharply for faster discharges. This was a "trend," albeit very non-linear. In general, the reader should note that the power law curves fitted the data imperfectly, thus extrapolation of the fit curves did not provide quantitative prediction. Still, the finding of complex "trends" in a few cases did not detract from the primary message of the paper: Immersing a parallel plate capacitor in DI or low salt solution dramatically increased capacitance.

The value of the dielectric constant, remarkably high in all cases, was found to be a function of the electrode separation. Specifically, it was found that the dielectric constant was consistently higher for an electrode separation for 6 mm than it was for a separation of 20 mm (Figure 53). It was also found that the dielectric constant for salt water in the S-

DOC was consistently higher than for the S-DIC configuration both for the 6 mm capacitor (shown) and the 20 mm capacitor.

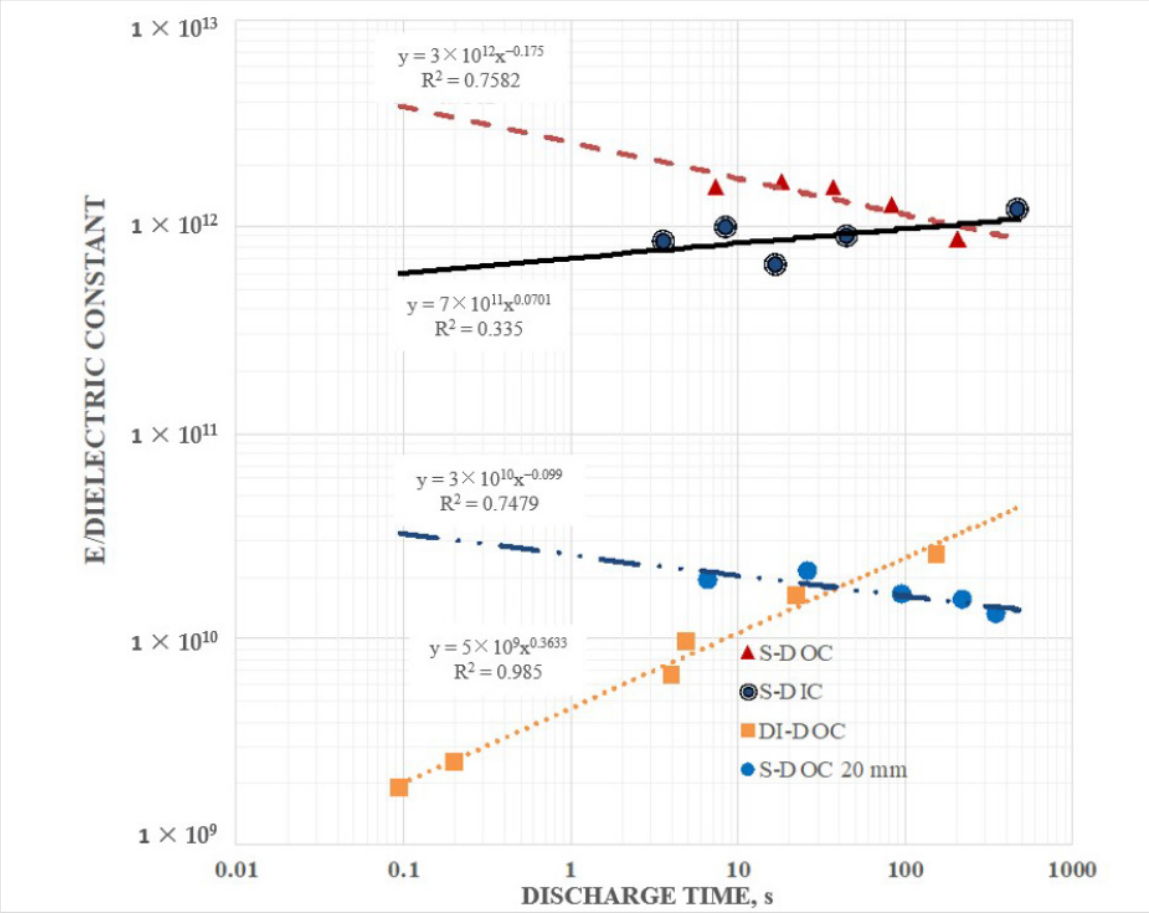

Effective dielectric values below 1 V for the S-DOC and DI-DOC configurations (0.5% NaCl, 10 V charge, 200 s hold) for the 6 mm capacitor. It is notable that the power law fits were imperfect, indicating that extrapolation of the curves was not necessarily valid.

Figure 53. Effective Dielectric Values for a 6 mm Capacitor S-DOC and DI-DOC Source: [1].

4. Energy Density

In Figure 54, quantitative plots of energy density for dielectric "outside" configurations of the 20 mm capacitor at different salt levels are shown. Note that all data was in terms of "effective" values. That is, only the volume between the plates was employed as the volume in computations, yet it was clear that dielectric outside this volume

was dramatically impacting the results. Although it was clear that the energy density of the S-DOC were higher than those of the DI-DOC, the trends suggest that for very slow discharges the energy densities for all salt levels might converge.

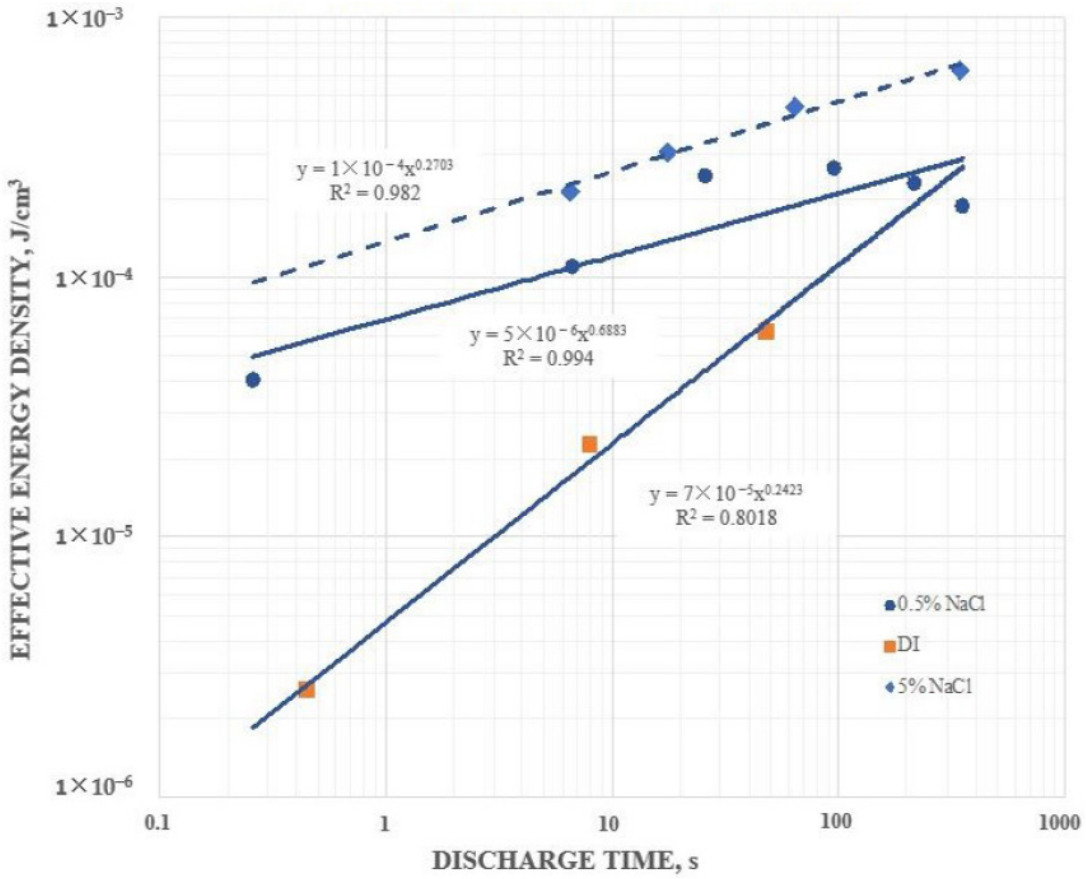

The three curves, based on the full voltage discharge, were obtained with the 20 mm capacitor and were all for a super dielectric outside/ambient air dielectric inside configuration, all based on a program of charging to ±10 V and holding for 200 s at ±10 V.

Figure 54. Effective Energy Density as a Function of the Salt Concentration Source: [1].

Similar broad trends in energy density were found for both the 6 mm and the 20 mm capacitors (Figure 55). Indeed, for the 6 mm capacitor energy density was highest for salt water (0.5 wt % all cases) on the outside (triangles), and in all equivalent cases, only salt concentration modified, the energy density was higher for salt water than for DI. The 6 mm capacitor consistently had higher energy density than the 20mm capacitor in all

equivalent configurations. This result was anticipated as in both the SDM and standard model of parallel plate capacitors energy density was inversely proportional to the electrode distance squared. In this study, the effective dielectric constant for salt water on the outside also increased as the electrode distance was reduced. This is another reason the increase in energy density with a decrease in electrode separation, was anticipated. It was also clear that the S-DOC pattern (not a clear trend for either data of these data sets) in energy density for longer discharge times (>10 s) was remarkably similar for the 20 mm and 6 mm capacitors.

As noted for other parameters, given the poor fit of some of the power law curves, quantitative extrapolation was not valid. Note: For the two "DOC" configurations shown the energy density was the effective energy density.

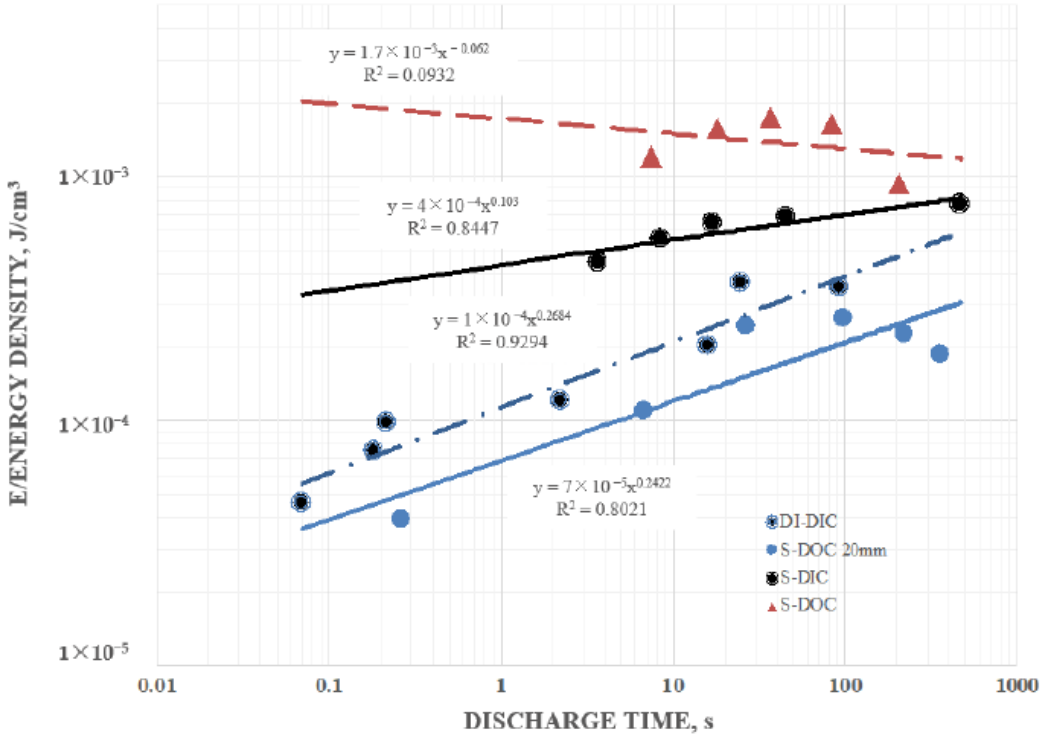

The 6 mm capacitor consistently had higher energy density than the 20 mm capacitor in all equivalent configurations. Parameters: ±10 V and holding for 200 s at ±10 V. Note: For the two "DOC" configurations shown the energy density was the effective energy density.

Figure 55. Energy Density 6 mm Capacitor Source: [1].

5. Power Density

In contrast to energy density, for all reported SDM based capacitors [2], [3], [7], [11]–[20] , power increases as the discharge time decreases. This indicates that for SDM based capacitors energy released during discharge is decreasing less quickly than the discharge time. This was also found true in the present study of SDM on the outside (Figure 56). As anticipated, with all other parameters constant, salt significantly also increased the power density; the power produced by S-DOC was at least an order of magnitude higher than equivalent DI-DOC at all discharge rates. Yet, it was also clear that DI-DOC performed extremely well.

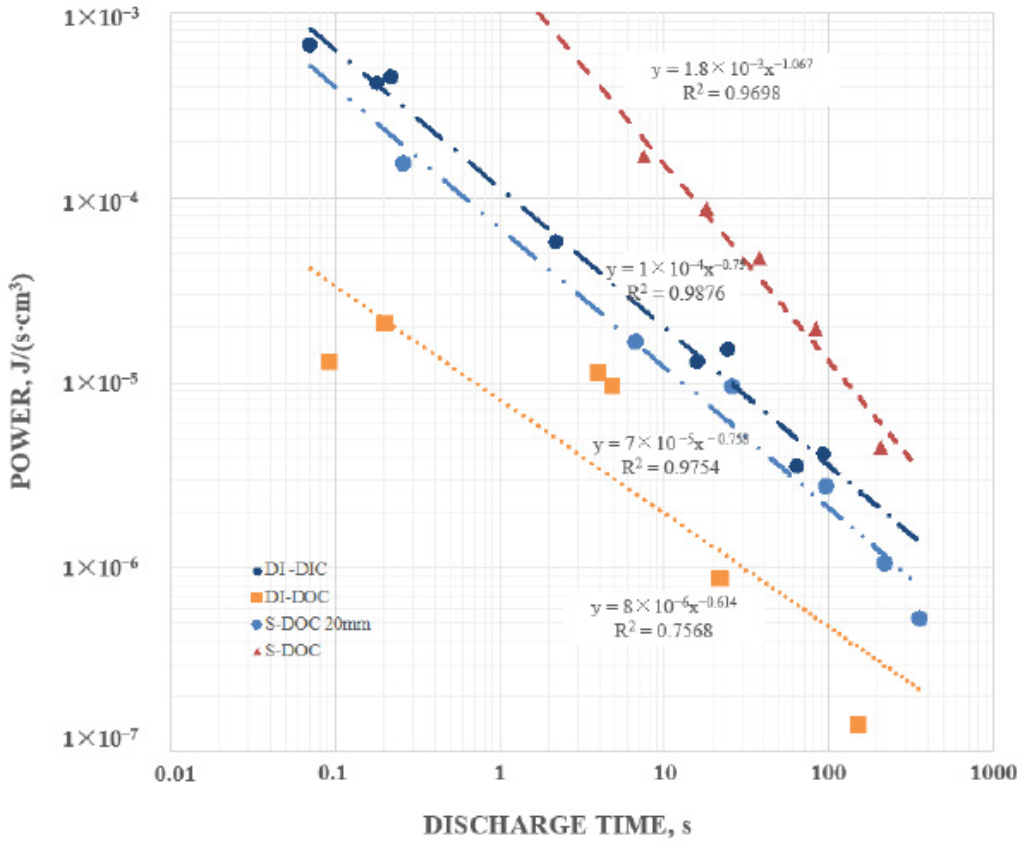

The highest power, based on energy determined by integration over the full discharge, was found for S-DOC for the 6 mm capacitor and the lowest for the DI-DOC for the 6 mm capacitor; however all configurations produced high power and showed the same trend with discharge time.

Figure 56. Increases with Decreasing Discharge Time Source: [1].

D. DISCUSSION

The mathematics employed in standard dielectric theory indicates an implicit assumption: The nature of the material on the "outside" of a capacitor is irrelevant. A good example is the mathematics of the most ubiquitous capacitor, a parallel plate capacitor. To determine the dielectric constant of a material that fills the space between the electrodes of a parallel plate capacitor three values are required: Measured capacitance, the area of the electrodes, and the distance between them (Equation (4)). There is no mathematical provision made to account for the properties of material not between the electrodes. True also: In standard narrative descriptions of the impact of dielectrics on capacitance there is never consideration given to properties of material outside the volume enclosed by the electrodes. In contrast, in SDM theory the properties of all dielectric materials, both between the plates and outside the plates, must be considered. One notable shortcoming of the SDM theory is that there is no simple equation linking geometric and materials properties equivalent to Equation (4), thus at present the theory is only qualitative.

This study regards the use of a very simple test to contrast the predictions of the standard dielectric theory with the SDM theory. In this study parallel plate capacitors were constructed such that in most cases only ambient laboratory air was between the electrodes. The capacitors were then "immersed" in different media (1) ambient laboratory air, (2) DI water, (3) DI water containing 0.5 wt % NaCl, and (4) DI water containing 5.0 wt % NaCl. According to standard theory the impact of the dielectric properties of material outside the region between the plates is irrelevant, hence all four capacitors "immersed" configurations should operate identically. In contrast, according to SDM theory, the measured capacitance of the test capacitors immersed in water or salt water should be substantially higher than those embedded in ambient laboratory atmosphere. The results, in brief, were that those capacitors immersed in water or salt water had a capacitance at least seven orders of magnitude higher than measured for the same capacitors immersed in air. In fact, for the 5 wt % NaCl case the effective dielectric constant below 1 V was spectacular, more than >10,000,000,000 x larger than the same capacitor immersed in laboratory air. Thus, the outcome of the experiments was only consistent with the SDM hypothesis.

This was not the first report of dielectric material outside the volume between the electrodes profoundly impacting performance. All the results reported were consistent with an earlier report from our laboratory, on the behavior of parallel plate capacitors covered with an SDM "gel" outside the volume between the electrodes [7]. As noted earlier, the intent of the present study was to confirm and "generalize" the conclusions reached in the first publication on the topic.

1. Secondary Findings

Secondary information found in the data included the following: (1) Pure water at short periods, order 1 s (roughly equivalent to a frequency of 1 Hz), had a dielectric constant in excess of 10^7, as reported elsewhere. (2) Salt does increase the dielectric constant. DI with even low dissolved salt concentrations (ca. 0.5 wt % NaCl) could have remarkably high dielectric values, $>10^{10}$, even for a one second hold time at 10 V. At one second discharge time the difference in the effective dielectric constant between DI, and 5 wt % NaCl in DI, was almost three orders of magnitude. (3) Increasing salt concentration did increase effective dielectric constant. Consistently, a bath of salt with 5 wt % NaCl produced higher capacitance, energy density, etc., values than a bath with 0.5 wt % NaCl. (4) There was evidence of a maximum, or "saturation" value to energy density achievable with salt water dielectric. In this study even as the discharge time was increased, effective dielectric constant remained relatively constant over a range of discharge times from about 1 s to 250 s. (5) Effective dielectric constant values were similar in magnitude to the dielectric constants of the same materials "between the plates." (6) Finally, in this study it was found that the effective dielectric constant of a dielectric material was always measured to be higher if it were outside the region between the electrodes than if it was placed between the electrodes. All of these secondary findings were only semi-quantitative and more detailed investigation is justified.

Most of these findings were consistent with earlier work on SDM, and expectations developed on the basis of those studies. Indeed, the high effective dielectric constant values for salt water were within an order of magnitude of those published previously for SDM

gels on the outside of parallel plate capacitors [7] as well as SDM, in various configurations, “between the electrodes” [3], [11]–[20].

It is notable that other groups studying the dielectric value of water at low frequency (ca. near 1 Hz) report values of dielectric constant very similar to those reported here [21], [22]. Moreover; those teams used other methods, not the constant current method employed herein. Thus, the present results further demonstrate the generality and reliability of the results.

2. Theory

It is illustrative to compare models of the origin of high dielectric value found in the literature for DI water at low frequency, which is the standard model vs. SDM model. The standard model is that the extremely high dielectric values (ca. 107 at 1 Hz) result from charged species in the water (e.g., OH^-, H_3O^+) forming oppositely charged electric double layers at each electrode [22]. According to the model, at the positive electrode OH^- forms a double layer, and at the negative electrode H_3O^+. For several reasons it is not at all clear how the remarkably high net dielectric values observed are consistent with that model: (1) In standard supercapacitor models it is assumed the dielectric value of the double layer is in the low double digits [2] at low frequency. (2) This standard model cannot explain why the dielectric constant of water is at least five orders of magnitude greater than solid titanates [2]. Generally, some double layer like feature is proposed to explain the dielectric value of solid dielectrics [28]–[30]. (3) The model is not consistent with the fact that voltage is a state property. Given all paths yield equivalent voltage, how does the double layer reduce the voltage for a charge that travels between the electrodes via a path outside the volume between the electrodes?

The SDM model, it is argued, is consistent with all observations, and all laws of physics [35], [36]. As explained in more detail elsewhere [2], [3], [7], [11], and illustrated in Figure 57, the theory is based on the field strength and direction of the field generated by a dielectric, placed between electrodes or surrounding the electrodes, “partially cancelling” the quasi dipole field produced by charges on the electrodes. The field generated by polarizing the dielectric will also be quasi-dipole, with a vector direction

necessarily opposite at every point in space to that of the “dipole” field generated by charges on the electrodes. Thus, the field produced by the dielectric reduces the electric field produced by the charge on the electrode at every point in space, both between the electrodes and outside the volume between electrodes. As the voltage is the line integral of the field, for any given charge density on the electrodes, that line integral, and concomitantly the voltage, is lowered. Hence, given a constant charge, capacitance (charge/voltage) is increased by the presence of the dielectric.

The SDM model predicts, consistent with the data presented herein, and contrary to the standard model, that dipoles outside the volume between the electrodes will increase capacitance. The dipoles formed in the dielectric reduce the field at every point in space whether the dielectric is in the volume between the electrodes, or outside that volume, a concept completely consistent with the standard E/M theory [37]: The electric field at any point is space is the vector sum of the fields of all charges in the universe. In either geometry the field at all points in space produced by the charges on the electrodes is reduced by the oppositely polarized dipoles of the dielectric. Also, unlike the standard model, there is no need to postulate either a double layer, or a high field region near the electrodes. According to the SDM model the electric field distribution in space is nearly the same for a particular voltage, including the region adjacent to the electrodes, with and without a dielectric [2].

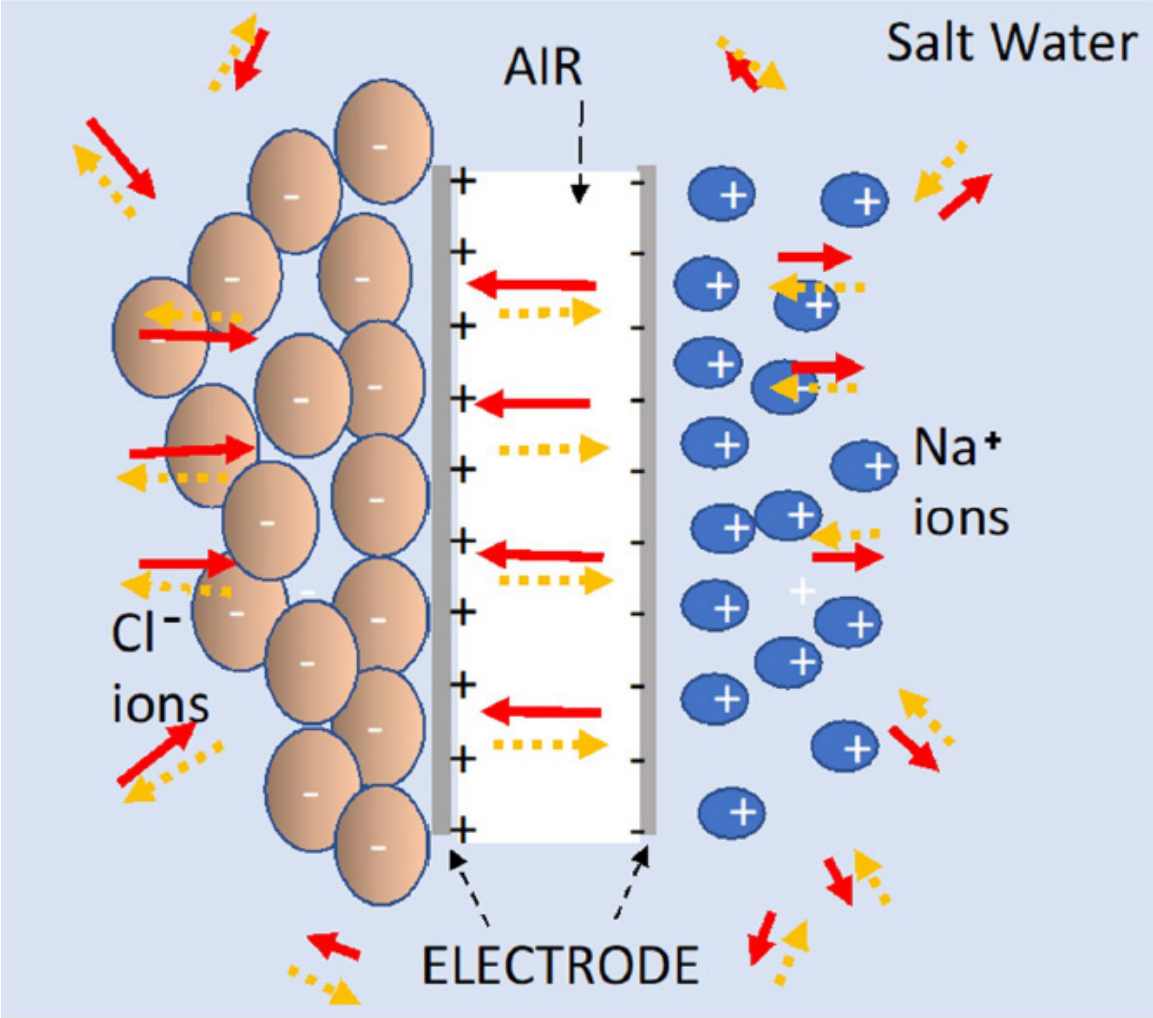

Top view schematic of super dielectric material (SDM) theory for a parallel plate capacitor submerged in a salt solution. In the S-DOC configuration illustrated at all points in space, both "outside" the capacitor and between the electrodes, the field due to charge on the electrodes (solid arrows) is partially cancelled by the field created by the ions (dashed arrows), or by water molecules (not shown) organized into a "liquid crystal" like arrangement.

Figure 57. Top View of SDM Example Source: [1].

The SDM model applies to all dielectrics, solids, and liquids. Two factors [2], [3], [7], [11] should impact the observed dielectric constant at low frequency; (1) the dipole density in the dielectric and, (2) the dipole length in the dielectric. There is no fundamental difference in the "action" of a solid (e.g., barium titanate) or a liquid dielectric. Both reduce the field created by charges on the electrode at all points in space via the formation of dipoles oriented opposite to the dipole orientation of the electrodes. Indeed, according to

SDM theory the underlying physical explanation for the enormous difference in a dielectric constant at low frequency (ca. 1 Hz) between salt water and barium titanate is the length of the dipoles. In barium titanate it is well under10^{-10} m, and in the salt water it can clearly be even centimeters long [2], [3], [7], [11]–[20]. Calculations show that NaCl saturated water has about 30% as many dipoles per volume as barium titanate. The longer dipoles of salt water lead to higher dipole fields at all points in space, hence more significant cancellation of electrode charge produced field, and concomitantly higher capacitance. That is, barium titanate, with far shorter dipoles, according to SDM theory should have far lower dielectric constant than salt water, as observed.

Some features of the data collected for the present work can readily be shown consistent with the SDM model. First, water should be an excellent dielectric at low frequencies because, as suggested elsewhere [22], the dipoles of water molecules align in the presence of an electric field. The structure of water in this condition is not known. Once, aligned, the water molecules will effectively "cancel" the field of the charges on electrodes, leading to extraordinarily high dielectric constants. Second, dissolved ions will further reduce the net field at all points in space by forming an effective large dipole with a length greater than the distance between the electrodes (Figure 57). The magnitude of this dipole may even explain why it was observed that S-DOC outperformed S-DIC as S-DIC dipoles, restricted by the internal volume, are necessarily shorter than those found in the S-DOC configuration. Third the effect of ion separation should increase with hold time. That is, the longer the hold time, the more charges can travel from elsewhere in the liquid bath to arrive at the proper electrode. In contrast, hold time has virtually no impact on the capacitive behavior of DI. Indeed, there is no need to provide time for ions to travel, only enough time for the water molecule alignment, clearly a far faster process.

Further study of a variety of related topics is arguably justified. What is the impact of salt type? For example, is KCl or NH_3Cl better than NaCl? Is KOH a better ion source than NaCl? How does the pH of salt-free water impact behavior? Is there a trend in the energy density as a function of inter-electrode distance?

3. Application

Potential significant applications of the SDM theory supported by these experiments, are: (1) Possible novel energy storage devices, and (2) improved understanding of charge/discharge mechanisms in nerve tissue. Regarding the former: As noted elsewhere, the high dielectric constant value of "salt water" at low frequencies suggest capacitors can be created with higher energy densities than the best batteries. An "ideal" example: A parallel plate capacitor with a gap of 1 micron into which a material of dielectric constant of 1 x 10^{10} and specific gravity of 2 is placed, then charged to 1 V will have an energy density of about 6000 Wh/kg of dielectric. This compares rather well with a lithium ion battery with an energy density of order 150 Wh/kg. Even a less "ideal" capacitor, same dimensions, but a dielectric of only 10^9, and assuming the dielectric is only thirty percent of the weight, still yields an energy density as good as the best lithium ion batteries. The present work suggests an interesting variation: The SDM dielectric need not be in the space between the electrodes, but in fact can merely "surround" the electrodes. Regarding the latter: One third of the fluid in the body is interstitial water with a relatively high Na^+ ion concentration. The present work suggests the capacitance of any "solvated" circuit, such as a circuit of neurons, will be impacted by the effective dielectric constant of the surrounding fluid. The present results suggest the dielectric constant of the "salt water" in the body is far higher than previously believed. Thus, the capacitance and charge stored in "biological circuits," even the roll of ions in interstitial media, may need to be reconsidered.

E. CONCLUSIONS

All data was consistent with the central postulate of SDM theory: Dielectric material on the outside of a parallel plate capacitor is as effective at increasing capacitance, energy density, and power density as the same dielectric material between the electrodes. In contrast, all data was inconsistent with the standard model of dielectrics applied to parallel plate capacitors: As per Equation (4), only the dielectric material between the electrodes plays a role in determining capacitance, energy, and power density. Thus, the

data in this paper suggests the theory of dielectrics presented in standard textbooks [27]–[29] should be reconsidered.

IV. FUTURE WORK

Future work needs to be continue in research into higher concentrations of NaCl. Increased concentrations of ionic solution to find a saturation limitation for the energy storage. This study could consist of utilizing several different materials that are soluble in water such as potassium. Further investigation into the material characteristics and changes of oxide layer growth and ageing of the materials. The combination of a pre-aged material and ionic solution may be a viable option for energy storage. Investigation into the byproduct manufacturing, initial testing found micron sized particle growth and unique nucleation of fibrous structures at the Nano-scale. This includes further investigation into the thin layered lead oxides and effects on efficiency. Further investigation into different configurations of carbon electrodes. Such as oriented CNT fibers, or uniform spaced sized CNT sheets. Further discussion and research in to different configurations of capacitors, thickness size of exposed areas and the impacts of these changing parameters. Based on preliminary research, investigation into the transition and chemistry associated with changing of ion transport in conjunction with electrolysis of water based solutions.

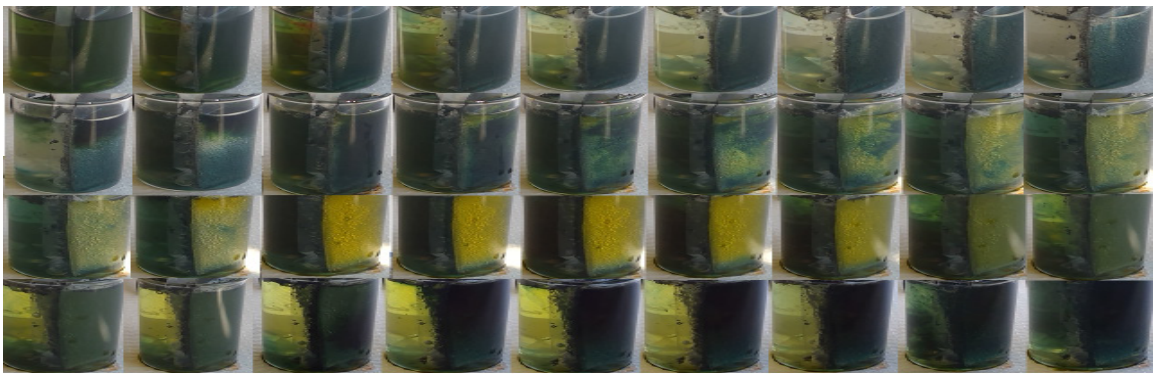

Two electrodes were placed in a NaCl solution separated by a wax paper barrier. One side was charged and held at a + voltage. The charged sides pH changed from neutral to a basic solution, while the opposite side became acidic. When the process was reversed the acidic and basic sides reversed.

Figure 58. Change of pH from High Electrolysis

THIS PAGE INTENTIONALLY LEFT BLANK

V. CONCLUSION

This research highlights some of the many changing variables of working with dielectrics and parallel plate capacitors. From the study the greatest combination of tested materials is a carbon based electrode with an ionic polar dielectric. This combination gives the greatest discharge times and energy densities. It operated best at the tested loading and necessitates further research to refine this possible future disruptive technology.

THIS PAGE INTENTIONALLY LEFT BLANK

VI. MATLAB SCRIPT

To process the EC-Lab files in MATLAB, the first step was to convert them from .mpr files to .mpt files. Using the built in function under "Experiment" then "Export to text" the file was converted to a text file.

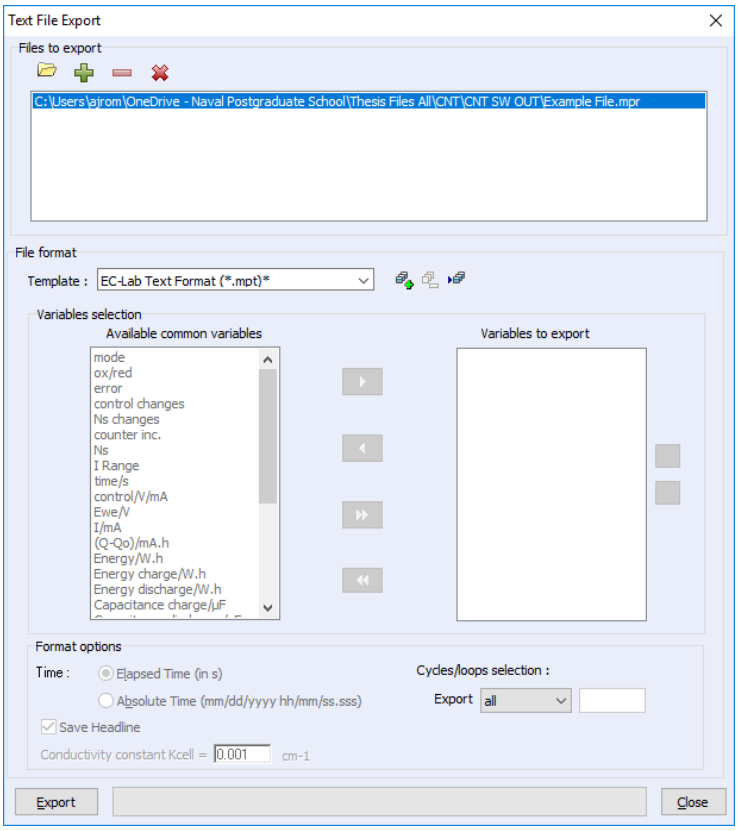

Figure 1. EC-Lab Text File Export Example

```
%% Give file generic name.
filename='Filename.mpt'

%% Load File as a table.
T = readtable(filename,'FileType','text','HeaderLines',101);
% Pull required data into a smaller table. 7-Sequence / 9-Time / 11-
% Voltage / 12-Current / 29-Cycle Count
T_all=T;
T = T(:,[7,9,11,12,29]);
% Label consolidated table
T.Properties.VariableNames={'Sequence','Time','Voltage','Current','Cycl
e'};
```

```
data_p=T(T.Sequence==2,:); % Data for sequence 2 only.
mean(data_p.Current) % Finds average discharge current.
data_m=T(T.Sequence==5,:); % Data for sequence 5 only.
mean(data_m.Current) %Finds average discharge current
T.Voltage=abs(T.Voltage);
T_Dis=T(T.Sequence==5 | T.Sequence==2,:);
a=min(T.Cycle);
b=max(T.Cycle);

for k=[a:b]
   T1=T_Dis(T_Dis.Cycle==k,:);
   T1A=table2array(T1);
% Pull all Plate A Data
  TA=T1(T1.Sequence==2,:);

  %% Find Linear Regression
                      if k==b
                      dt_a(k+1)=0;
                      inta(k+1)=0;
                      slopea(k+1)=0;
                      else
                      dt_a(k+1)= max(TA.Time)-min(TA.Time);
                      inta(k+1)=trapz(TA.Time,TA.Voltage);
                             TAA=table2array(TA);           z=TAA(:,3)<1;
y=nonzeros(TAA(:,3).*z);
                             x=nonzeros(TAA(:,2).*z);  mdl=fitlm(x,y);
                     slopea(k+1)=table2array(mdl.Coefficients(2,1));
                     end
 TA_c(k+1)=abs(mean(TA.Current));

 % Pull All Plate B Data

  TB=T1(T1.Sequence==5,:);
                     if k==a
                      dt_b(1)=0;
                      intb(1)=0;
                      slopeb(1)=0;
                  else
                     TB=TB(1:(height(TB)-1),:);
                     dt_b(k+1)= max(TB.Time)-min(TB.Time);
                     intb(k+1)=trapz(TB.Time,TB.Voltage);


                     TAA=table2array(TB);                  z=TAA(:,3)<1;
y=nonzeros(TAA(:,3).*z);
                     x=nonzeros(TAA(:,2).*z);  mdl=fitlm(x,y);
                     slopeb(k+1)=table2array(mdl.Coefficients(2,1));
end
   TB_c(k+1)=mean(TB.Current);

end
Results_a=[inta;dt_a;TA_c;slopea]';
Results_b=[intb;dt_b;TB_c;slopeb]';
Results_c=[Results_a((1:6),:);Results_b((2:7),:)];
```

APPENDIX: XRD DATA

A. TI SHEET (ORANGE)

Measurement conditions

X-Ray	40 kV , 15 mA	Scan speed / Duration time	5.0000 deg/min
Goniometer	MiniFlex 300/600	Step width	0.0100 deg
Attachment	ASC-6	Scan axis	Theta/2-Theta
Filter	K-beta(x1)	Scan range	10.0000 - 90.0000 deg
CBO selection slit	-	Incident slit	1.250deg
Diffrected beam mono.	None	Length limiting slit	10.0mm
Detector		Receiving slit #1	13.0mm
Scan mode	CONTINUOUS	Receiving slit #2	13.0mm

Qualitative analysis results

Phase name	Formula	Figure of merit	Phase reg. detail	DB card number
Titanium, syn	Ti	0.663	ICDD (PDF-4+ 2018 RDB)	04-003-5533
Titanium Oxide	Ti2 O0.33	1.761	ICDD (PDF-4+ 2018 RDB)	04-006-8712
Titanium Oxide	Ti6 O	1.708	ICDD (PDF-4+ 2018 RDB)	04-007-2177

Phase name	Formula	Space group	Phase reg. detail	DB card number
Titanium, syn	Ti	194 : P63/mmc	ICDD (PDF-4+ 2018	04-003-5533
Titanium Oxide	Ti2 O0.33	163 : P-31c	ICDD (PDF-4+ 2018	04-006-8712
Titanium Oxide	Ti6 O	163 : P-31c	ICDD (PDF-4+ 2018	04-007-2177

Peak list

No.	2-theta(deg)	d(ang.)	FWHM(deg)	Size(ang.)	Phase name	DB card number	Size distribution RSD
1	35.153(7)	2.5509(5)	0.163(5)	534(18)	Titanium,	04-003-5533,04-006-	-
2	36.22(3)	2.478(2)	0.60(3)	146(8)	Unknown	0	-
3	38.485(4)	2.3373(2)	0.173(8)	509(24)	Titanium,	04-003-5533,04-006-	-
4	40.2421(19)	2.23920(10)	0.1701(19)	519(6)	Titanium,	04-003-5533,04-006-	-
5	53.070(2)	1.72425(7)	0.112(3)	828(21)	Titanium,	04-003-5533,04-006-	-
6	60.95(7)	1.5188(15)	0.62(10)	154(25)	Unknown	0	-
7	63.0069(17)	1.47411(3)	0.1027(16)	947(15)	Titanium,	04-003-5533,04-006-	-
8	69.00(12)	1.360(2)	1.8(9)	55(28)	Titanium	04-006-8712,04-007-	-
9	70.660(9)	1.33204(15)	0.598(5)	169.9(14)	Titanium Oxide(3,0,3)	04-006-8712	-
10	70.7122(4)	1.331181(6)	0.1044(4)	975(3)	Titanium,	04-003-5533,04-006-	-
11	76.259(2)	1.24756(3)	0.107(3)	987(24)	Titanium,	04-003-5533,04-006-	-
12	77.401(4)	1.23198(6)	0.132(6)	805(35)	Titanium,	04-003-5533,04-006-	-
13	82.327(7)	1.17029(8)	0.116(9)	952(77)	Titanium,	04-003-5533,04-006-	-
14	86.790(5)	1.12121(5)	0.135(6)	847(40)	Titanium,	04-003-5533,04-006-	-

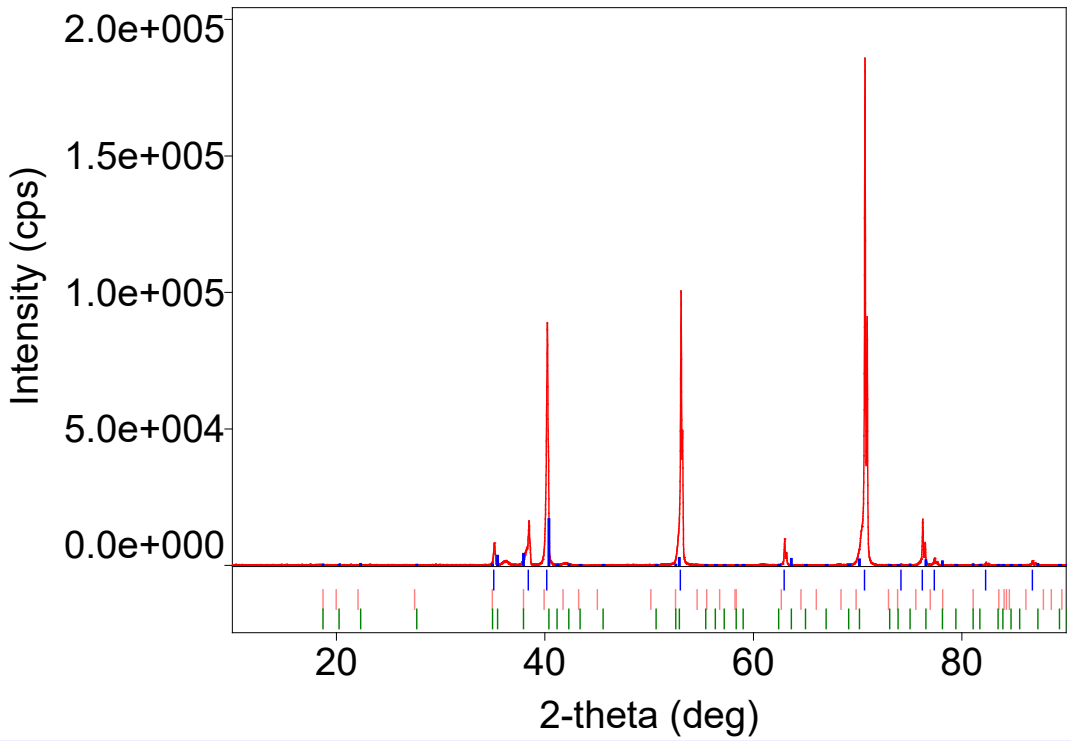

Crystal structure analysis results

Indexing

Phase name	Formula	Figure of merit	Phase reg. detail	DB card number
Titanium, syn	Ti	0.663	ICDD (PDF-4+ 2018 RDB)	04-003-5533
Titanium Oxide	Ti2 O0.33	1.761	ICDD (PDF-4+ 2018 RDB)	04-006-8712
Titanium Oxide	Ti6 O	1.708	ICDD (PDF-4+ 2018 RDB)	04-007-2177

Quantitative analysis results

Lattice information

Phase name	a(A)	b(A)	c(A)	alpha(deg)	beta(deg)	gamma(deg)	V(A^3)
Titanium, syn	2.947909	2.947909	4.678678	90.000000	90.000000	120.000000	35.211280
Titanium Oxide	5.105746	5.105746	9.358918	90.000000	90.000000	120.000000	211.287970
Titanium Oxide	5.103249	5.103249	9.357284	90.000000	90.000000	120.000000	211.044460

Phase name	Space group	Z	Z'	Calc. density(g/cm^3)
Titanium, syn	194 : P63/mmc	2	0.083	4.515
Titanium Oxide	163 : P-31c	6	0.500	4.766
Titanium Oxide	163 : P-31c	2	0.167	4.771

Structure determination

Refinement

Measurement range: 10.0000-90.0000deg. Refinement range: 10.0000-90.0000deg (1.09 A)
Number of refined parameters: 0

Phase name	Atomic coords	# of indep. reflns
Titanium, syn	Fractional coords	11
Titanium Oxide	Fractional coords	61
Titanium Oxide	Fractional coords	61

Rwp = - S = -

B. TI SHEET (BLUE)

Measurement conditions

X-Ray	40 kV , 15 mA	Scan speed / Duration time	5.0000 deg/min
Goniometer	MiniFlex 300/600	Step width	0.0100 deg
Attachment	ASC-6	Scan axis	Theta/2-Theta
Filter	K-beta(x1)	Scan range	10.0000 - 90.0000 deg
CBO selection slit	-	Incident slit	1.250deg
Diffrected beam mono.	None	Length limiting slit	10.0mm
Detector		Receiving slit #1	13.0mm
Scan mode	CONTINUOUS	Receiving slit #2	13.0mm

Qualitative analysis results

Phase name	Formula	Figure of merit	Phase reg. detail	DB card number
Titanium, syn	Ti	1.117	ICDD (PDF-4+ 2018 RDB)	04-006-2824
Titanium Oxide	Ti2 O	1.679	ICDD (PDF-4+ 2018 RDB)	04-015-8643

Phase name	Formula	Space group	Phase reg. detail	DB card number
Titanium, syn	Ti	194 : P63/mmc	ICDD (PDF-4+ 2018	04-006-2824
Titanium Oxide	Ti2 O	164 : P-3m1	ICDD (PDF-4+ 2018	04-015-8643

Peak list

No.	2-theta(deg)	d(ang.)	FWHM(deg)	Size(ang.)	Phase name	DB card number	Size distribution RSD
1	35.152(3)	2.5509(2)	0.147(3)	590(13)	Titanium,	04-006-2824,04-015-	-
2	36.18(2)	2.4806(15)	0.57(2)	154(6)	Unknown	0	-
3	38.33(2)	2.3462(14)	0.502(8)	175(3)	Titanium Oxide(0,0,2)	04-015-8643	-
4	38.474(2)	2.33796(13)	0.111(4)	794(30)	Titanium, syn(0,0,2)	04-006-2824	-
5	40.235(2)	2.23957(10)	0.167(2)	530(6)	Titanium,	04-006-2824,04-015-	-
6	53.060(2)	1.72454(7)	0.113(3)	823(20)	Titanium,	04-006-2824,04-015-	-
7	60.67(3)	1.5251(6)	0.60(12)	161(33)	Unknown	0	-
8	62.9987(15)	1.47428(3)	0.1071(13)	908(11)	Titanium,	04-006-2824,04-015-	-
9	70.476(15)	1.3351(3)	0.622(8)	163(2)	Unknown	0	-
10	70.6994(4)	1.331391(7)	0.1072(3)	949(3)	Titanium,	04-006-2824,04-015-	-
11	76.249(2)	1.24770(3)	0.109(3)	967(24)	Titanium,	04-006-2824,04-015-	-
12	77.396(5)	1.23205(6)	0.125(7)	854(48)	Titanium,	04-006-2824,04-015-	-
13	82.322(9)	1.17035(10)	0.129(11)	852(75)	Titanium,	04-006-2824,04-015-	-
14	86.778(5)	1.12133(5)	0.128(6)	890(43)	Titanium,	04-006-2824,04-015-	-

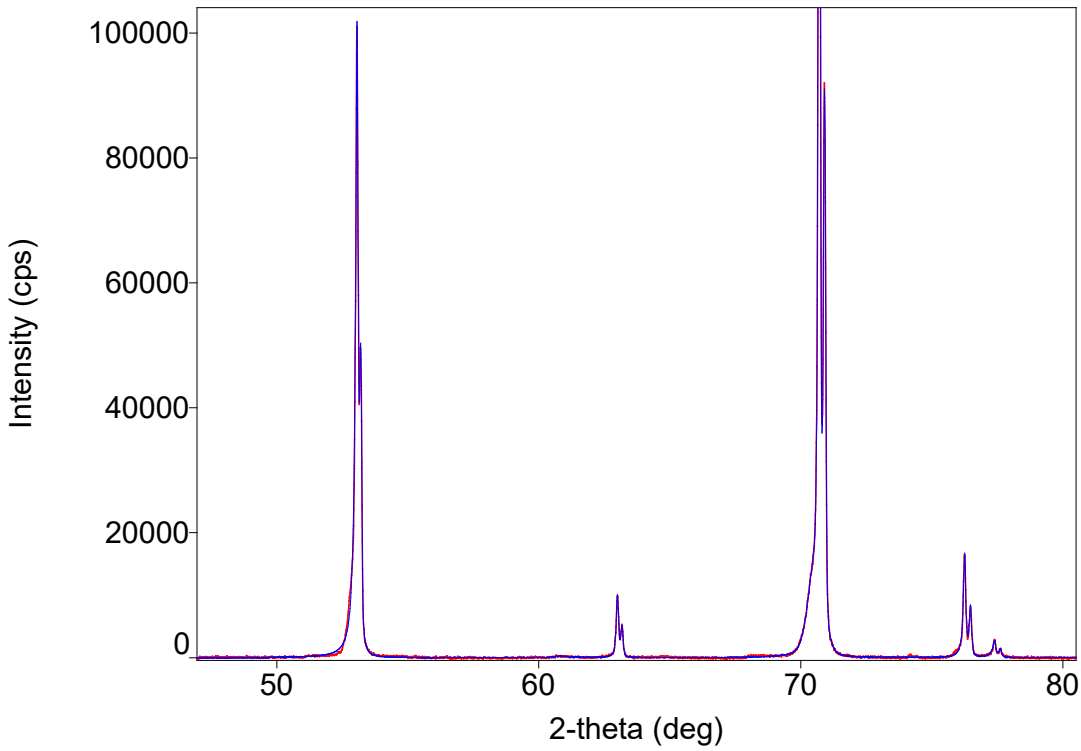

Crystal structure analysis results

Indexing

Phase name	Formula	Figure of merit	Phase reg. detail	DB card number
Titanium, syn	Ti	1.117	ICDD (PDF-4+ 2018 RDB)	04-006-2824
Titanium Oxide	Ti2 O	1.679	ICDD (PDF-4+ 2018 RDB)	04-015-8643

Quantitative analysis results

Lattice information

Phase name	a(A)	b(A)	c(A)	alpha(deg)	beta(deg)	gamma(deg)	V(A^3)
Titanium, syn	2.947926	2.947926	4.680910	90.000000	90.000000	120.000000	35.228480
Titanium Oxide	2.946607	2.946607	4.682691	90.000000	90.000000	120.000000	35.210375

Phase name	Space group	Z	Z'	Calc. density(g/cm^3)
Titanium, syn	194 : P63/mmc	2	0.083	4.513
Titanium Oxide	164 : P-3m1	1	0.083	5.269

Structure determination

Refinement

Measurement range: 10.0000-90.0000deg. Refinement range: 10.0000-90.0000deg (1.09 A)
Number of refined parameters: 0

Phase name	Atomic coords	# of indep. reflns
Titanium, syn	Fractional coords	11
Titanium Oxide	Fractional coords	19

Rwp = - S = -

C. LEAD OXIDE

Measurement conditions

X-Ray	40 kV , 15 mA	Scan speed / Duration time	10.0000 deg/min
Goniometer	MiniFlex 300/600	Step width	0.0200 deg
Attachment	ASC-6	Scan axis	Theta/2-Theta
Filter	None	Scan range	10.0000 - 90.0000 deg
CBO selection slit	-	Incident slit	1.250deg
Diffrected beam mono.	None	Length limiting slit	10.0mm
Detector		Receiving slit #1	13.0mm
Scan mode	CONTINUOUS	Receiving slit #2	13.0mm

Qualitative analysis results

Phase name	Formula	Figure of merit	Phase reg. detail	DB card number
Lead	Pb	1.392	ICDD (PDF-4+ 2018 RDB)	01-073-7078
Massicot, syn	Pb O	0.862	ICDD (PDF-4+ 2018 RDB)	04-005-4254
alpha-Pb3 O5	Pb3 O5	0.959	ICDD (PDF-4+ 2018 RDB)	01-076-1831
Lead Oxide	Pb2 O3	1.124	ICDD (PDF-4+ 2018 RDB)	04-013-9468
scrutinyite, syn, alpha-Pb O2	Pb O2	1.250	ICDD (PDF-4+ 2018 RDB)	04-011-9598
Lead Oxide	Pb O2	1.663	ICDD (PDF-4+ 2018 RDB)	04-020-6665

Phase name	Formula	Space group	Phase reg. detail	DB card number
Lead	Pb	194 : P63/mmc	ICDD (PDF-4+ 2018	01-073-7078
Massicot, syn	Pb O	57 : Pbma	ICDD (PDF-4+ 2018	04-005-4254
alpha-Pb3 O5	Pb3 O5	7 : P1a1,unique-b,cell-3	ICDD (PDF-4+ 2018	01-076-1831
Lead Oxide	Pb2 O3	11 : P121/m1,unique-b	ICDD (PDF-4+ 2018	04-013-9468
scrutinyite, syn, alpha-Pb O2	Pb O2	60 : Pbcn	ICDD (PDF-4+ 2018	04-011-9598
Lead Oxide	Pb O2	61 : Pbca	ICDD (PDF-4+ 2018	04-020-6665

Peak list

No.	2-theta(deg)	d(ang.)	FWHM(deg)	Size(ang.)	Phase name	DB card number	Size distribution RSD
1	11.134(8)	7.940(5)	0.182(11)	459(27)	alpha-Pb3 O5(0,1,2)	01-076-1831	-
2	14.958(2)	5.9179(9)	0.1295(18)	646(9)	Massicot, syn(0,0,1)	04-005-4254	-
3	21.00(11)	4.23(2)	2.5(3)	33(4)	Massicot,	04-005-4254,01-076-	-
4	28.575(11)	3.1213(12)	0.238(17)	359(25)	alpha-Pb3	01-076-1831,04-013-	-
5	28.950(9)	3.0817(9)	0.17(2)	490(65)	Massicot, syn(1,1,1)	04-005-4254	-
6	30.2410(13)	2.95302(12)	0.1357(15)	633(7)	Massicot, syn(0,0,2)	04-005-4254	-
7	33.956(9)	2.6380(6)	0.24(2)	361(30)	alpha-Pb3	01-076-1831,04-011-	-
8	35.973(8)	2.4945(5)	0.358(19)	244(13)	Lead(1,0,1),Massicot,	01-073-7078,04-005-	-
9	45.048(9)	2.0108(4)	0.158(19)	570(67)	Massicot,	04-005-4254,01-076-	-
10	46.1086(16)	1.96703(6)	0.141(2)	642(10)	Massicot,	04-005-4254,01-076-	-
11	53.04(2)	1.7250(6)	0.21(2)	433(47)	Massicot,	04-005-4254,01-076-	-
12	58.324(11)	1.5808(3)	0.13(2)	726(125)	Lead	04-013-9468,04-020-	-
13	59.16(4)	1.5604(10)	0.47(5)	203(22)	Massicot,	04-005-4254,04-013-	-
14	62.977(2)	1.47475(5)	0.149(2)	652(10)	Massicot,	04-005-4254,04-013-	-
15	67.48(4)	1.3868(7)	0.44(5)	227(25)	Massicot,	04-005-4254,04-013-	-
16	71.610(7)	1.31668(10)	0.244(10)	419(17)	Massicot,	04-005-4254,04-013-	-
17	76.30(3)	1.2470(4)	0.55(3)	192(10)	Lead(2,0,2),Massicot,	01-073-7078,04-005-	-
18	81.543(4)	1.17955(5)	0.189(5)	579(14)	Massicot,	04-005-4254,04-013-	-

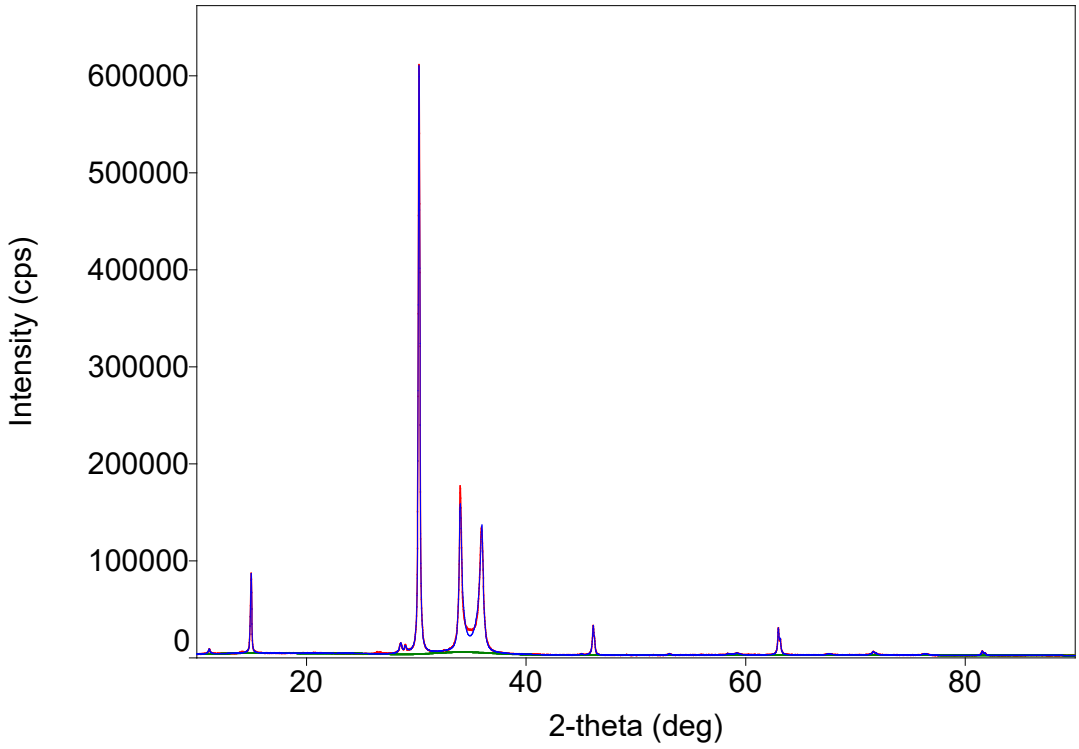

Crystal structure analysis results

Indexing

Phase name	Formula	Figure of merit	Phase reg. detail	DB card number
Lead	Pb	1.392	ICDD (PDF-4+ 2018 RDB)	01-073-7078
Massicot, syn	Pb O	0.862	ICDD (PDF-4+ 2018 RDB)	04-005-4254
alpha-Pb3 O5	Pb3 O5	0.959	ICDD (PDF-4+ 2018 RDB)	01-076-1831
Lead Oxide	Pb2 O3	1.124	ICDD (PDF-4+ 2018 RDB)	04-013-9468
scrutinyite, syn, alpha-Pb O2	Pb O2	1.250	ICDD (PDF-4+ 2018 RDB)	04-011-9598
Lead Oxide	Pb O2	1.663	ICDD (PDF-4+ 2018 RDB)	04-020-6665

Quantitative analysis results

Lattice information

Phase name	a(A)	b(A)	c(A)	alpha(deg)	beta(deg)	gamma(deg)	V(A^3)
Lead	3.261720	3.261720	5.398670	90.000000	90.000000	120.000000	49.740570
Massicot, syn	5.486449	4.783608	5.890041	90.000000	90.000000	90.000000	154.584256
alpha-Pb3 O5	7.679129	10.752771	22.798659	90.000000	88.699997	90.000000	1882.044420
Lead Oxide	7.067039	5.629573	3.874341	90.000000	80.099998	90.000000	151.843158
scrutinyite, syn,	4.937444	6.045955	5.366813	90.000000	90.000000	90.000000	160.207789
Lead Oxide	10.025331	5.268950	5.177864	90.000000	90.000000	90.000000	273.510144

Phase name	Space group	Z	Z'	Calc. density(g/cm^3)
Lead	194 : P63/mmc	2	0.083	13.834
Massicot, syn	57 : Pbma	4	0.500	9.590
alpha-Pb3 O5	7 : P1a1,unique-b,cell-3	16	8.000	9.904
Lead Oxide	11 : P121/m1,unique-b	2	0.500	10.113
scrutinyite, syn, alpha-Pb O2	60 : Pbcn	4	0.500	9.917
Lead Oxide	61 : Pbca	8	1.000	11.618

D. SILVER OXIDE

Measurement conditions

X-Ray	40 kV , 15 mA	Scan speed / Duration time	5.0000 deg/min
Goniometer	MiniFlex 300/600	Step width	0.0100 deg
Attachment	ASC-6	Scan axis	Theta/2-Theta
Filter	K-beta(x1)	Scan range	10.0000 - 90.0000 deg
CBO selection slit	-	Incident slit	1.250deg
Diffrected beam mono.	None	Length limiting slit	10.0mm
Detector		Receiving slit #1	13.0mm
Scan mode	CONTINUOUS	Receiving slit #2	13.0mm

Qualitative analysis results

Phase name	Formula	Figure of merit	Phase reg. detail	DB card number
Silver Oxide	Ag2 O	1.074	ICDD (PDF-4+ 2018 RDB)	00-012-0793
Silver, syn	Ag	0.332	ICDD (PDF-4+ 2018 RDB)	04-002-1347
Silver Oxide	Ag2 O	0.518	ICDD (PDF-4+ 2018 RDB)	01-078-5868

Phase name	Formula	Space group	Phase reg. detail	DB card number
Silver Oxide	Ag2 O	224 : Pn-3m,choice-2	ICDD (PDF-4+ 2018	00-012-0793
Silver, syn	Ag	225 : Fm-3m	ICDD (PDF-4+ 2018	04-002-1347
Silver Oxide	Ag2 O	224 : Pn-3m,choice-2	ICDD (PDF-4+ 2018	01-078-5868

Peak list

No.	2-theta(deg)	d(ang.)	FWHM(deg)	Size(ang.)	Phase name	DB card number	Size distribution RSD
1	26.669(11)	3.3399(14)	0.180(11)	474(28)	Silver Oxide(1,1,0)	00-012-0793	-
2	32.120(17)	2.7845(15)	0.22(3)	397(48)	Silver Oxide(1,1,1)	01-078-5868	-
3	32.774(4)	2.7304(3)	0.204(4)	424(9)	Silver Oxide(1,1,1)	00-012-0793	-
4	38.0308(15)	2.36416(9)	0.187(3)	469(8)	Silver	00-012-0793,04-002-	-
5	44.222(3)	2.04646(15)	0.252(8)	356(12)	Silver, syn(2,0,0)	04-002-1347	-
6	54.922(4)	1.67039(10)	0.278(4)	336(5)	Silver Oxide(2,2,0)	00-012-0793	-
7	64.364(4)	1.44627(8)	0.224(6)	438(12)	Silver, syn(2,2,0)	04-002-1347	-
8	65.52(3)	1.4235(6)	0.30(4)	327(44)	Silver Oxide(3,1,1)	00-012-0793	-
9	77.348(5)	1.23269(7)	0.305(8)	349(9)	Silver, syn(3,1,1)	04-002-1347	-
10	81.472(9)	1.18039(11)	0.238(13)	461(25)	Silver	00-012-0793,04-002-	-

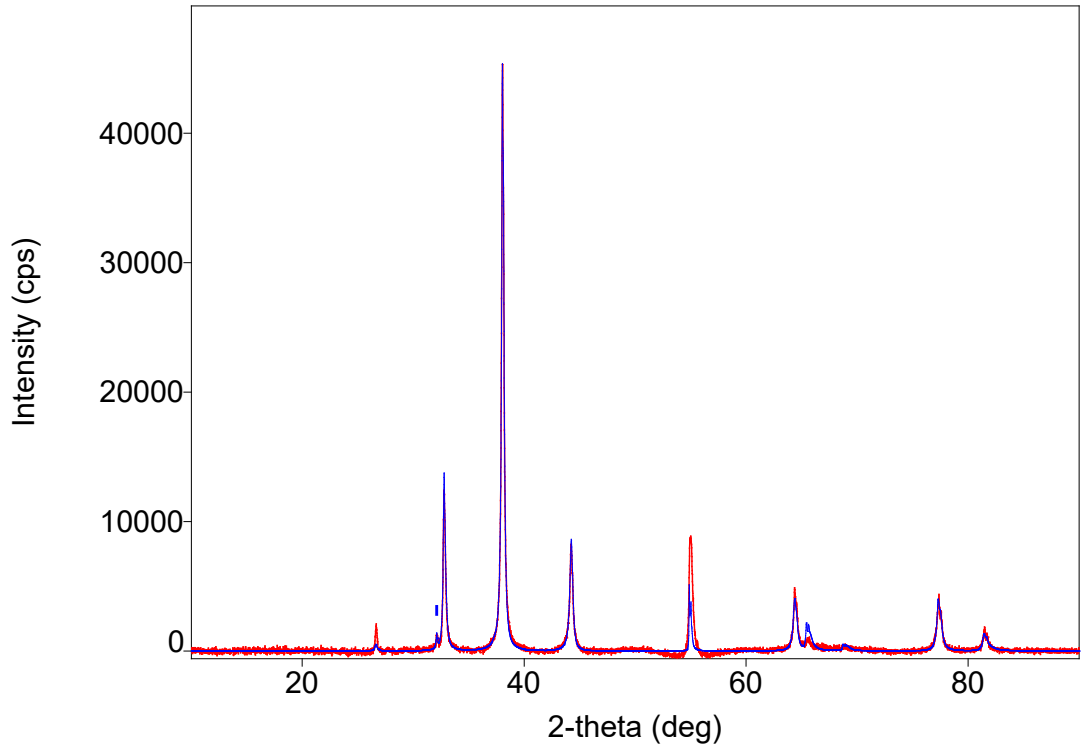

Crystal structure analysis results

Indexing

Phase name	Formula	Figure of merit	Phase reg. detail	DB card number
Silver Oxide	Ag2 O	1.074	ICDD (PDF-4+ 2018 RDB)	00-012-0793
Silver, syn	Ag	0.332	ICDD (PDF-4+ 2018 RDB)	04-002-1347
Silver Oxide	Ag2 O	0.518	ICDD (PDF-4+ 2018 RDB)	01-078-5868

Quantitative analysis results

Lattice information

Phase name	a(A)	b(A)	c(A)	alpha(deg)	beta(deg)	gamma(deg)	V(A^3)
Silver Oxide	4.72773(17)	4.72773(17)	4.72773(17)	90.000000	90.000000	90.000000	105.672(6)
Silver, syn	4.0907(3)	4.0907(3)	4.0907(3)	90.000000	90.000000	90.000000	68.453(8)
Silver Oxide	4.8222(19)	4.8222(19)	4.8222(19)	90.000000	90.000000	90.000000	112.14(8)

Phase name	Space group	Z	Z'	Calc. density(g/cm^3)
Silver Oxide	224 : Pn-3m,choice-2	2	0.042	7.286
Silver, syn	225 : Fm-3m	4	0.021	10.457
Silver Oxide	224 : Pn-3m,choice-2	2	0.042	6.861

Structure determination

Refinement

Measurement range: 10.0000-90.0000deg Refinement range: 10.0000-90.0000deg (1.09 A)
Number of refined parameters: 54

Phase name	Atomic coords	# of indep. reflns
Silver Oxide	-	14
Silver, syn	Fractional coords	5
Silver Oxide	-	15

Rwp = 8.56% S = 1.6979

LIST OF REFERENCES

[1] J. Phillips and A. Roman, "Understanding Dielectrics: Impact of External Salt Water Bath," *Materials*, vol. 12, no. 12, p. 2033, Jun. 2019. [Online]. doi:10.3390/ma12122033

[2] F. J. Q. Cortes, A. Suarez, and J. Phillips "Toward a Universal Model of High Energy Density Capacitors." *Innovation in Engineered Porous Materials for Energy Storage Applications.* CRC Press, Boca Raton 2018. :pp 343 (in press)

[3] F. Cortes and J. Phillips, "Tube-Super Dielectric Materials: Electrostatic Capacitors with Energy Density Greater than 200 J·cm−3," *Materials*, vol. 8, no. 9, pp. 6208–6227, Sep. 2015.

[4] FinancialBuzz.com, "Cobalt's Scarcity Influences the Lithium-ion Battery Market." [Online]. Available: https://www.prnewswire.com/news-releases/cobalts-scarcity-influences-the-lithium-ion-battery-market-685240801.html

[5] P. W. Parfomak, "Energy Storage for Power Grids and Electric Transportation: A Technology Assessment," Washington, DC, USA, CRS Report No. R42455, 2012. [Online]. Available: https://crsreports.congress.gov/product/pdf/R/R42455

[6] T.W. McKnight, "Study of super dielectric material for novel paradigm capacitors." M.S. thesis, Naval Postgraduate School, Monterey, CA, 2018. [Online]. Available: http://hdl.handle.net/10945/58339

[7] J. Phillips, "Toward an Improved Understanding of the Role of Dielectrics in Capacitors," *Materials*, vol. 11, p. 1519, Aug. 2018.

[8] Nanocomp Technologies,"Miralon_Sheets_Tape.pdf." Merrimack, NH.

[9] "Our Ingredients," *Johnson's® Baby*. [Online]. Available: https://www.johnsonsbaby.com/safety-standards/ingredients.

[10] M. V. Diamanti, B. Del Curto, and M. Pedeferri, "Interference colors of thin oxide layers on titanium," *Color Res. Appl.*, vol. 33, no. 3, pp. 221–228, Jun. 2008.

[11] F. Cortez and J. Phillips, "Novel Materials with Effective Super Dielectric Constants for Energy Storage," *Journal of Electronic Materials*, Vol 44, no 5, pp. 1367–1376, May. 2015. [Online]. https://doi.org/10.1007/s11664-015-3641-8

[12] J. Gandy, F. J. Q. Cortes, and J. Phillips, "Testing the Tube Super-Dielectric Material Hypothesis: Increased Energy Density Using NaCl," *Journal of Electronic Materials*, vol. 45, no. 11, pp. 5499–5506, Nov. 2016.

[13] J. Phillips, “Novel Superdielectric Materials: Aqueous Salt Solution Saturated Fabric,” *Materials*, vol. 9, no. 11, p. 918, Nov. 2016

[14] S. Fromille and J. Phillips, “Super Dielectric Materials,” *Materials*, vol. 7, no. 12, pp. 8197–8212, Dec. 2014.

[15] J. Phillips and S. S. Fromille, “Super Dielectric Materials,” U.S. Patent 9530574, Dec. 27, 2016.

[16] N. Jenkins, C. Petty, and J. Phillips, “Investigation of Fumed Silica/Aqueous NaCl Superdielectric Material,” *Materials*, vol. 9, no. 2, p. 118, Feb. 2016.

[17] M. Lombardo , Steven and J. Phillips, “*Performance of Aqueous Ion Solution/Tube-Super Dielectric Material-Based Capacitors as a Function of Discharge Time*.” InTech: London, UK (2018). http://hdl.handle.net/10945/59935

[18] J. Phillips, “Capacitor with Ionic-Solution-Infused, Porous, Electrically Non-Conductive Material,” U.S. Patent 9,711,293, Jul 1, 2017.

[19] Phillips, J. “Super Dielectric Capacitor Using Scafold Dielectric,” U.S. Patent 9870875, Jan. 16, 2018.

[20] C. W. Petty and J. Phillips, “Super Dielectric Material Based Capacitors: Punched Membrane/Gel,” *Journal of Electronic Materials*, vol. 47, no. 8, pp. 4902–4909, Aug. 2018.

[21] P. M. Geethu, V. T. Ranganathan, and D. K. Satapathy, “Inferences on Hydrogen Bond Networks in Water from Isopermitive Frequency Investigations,” *Journal of Physics: Condensed Matter*, vol. 30, no. 31, p. 315103, Jul. 2018.

[22] P. B. Ishai, Z. Sobol, J. D. Nickels, A. L. Agapov, and A. P. Sokolov, “An Assessment of Comparative Methods for Approaching Electrode Polarization in dielectric Permittivity Measurements,” *Review of Scientific Instruments*, vol. 83, no. 8, p. 083118, Aug. 2012.

[23] R. Farma *et al.*, “Physical and Electrochemical Properties of Supercapacitor Electrodes Derived from Carbon Nanotube and Biomass Carbon,” *International Journal of Electrochemical Science*, vol. 8, pp. 257–273, Jan. 2013.

[24] H. Li, J. Wang, Q. Chu, Z. Wang, F. Zhang, and S. Wang, “Theoretical and Experimental Specific Capacitance of Polyaniline in Sulfuric Acid,” *Journal of Power Sources*, vol. 190, no. 2, pp. 578–586, May 2009.

[25] E. Barsoukov and J.R. Macdonald, *Impedance Spectroscopy: Theory, Experiment, and Applications.* Hoboken, NJ, USA: John Wiley and Sons, 2018.

[26] J. A. Connelly, *Low-Noise Electronic System Design*, 1st ed. New York, NY, USA: John Wiley & Sons, Inc., 1993.

[27] J. R. Macdonald and W. R. Kenan, *Impedance Spectroscopy: Emphasizing Solid Materials and Systems*. New York, NY, USA : John Wiley and Sons, 1987.

[28] Resnick, R. and D. Halliday. *Physics.* New York, NY, USA : John Wiley and Sons, 1968.

[29] Walker, J. *Physics.* Upper Saddle River, NJ, USA: Pearson Prentice Hall, 2007.

[30] K.C. Kao, *Dielectric Phenomena in Solids: With Emphasis on Physical Concepts of Electronic Processes.* Cambridge, NY, USA : Academic Press, 2004.

[31] "Test Procedures for Capacitance, ESR, Leakage Current and Self-Discharge Characterizations of Ultracapacitors; 1007239-EN.2," San Diego, CA, USA : Maxwell Technologies, 2015.

[32] "Murata Supercapacitor Technical Note No. C2M1CXS-053M," Kyoto, Japan :Murata, 2014.

[33] C. G. Malmberg and A. A. Maryott, "Dielectric Constant of Water from 0 to 100 C," *J. RES. NATL. BUR. STAN.*, vol. 56, no. 1, p. 1, Jan. 1956.

[34] G. J. Reynolds, M. Kratzer, M. Dubs, H. Felzer, and R. Mamazza, "Electrical Properties of Thin-Film Capacitors Fabricated Using High Temperature Sputtered Modified Barium Titanate," *Materials*, vol. 5, no. 4, 2012.

[35] Faraday Michael, "Experimental Researches in Electricity," *Philosophical Transactions of the Royal Society of London*, vol. 122, pp. 125–162, Jan. 1832.

[36] Maxwell, J.C. *A Treatise on Electricity and Magnetism,* 3rd ed., Oxford, UK : Clarendon Press, 1873.

[37] Jackson, J.D. *Classical Electrodynamics,* 2nd ed. Hoboken, NJ, USA : John Wiley and Sons, 1999.

THIS PAGE INTENTIONALLY LEFT BLANK

INITIAL DISTRIBUTION LIST

1. Defense Technical Information Center
   Ft. Belvoir, Virginia

2. Dudley Knox Library
   Naval Postgraduate School
   Monterey, California